OPEN ACCESS

Greenhouse Gas Theories and Observed Radiative Properties of the Earth's Atmosphere

Klimarealistene
P.O. Box 33,
3901 Porsgrunn
Norway
ISSN: 2703-9072

Correspondence: mis-kolczif@gmail.com

Vol. 3.3 (2023)

pp. 232-289

Ferenc Miskolczi

Foreign Associate Member of the Hungarian Academy of Sciences, Budapest, Hungary

Abstract

In the last decade fundamental theoretical equations were developed for describing and understanding the global average radiative equilibrium state of the Earth-atmosphere system. It is shown that using the well-established laws of radiation physics the key climate parameters of the planet can be deduced theoretically, from purely astrophysical considerations and some plausible assumptions on the material composition of the planetary surface and the structure of the atmosphere. It is also shown, that the Earth-atmosphere system is in radiative equilibrium with a theoretical solar constant, and all global mean flux density components satisfy the theoretical expectations. The greenhouse effect predicted by the Arrhenius greenhouse theory is inconsistent with the existence of this radiative equilibrium. Hence, the CO_2 greenhouse effect as used in the current global warming hypothesis is impossible. The greenhouse effect itself and the CO_2 greenhouse effect based global warming hypothesis is a politically motivated dangerous artifact without any theoretical or empirical footing. Planet Earth obeys the most fundamental laws of radiation physics.

Keywords: Greenhouse effect theory; radiative equilibrium; climate change

Submitted 2023-03-09; Accepted 2023-07-08. https://doi.org/10.53234scc202304/05

1. Introduction

All planets in our solar system are isolated celestial objects orbiting around the Sun. Isolated objects can only exchange energy with other objects and the surrounding space environment by mains of radiation (Peixoto & Oort (1992) [64], page 104: *"all exchange of energy between the Earth and outer space is through radiative transfer"*). The exchange of *shortwave* (SW) and *infrared* (IR) − or *long-wave* (LW) − radiant energy happens through the *active planetary surface* (APS). By definition, APS is the sum of the identifiable clear and cloudy (solid or liquid) surface areas which contributes to the exchange of radiant energy with the atmosphere above and, − in case of semi-transparent atmospheres − directly with the Sun and the space environment. The atmosphere above the APS has its own SW and LW upward contribution to the total radiation leaving the planet.

The APS may receive inward radiation from the full 4π solid angle, and emits and reflects (or scatters) radiation into the full 4π solid angle. Planets with semi-transparent condensing *greenhouse gas* (GHG) atmospheres usually have complex multi-layer adaptive APS which must be able to configure itself to the planetary *radiative equilibrium* (RE) state. Some GHGs (CO_2, CH_4) are practically uniformly mixed in the atmosphere, others (H_2O, O_3) have vertical structures and diverse geographical patterns.

Further on, we shall use the concept of a *passive* planet. A passive planet has negligible internal source of thermal energy (from non-radiative processes) propagating through the APS and the atmosphere above and will contribute to the *top of the atmosphere* (TOA) net radiation.

Compared to the magnitude of the flux densities involved in the planetary radiative processes, the combined effect of the thermal energy released by geothermal flux, tidal friction, plate tectonics, surface erosion, volcanism, forest fires, human energy production, or other natural and non-natural sources is far too small to give a reasonable estimate of their role in the long-term climate change, Kandel & Viollier (2005) [1].

In this study any power dissipation in the system that is *unrelated* to the incoming solar radiation will be disregarded partly because it cannot be accurately quantified, and partly because later, when the observational evidence of their global scale net contributions will be available, it may be considered (as part of the net heat conduction, or the net dissipation due to latent heat transfer among the geological reservoirs).

Due to the stochastic dynamical nature of the climate it is impossible to quantitatively decompose the thermal structure (and in fact the GHG structure) of the atmosphere showing the individual contributions of the processes mentioned above. For example, the 0.06 – 0.086 Wm^{-2} heat flow from the planetary interior in [1] can never be associated with the global mean thermal structure or the surface temperature.

However, one must acknowledge, that the real (empirically observed) atmospheric thermal structure implicitly involves all the power dissipation in the system independently of the origin. In other words, working with real radiosonde data one must be sure, that the nature knows very well how to establish the global average thermal structure as the function of the power dissipation from any source. For better understanding let us quote the following statement from the Science magazine, Lacis et al. (2010) [13]:

"Because the solar-thermal energy balance of Earth [at the top of the atmosphere (TOA)] is maintained by radiative processes only, and because all the global net advective energy transports must equal zero, it follows that the global average surface temperature must be determined in full by the radiative fluxes arising from the patterns of temperature and absorption of radiation. This then is the basic underlying physics that explains the close coupling that exists between TOA radiative fluxes, the greenhouse effect, and the global mean surface temperature."

From practical point of view working with the concept of a passive planet at the end of the complete flux density simulations the planetary radiative balance will clearly show if there is a need for a correction term (attributed to unaccounted power dissipations in the system) to establish the Sun-Earth radiative equilibrium. Planets or Moons without atmosphere have limited capabilities to regulate their radiative budget and their equilibrium state is not discussed here. In the steady-state RE (at the TOA of an isolated passive planet) the long term global mean radiation field must satisfy the next two requirements:

- The energy conservation principle dictates that the sum of the reflected and absorbed parts of the effective available (or intercepted) solar flux at the TOA must be equal.
- According to the flux form of the Kirchhoff law at the TOA the total outgoing LW radiation and the absorbed SW solar radiation must be equal.

Expressed in analytic equations we may write:

$$F_0 / 4 = F_E = F_A + F_R = F_E(1-\alpha_B) + \alpha_B F_E , \quad (1)$$

$$OLR^A = F_A = F_E(1-\alpha_B) , \quad (2)$$

where F_0 is the local solar constant, $F_E = F_0 / 4$ is the *effective available solar flux* over a unit area on the Earth (at the TOA), F_A and F_R are the absorbed and reflected SW flux density components of F_E, $\alpha_B = F_R / F_E$ is the Bond albedo (by definition), and OLR^A is the total outgoing LW radiation. The ¼ scaling factor of F_0 in (1) converts the intercepted solar flux to flux density available over a unit surface area of a planet (or any spherical celestial object). Such a planet will obey the energy and momentum conservation principles of the radiation field in its simplest form where all planetary LW flux density components are scaled with the solar luminosity. These are the top-level constraints imposed on the radiation field of the Sun-planet system, and assures, that an isolated passive planet cannot change the local solar constant. Obviously, such a planet is an abstraction, but observations show that it is not an unrealistic one.

It is quite reasonable to assume that after the formation and during the billions of years of planetary evolution planets have always sufficient time to maintain the average quasi-static state of the *Chandrasekhar-type radiative equilibrium* (CRE), Chandrasekhar (1960) [2], page 200. Equations (1,2) are not a kind of wish-list, they are the direct consequences of the energy and momentum conservation, energy minimum (or entropy maximum) principles of nature.

Climate change (the observed, as opposed to declared) are to be investigated either as a consequence of mere fluctuations between regions (which upsets at localities what was earlier regarded as normal) or due to external perturbations of the total energy input to the Earth-atmosphere system. Here climate change will be regarded as deviations of the basic (radiative and thermodynamic) global mean climate parameters from their long-term average value, due to possible internal (natural or random) fluctuations, or external perturbations of the total energy input to the Earth-atmosphere system (through the upper and lower boundaries). Internal fluctuations are due to the chaotic nature of the dissipative dynamic climate system, and they do not alter the long-term radiative balance. Regarding the large variety of time scales of the possible internal fluctuations and external perturbations that may occur one has to be careful with selecting the length of a characteristic averaging time interval, over which the radiative equilibrium is established, Scafetta (2010) [3], Scafetta et al. (2018) [51].

In Figure 1 the exponential increase of the atmospheric CO_2 concentration in the last 75 years is an empirical fact, Andrews (2023) [6]. However, it is an open question how these changes in the GHG content of the atmosphere may alter the radiative equilibrium state of the planet, i.e. the validity of (1,2). The light blue regression function was established between the time differences from the reference year of 1948 and the Mauna Loa 63 annual mean data between 1959 and 2021. Although the relationship between the thermal history of the Earth and the composition of the atmosphere on evolutionary time scale is an interesting subject, the man-made CO_2 greenhouse problem is only relevant to the last century.

Planets with large amount of latent heat storage (in geological reservoirs) may moderate the internal and external fluctuations by phase pinning (Maxwell rule). In the Earth's atmosphere the *water vapor* (WV) is the only condensing GHG, therefore the triple point temperature (we call it phase temperature) of the H_2O at $t_P = 273.16$ K (0 °C) has a unique role in the climate system. Notice, that in the Kelvin scale the reference temperature $t_{ZERO} = -273.16$ °C, that is, t_P in K practically equal to $-t_{ZERO}$ in °C.

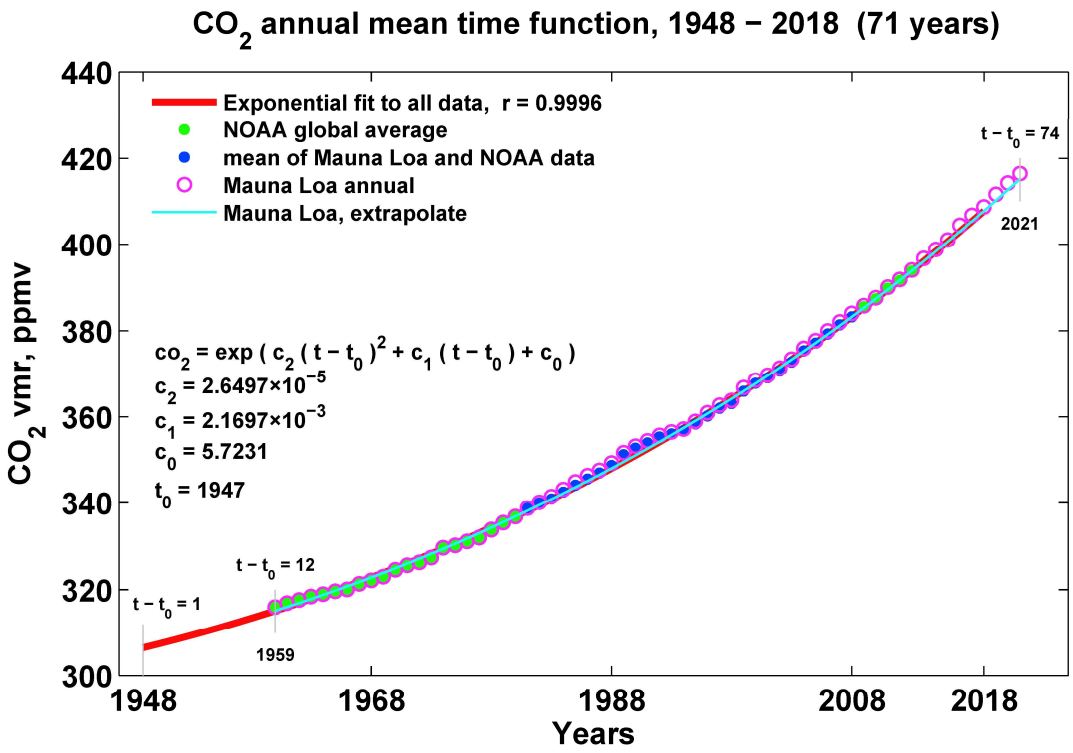

Figure 1: Time dependence of the CO_2 volume mixing ratio in the last 75 years. Our empirical exponential fit was based on the publicly available numerical annual mean data in the NOAA NCEP/NCAR Reanalysis data time series. The origin of the observed ~35 % increase is not yet identified. The Mauna Loa weekly data shows significant seasonal fluctuation, probably related to the seasonal changes of the SW radiation input.

The purpose of this paper is to answer two greenhouse effect related fundamental questions:

- Do greenhouse gas theories contradict energy balance equations?
- Is the proposed greenhouse effect due to anthropogenic carbon dioxide emissions supported by observed atmospheric thermal and humidity structures and global scale simulations of the infrared absorption properties of the Earth's atmosphere?

In 2017 these two questions were explicitly raised by the *Supreme Court of British Columbia* in the libel cases of Michael Mann vs. Timothy Ball and Andrew Waver vs. Timothy Ball. This paper was built on the testimony presented to the Court in the above cases, Miskolczi (2016) [4]. Further on we shall also address some problems of recent global radiative budget schemes and present a realistic planetary radiative budget by establishing new theoretical approach to the greenhouse effect.

We also wish to demonstrate that the theoretical expectations are fully consistent with the observations. The special orbit of the Earth, the unique GHG composition of the atmosphere, the huge amount of water (in all three phases), the partial cloud cover, and the existence of the biosphere make our planet a very distinguished member of the solar system. Although the general constraint of the energy conservation principle (1) and Kirchhoff law (2) is valid for any isolated passive celestial object, other planets or moons have entirely different physical environments therefore, we shall not discuss (in details) the *relevance* of our new greenhouse effect related theoretical considerations here.

In what follows, we shall introduce some definitions and present observed empirical facts on the radiative structure of the Earth-atmosphere system (section **2**); discuss the methodology of the greenhouse effect validations (section **3**); present relevant recently developed radiative transfer background information (section **4**); summarize the new results (section **5**); and state the conclusions (section **6**).

In the Appendix the Planck radiation laws and the new (theoretical) *law of radiation-temperature duality* – a relationship between the flux density and temperature – are discussed in some detail.

2. Greenhouse gas theories and radiative balance equations

Although the use of the radiative *greenhouse effect* (GE) terminology associated with the Earth's climate goes back about two centuries, the physically meaningful definition, and the structured theoretical foundation of the planetary GHG GE is still missing.

The root of the problem is in the difficulties of characterizing the planetary climate with a single, properly chosen (scalar) physical quantity. It is no wonder, that humans living on the Earth's surface are very much interested in the average surface temperature of their immediate environment. The variability of ground surface temperature on different time scales and geographical locations affect people's every day's life.

In case of the *local thermodynamic equilibrium* (LTE), the isotropic source function at the lower boundary of the atmosphere and the isotropic upward flux density from a perfectly black surface (in direct contact with the atmosphere above) are equal, Mihalas & Mihalas (1984) [48], page 328. Accordingly, there is no discontinuity or jump in the temperature at surface, and the boundary layer can be characterized with a single radiative temperature t_S from the source function, Manabe & Wetherald (1967) [5], Van Wijngaarden & Happer (2020) [57].

The extrapolation of the average local or regional surface temperature to global scale and longer periods of time leads to the concepts of global climate change, and ultimately to the CO_2 related *anthropogenic global warming* (AGW). We believe the temporal and areal averages of any single physical quantity should be meaningful. However, in the greenhouse effect literature one may find articles stating (without proof) that the assumption of uniform temperature for the whole global surface is inadequate, le Pair & de Lange (2022) [7], Kramm & Dlugi (2011) [8].

2.1 Definitions of basic greenhouse parameters

In climate science the GHG GE is arbitrarily defined as the Δt_A temperature difference between the ground surface *radiative temperature* t_S and the planetary SW *absorption temperature* t_A:

$$\Delta t_A = t_S - t_A, \tag{3}$$

where $t_A = (F_A / \sigma)^{1/4}$, $t_S = (S_U / \sigma)^{1/4}$, S_U is the isotropic ground surface upward flux density, and $\sigma = 5.6699833 \times 10^{-8}$ $\mathrm{Wm^{-2}K^{-4}}$ is our adopted *Stefan-Boltzmann* (SB) constant. Unless specified otherwise, all physical constants were taken from the *National Institute of Standards and Technology* (NIST), Mohr et al. (2007) [9]. Using the SB law, any flux density may be converted to *equivalent blackbody temperature* (EBT), which facilitates the convenient comparison of temperatures (instead of fluxes) without referencing to any real radiating surface. Associated with the local solar constant, it is customary to define the $t_0 = (F_0 / \sigma)^{1/4} = 394.117$ K effective temperature which is the EBT for our adopted $F_0 = 1367.95\ \mathrm{Wm^{-2}}$ solar constant, (see paragraph *4.2*). In addition to (3), GE may also be expressed by the greenhouse factor G_A, which is the difference of the respective flux densities from the SB law:

$$G_A = \sigma t_S^4 - \sigma t_A^4 = S_U - F_A . \quad (4)$$

Raval & Ramanathan (1989) [10] introduced the normalized greenhouse factor which is the ratio of G_A to S_U:

$$g_A = (S_U - F_A)/S_U . \quad (5)$$

For real − not perfectly black − ground surfaces one may also define a t_G *hypothetical* EBT via the $\varepsilon_B S_G = \varepsilon_B \sigma t_G^4 = \sigma t_S^4 = S_U$ equation, where ε_B is the LW flux emissivity. Perfectly black surfaces will have ε_B equal to 1.0 , $t_G = t_S$, and $S_U = S_G$. Here S_G is the surface upward blackbody radiation associated with the change of thermal energy due to processes of non-radiative origin (evaporation, condensation, sublimation, heat conduction, etc.).

Apparently, F_A from (2) depends only on the long term means of F_0, and α_B. Therefore, t_A may be written as:

$$t_A = ((1-\alpha_B)F_E/\sigma)^{1/4} = ((1-\alpha_B)F_0/(4\sigma))^{1/4} . \quad (6)$$

Since in (6) t_A does not depend on the LW absorption and emission properties of the system, the arbitrarily defined Δt_A, G_A , and g_A cannot be related to the GHG content of the atmosphere. They are only dependent on the choice of the global mean t_S, consequently, the planetary greenhouse effect is not a GHG dependent observed global radiative phenomenon.

In astrophysics textbooks the t_{APS} *effective (equivalent) planetary surface temperature* of the APS used to be defined by the SB law and the F_E effective available SW solar flux. t_{APS} may be expressed with different astronomical quantities, Ahren (2004) [11]:

$$t_{APS} = (L_0/(\pi\sigma))^{1/4}/(2d_E^{1/2}) = (E_0 A_{SUN}/(\pi\sigma))^{1/4}/(2d_E^{1/2}) = (F_E/\sigma)^{1/4} , \quad (7)$$

where L_0 is the solar *luminosity*, E_0 is the solar *surface emission*, d_E is the *semi-major axis of the Earth's orbit*, $A_{SUN} = 4\pi r_0^2$ is the *solar surface area*, and r_0 is the solar radius. The right side of (7) is the definition of t_{APS} by the F_E *effective available solar flux*, as it was given in (1). Using F_R one may also define the t_R *equivalent reflection temperature* by the SB law: $t_R = (F_R/\sigma)^{1/4}$. Similarly to the definitions of the climatological Δt_A, G_A , and g_A, the APS and reflection greenhouse parameters are:

$$\Delta t_{APS} = t_S - t_{APS}, \quad G_{APS} = \sigma t_S^4 - \sigma t_{APS}^4, \quad g_{APS} = G_{APS}/S_U , \quad (8)$$

and

$$\Delta t_R = t_S - t_R, \quad G_R = \sigma t_S^4 - \sigma t_R^4, \quad g_R = G_R/S_U . \quad (9)$$

The important fact is that t_A and G_A in (3,4) are constrained by the conservation principles of radiation energy and momentum, and by the SB law:

$$G_A = G_{APS} + F_R , t_A = (t_{APS}^4 - t_R^4)^{1/4} . \quad (10)$$

These constraints tell us that t_A is not a free parameter, but the sole function of F_0, and α_B. Based on (2) F_A and OLR^A must be equal, which implies the $F_A = OLR^A(S_U^A, \tau)$ functional relationship. Here τ is the *flux optical thickness* representing the all-sky LW absorption properties of a global average atmospheric air column, computed from the all-sky global average atmospheric structure. This quantity can only be accessed by extremely complex *radiative transfer* (RT) computations.

Since in definition (3) $t_S = (S_U / \sigma)^{1/4}$ is the ground surface radiative temperature, the assumed equilibrium relationship is:

$$F_A(F_0, \alpha_B) = OLR^A(S_U, \tau), \tag{11}$$

which obviously violates the (1,2) RE conditions. That is, keeping the left-hand side of (11) constant (no change in F_0 and α_B) the reduced OLR^A (due to increased GHG) cannot be restored to the original value simply by adjusting S_U, without adding thermal energy to the system (from somewhere). Remember, that the APS of a planet with condensing GHGs (clouds) is the sum of the clear and cloudy areas, which is a physically (and practically) identifiable mixture of solid and liquid surfaces. Applying definitions (3-5) for the whole planet, S_U must be the S_U^A (scaled to the TOA), and OLR^A must be the all-sky TOA LW radiation.

It is well known from mathematics that (11) type of equations hold only if the left and right sides are independent identical constants. The fate of the terrestrial greenhouse effect entirely depends on the existence of the long term radiative equilibrium state of the Earth. If the radiative equilibrium (independently of the GHG content) holds, then the GHG greenhouse effect does not exist, and definitions (3-5) are artifacts. Since the ground surface temperature is governed by CRE state of the planet, from the point of view of the CO_2 based AGW, the (3-5) GE parameters may be calculated, but they are useless, and physically meaningless quantities.

To determine Δt_A one needs to know t_S, F_0, α_B, and OLR^A. All these quantities can routinely be measured by ground based and satellite observing systems. The most quoted textbook data of t_S, F_0, α_B, and OLR^A are: 288 K, 1368 Wm^{-2}, 0.3, and 239 Wm^{-2}, subsequently, Schmidt et al. (2010) [12], Lacis et al. (2010) [13]. These numerical data show that the greenhouse temperature, and the flux density differences are about 33 K, and 151 Wm^{-2}. In this example the planetary RE condition is explicitly assumed, and no surprise that the imbalance at the TOA is close to zero.

There are several problems with the estimates above. It should be known that the assumed 288 K surface temperature is not an empirically measured quantity, but it is based on an international agreement dated back to 1924, (*International Commission for Air Navigation*, NOAA (1976) [14], therefore the real meaning of the 33 K is questionable. In fact, there is no standard, widely accepted definition of an empirically verified global mean surface temperature. Another serious mistake is the simultaneous use of t_A and OLR^A with t_S and ground surface upward flux S_U. Because of the permanent presence of the global average cloud cover, the radiation field of S_U and OLR^A are decoupled. Physically meaningful GHG GE may only be defined for clear-sky conditions, that is, GHG GE only exists over clear and above-cloud air columns, or perhaps above the whole APS, [10]. For the fluxes from the whole APS, (and similarly for t_{APS}), one cannot assign a definite physical altitude, but using the known source function profile, an effective altitude maybe attributed by the SB law.

The spectral aspects of the greenhouse effect are presented in Figure 2. In this simplified view the *Planck equivalent blackbody spectral flux densities* (EBFs) are plotted for the assumed 288 K surface temperature (green curve) and the 255 K SW absorption temperatures (red curve). Notice that in the wavenumber domain the areas under each curve are proportional with the spectrally integrated flux densities. The $\Delta t_A = 288 - 255 = 33$ K and $G_A = S_U - F_A = 151$ Wm^{-2} quantities are just arbitrary definitions used by the climatologists to indicate that the surface emits more IR radiation than the absorbed SW solar radiation. The light blue curve of the $G_{A,\nu}$ spectral greenhouse factor is the EBF at $t = (G_A / \sigma)^{1/4} = ((S_U - F_A) / \sigma)^{1/4} = 227$ K temperature.

According to the conservation of radiative energy the area under $G_{A,\nu}$ must be equal to the dark blue shaded area, that is, $\sigma t_s^4 - \sigma t_A^4 = G_A = \sigma t^4 = 151\,\mathrm{Wm^{-2}}$. Since $G_{A,\nu}$ does not depend on any GHG absorption, therefore the statement that the $\Delta t_A = 33\,\mathrm{K}$ is caused by the GHG absorption is not justified. The signatures of the spectral absorption of any GHG are not present in this figure. Although the maximum of the spectral greenhouse factor is close to the center of a strong CO_2 IR absorption band (black dot on the light blue curve), this figure does not have any useful information on the relationship between the surface temperature and the amount of the GHGs.

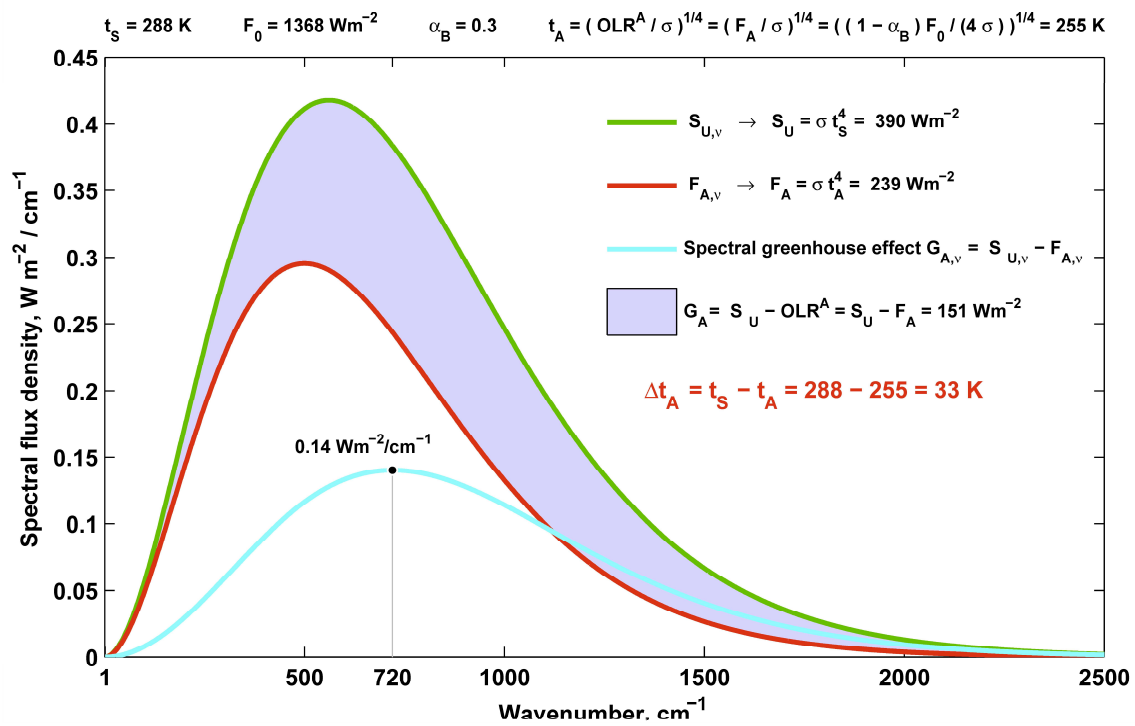

Figure 2: Spectral greenhouse effect. The curves are the Planck spectral flux density distributions belonging to the equivalent blackbody temperatures. In this view the ground surface is assumed to be perfectly black, $t_G = t_S$.

2.2 Violation of the energy conservation principle

Beside the empirical knowledge of the material composition of an average atmospheric structure, RT computation of the GE requires a theoretically founded functional relationship between the clear-sky S_U, OLR, and the amount of atmospheric GHGs. All of the different GHG column amounts must be explicitly and simultaneously involved in the computations of flux transmittance, absorption, and optical thickness of a semi-transparent global average air column.

Here we define some frequently used RT quantities and relationships. Trivially, $S_U = S_T + A_A$ where S_T and A_A are the transmitted and absorbed part of S_U. The flux transmittance T, flux absorption A, and flux optical thickness τ are defined as: $T = S_T / S_U$, $A = (S_U - S_T)/S_U$, and $\tau = -\ln(S_T / S_U)$. Further on, parameters referenced to the air column above an optional cloud-top are marked by an upper index 'c'.

In the classic radiative transfer and greenhouse effect literature a general $OLR(S_U,\tau)$ function for semi-transparent planetary atmospheres does not exist. The first published relationship of this kind appeared about 20 years ago in Miskolczi & Mlynczak (2004) [15]. Later it was shown with sufficient mathematical rigor that the clear-sky OLR and the surface upward LW radiation S_U in clear-sky radiative equilibrium are related by the next analytical equations:

$$OLR = S_U f(\tau) = S_U \frac{2}{1+\tau+\exp(-\tau)}, \tag{12}$$

where $f(\tau)$ is the newly introduced *transfer function* (and, by definition, $g(\tau)=1-f(\tau)$ is the *greenhouse function*), Miskolczi, (2007) [16]. The theoretical derivation of (12) was the missing link, which − through the transfer function and flux optical thickness − connects the surface temperature to the GHG content of the atmosphere. Here we should note, that in practice (12) is not a general requirement for an atmospheric air column. The instantaneous local or global mean atmospheric structures may or may not be in exact radiative balance. However, a realistic time-averaged structure should have a τ close to the planetary equilibrium value, which is the solution of the $OLR/S_U = f(\tau_E) = f_E$ equation. As an example, for the *global average TIGR2* (GAT) atmosphere (Scott (2009) [31]) : $\tau = 1.8691$, $\tau_E = 1.8602$, (they are close). For the *US Standard Atmosphere 1976* (USST76) atmosphere (NOAA, 1976 [14]): $\tau = 1.5092$ and $\tau_E = 1.8672$, and, evidently, the USST76 structure *is badly out of radiative balance*, and should not be used in radiative budget studies. Similarly to (12), the radiative equilibrium requirement above the cloud top is:

$$OLR^C = S_U^C f^C(\tau^C) = S_U^C \frac{2}{1+\tau^C+\exp(-\tau^C)}, \tag{13}$$

where S_U^C is the upward flux from the cloud top, τ^C is the flux optical thickness of the air column above the cloud top. While (12) is closely satisfied for the clear-sky portion of the atmosphere, (13) does not hold, indicating that the radiative structure above the cloud top is affected by other dynamical processes. In particular, instead of (13) the $OLR - OLR^C = A_A - E_D$ equation holds, where A_A is the absorbed isotropic surface upward flux and E_D is the anisotropic downward flux from the clear atmosphere. For more details on the theoretical RT functions see paragraph *3.3*. We shall see later, that the radiative equilibrium condition above the cloud top may be expressed by the $OLR^C = E_D^C$ relationship, where E_D^C is the atmospheric downward flux density arriving at the cloud top. As we have already mentioned, in the stochastic dissipative climate system locally and regionally the RE is not a constraint, τ and S_U in (12) can take any value. However, for an isolated planet, and on global scale the radiative equilibrium is a strict constraint. For planets with partial cloud cover − instead of (11) − the correct relationship between OLR^A and F_A must have the functional form of

$$OLR^A(\tau, S_U, \beta, S_U^C) = F_A(F_0, \alpha_B), \tag{14}$$

where β is the cloud cover, $S_U^C = S_U^C(h^C)$ is the upward flux density from the cloud top, and h^C is the equilibrium cloud top altitude. Evidently α_B will also depend on the cloud cover and cloud altitude: $\alpha_B = \alpha_B(\beta, h^C)$. Shortly, the practical derivation of the equilibrium cloud cover is based on the empirical fact that the clear air column above a characteristic h^C is in a special dynamical equilibrium which assures the $OLR^C = E_D^C$ equality (black circle, shown in Figure 6). The cloud top at this altitude is in thermal and radiative equilibrium with the local source function. More detail is given in paragraph *4.4*, or in Miskolczi (2014) [17].

The principle of the conservation of the radiant energy dictates that the true all-sky TOA OLR^A must be a strictly linear function of the cloud cover, it has to be the weighted sum of the clear-sky OLR and cloudy sky OLR^C by the fractional clear and cloudy areas of the APS:

$$OLR^A = sc((1-\beta)OLR + \beta OLR^C, \tag{15}$$

where sc is a spherical correction factor, necessary for the conversion of the fluxes from any reference altitude to TOA fluxes. Similar equation holds for the upward flux from the APS:

$$S_U^A = sc((1-\beta)S_U + \beta S_U^C. \tag{16}$$

From (16) immediately follows the analytical relationship between the t_S ground surface radiative temperature, and the F_0, sc, β, and S_U^C parameters:

$$t_S = ((F_0/(4sc) - \beta S_U^C)/(1-\beta)/\sigma)^{1/4}. \tag{17}$$

Obviously t_S in (17) does not depend directly on any amount of non-condensing GHGs. In a two-level radiating system (cloud-free surface and cloud top) the Δt_A, G_A, and g_A can never be directly associated with the GHG content of the atmosphere. So far GE theories are not capable to predict a-priori the observed equilibrium t_S. The reason is that the definition (3) completely ignores the radiative effect of the cloud cover, and consequently, the radiative constraint on dependence of S_U^C on the GHGs cannot be asked. Ignoring the radiative balance requirements represented by (12-17), discussion on the GE and the related global climate change does not have much merit. Without any theoretical or experimental proofs, in the GE literature Δt_A is simply attributed to the absorption and re-emission of the surface upward radiation by the IR active atmospheric gases. In 1896 Svante Arrhenius put forward the question:

"*Is the mean temperature of the ground in any way influenced by the presence of heat-absorbing gases in the atmosphere?*",

and he tried to quantify the effect of the CO_2 and associate it with the ice-ages in the planetary climate history, Arrhenius (1896) [18]. The official − *Intergovernmental Panel on Climate Change* (IPCC) approved − CO_2 greenhouse effect hypothesis states that:

increasing CO_2 content of the atmosphere will increase the absorbed upwelling LW radiation from the surface, will reduce the outgoing LW radiation, and will increase the downward LW radiation received by the surface. As a result, the surface will warm up until the top of the atmosphere radiative balance is restored,

Pierrehumbert (2011) [19], Lindzen (2007) [20], Nurse & Cicerone (2014) [21], Smith (2008) [22]. Of course, this is not a greenhouse theory but an unproven hypothesis which poses deliberate constraint on the atmospheric response to increased GHG content.

The key information badly missing here are the theoretical radiation laws governing the radiation climate and the long time theoretical and empirical RE state of the atmosphere. To talk about planetary GE is not smart without having the slightest idea of both the governing theoretical con-straints, and the quasi-static equilibrium state of the system. In this article we shall not waste the time to critically evaluate the tons of supporting literature of the (climate model based) AGW theory, we shall quote only some (frequently referenced) representative examples from the well-known, world famous radiative transfer giants mentioned above.

Climate modelers generally assume a hypothetical positive feedback process which amplifies the initial warming: higher surface and atmospheric temperatures will increase the water vapor content of the atmosphere, and the increased water vapor absorption will further increase the warming effect.

Since the magnitude and quantitative constraint of this effect is unknown, *global climate models* (GCMs) are stabilized with diverse ad-hoc H_2O feedback parameterizations, aimed to fit model outputs to some expected climate scenarios, to real world empirical data, or just to set a desired (acceptable) GHG climate sensitivity.

The unphysical assumption of positive feedback (known as the Simpson paradox) stems from the Schwarzschild solution of the RE state in stellar atmospheres, which predicts unconstrained temperature grows with increasing optical depth, see for example Schwarzschild (1906) [23] (page 28, equation 11), or in the semi-gray treatment of the runaway GE in Shaviv (2012) [37]. The Schwarzschild solution also predicts a large (never observed) surface temperature jump at the lower boundary, and at the small optical thickness limit it violates the law of conservation of radiant energy (an airless planet should have a surface radiative temperature equal to the temperature of the APS).

3. Quantitative validation of the CO_2 greenhouse effect

There is an on-going debate on the origin and the cause of the increase in the atmospheric CO_2 concentration shown in Figure 1. Several publications suggesting that most of the sources of the atmospheric CO_2 are unrelated to human activity, Harde (2019) [62]; Berry (2021) [63]. Recent estimate of the man-made contribution to the observed ~35 % changes is only about 6 %, Poyet (2022) [24]. From our point of view this problem is irrelevant, and in fact we try to focus on the real problem of establishing the theoretical relationships between the atmospheric GHG content and the surface radiative temperature. It is not our purpose discuss the GE definition of (3) and the pretty much useless $\Delta t_A \approx 33$ K temperature difference. To properly attribute the increase of GHGs to the AGW hypothesis one needs a sound physical theory, and one has to relay on relevant empirical facts for validation.

3.1. The global mean picture

The practical approach to the validation effort is to collect long term geographically diverse global radiosonde data sets containing information about the state of the surface and the atmosphere and perform high quality radiative transfer computations to obtain the true long time global average radiative structure of the system. Once the reliable global mean flux density components of the system are known, then the simple task is to compare the global mean observed surface temperature to the predicted one by the RT theory, that is, by validating the key parameters (t_S, F_0, sc, β, and S_U^C) in (17).

The first obvious requirement to conduct such studies are the availability of global scale primary radiosonde observations. Readily available sources of the vertical temperature, water vapor and ozone structures are the world climate data centers and the national meteorological data archives. In our validation efforts we frequently used the following radiosonde data sets: two archives − known as TIGR2 and TIGR2000 sets − of global radiosonde observations between 1976 and 1989, Scott (2009) [31]; 61 annual global mean soundings for years 1948-2008 from the NOAA-R1 archive *National Oceanic and Atmospheric Administration* (NOAA) NCEP (2012) [32]; one full year of high resolution (6 second) morning and evening soundings from the former NOAA *testing facility in Sterling Virginia* (NOAA-S). Several simulations were also performed for the different versions of the USST76 atmosphere, and for some research grade (1 second) soundings from special locations and purposes. Raw radiosonde observations in their original structures are not suitable for direct radiative transfer computations. They must be cleaned of any thermodynamical inconsistencies, sensor errors, and the altitude levels should be optimized for the purpose of the particular applications. In Figure 3 a radiosonde observation from Barrow (Alaska) is shown with cleaned and re-layered structure needed for flux density computations.

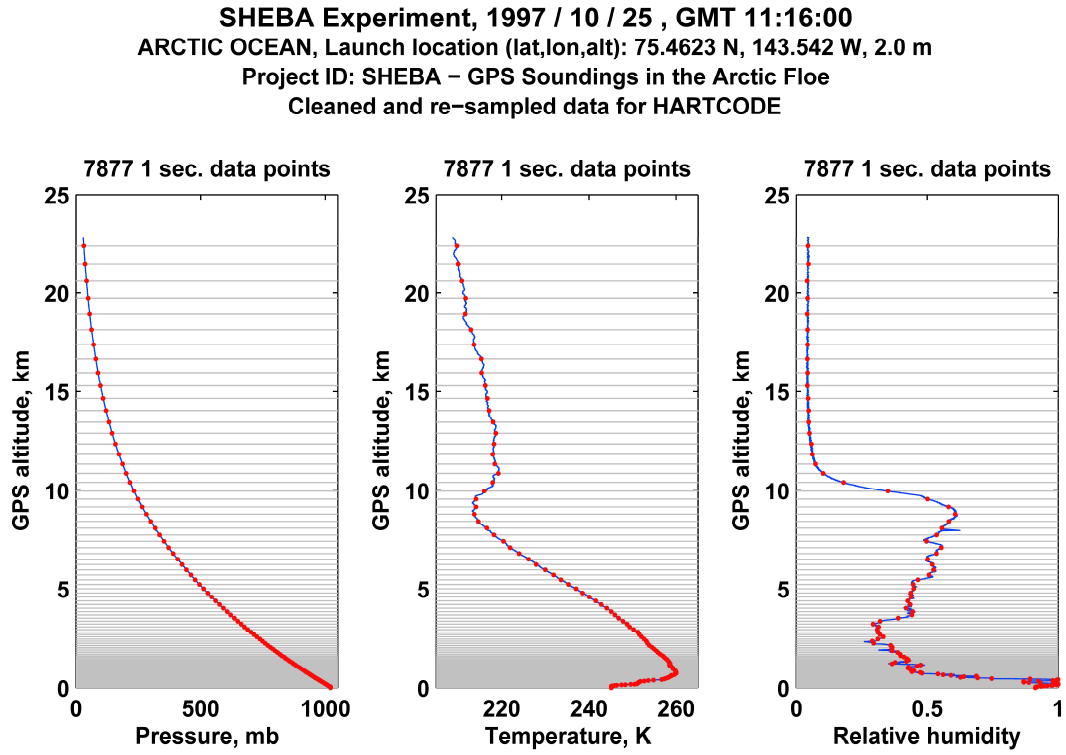

Figure 3: Radiosonde observation taken at Barrow (Alaska). The raw data has to be re-shaped to make it suitable for RT computations. The 140 exponentially spaced gray lines are the levels where the RT code computes the upward and downward fluxes. Between the lines the atmosphere assumed to be homogeneous.

In Figure 4 comparisons of the thermal and water vapor structures of the GAT [31], and the USST76 atmospheres are presented. Both of them are frequently used in radiative budget studies. Compared to the USST76 atmosphere the significant differences in the vertical temperature and H_2O structures are obvious. It is not shown here, but the GAT vertical ozone structure and the global mean column amount of ozone are also different, the USST76 ozone amount is about 10 % higher.

Notice that the USST76 tropospheric lapse rate is much higher, the isothermal stratosphere does not exist, and the H_2O column amount is about half of the global average. Unfortunately, on the top of the inherent uncertainties, global climatological data sets are also subject to deliberate data manipulations, therefore extreme care is needed to identify a suitable clean archive.

The second obvious requirement is adequate high quality RT software. It must be quite clear that the accuracy of a research *line-by-line* (LBL) RT code should not be restricted by speed requirements, vertical resolution, or absorption band selections common in radiative transfer modules in climate models. Our choice was the *High-resolution Atmospheric Radiative Transfer Code* (HARTCODE) which was explicitly developed for extreme numerical accuracy, Miskolczi (1989) [25], Rizzi et al. (2002) [26].

Test computations show that HARTCODE adequately responds to extremely small changes of the most important input parameters, for example, 1.0 ppm increase in the CO_2 volume mixing ratio, Miskolczi (2010) [27]. Routine comparisons of RT codes from different authors and their empirical validations may be found in Kratz et al. (2005) [28], and Saunders et al. (2007) [29].

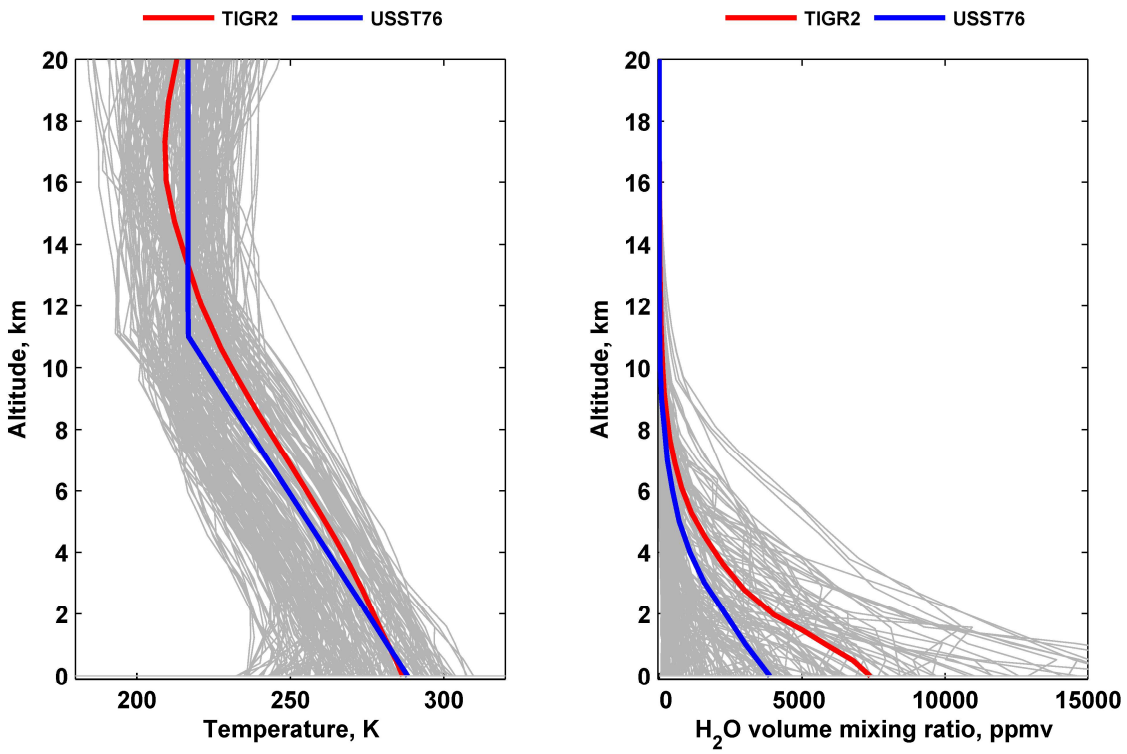

Figure 4: Comparisons of the vertical thermal and humidity profiles of the global average TIGR2 (GAT) and theUSST76 atmospheres. Thin gray lines are the individual radiosonde data as it was observed by the TIGR2 global radiosonde archive. One has to notice the significant differences between the averages in both the thermal and humidity profiles (blue and red lines). Such differences adversely affect the flux density simulations.

Further unique features of HARTCODE are the strict preservation of the monochromatic Beer-Lambert law, the Helmholtz reciprocity principle, and the spherical refractive computation of the directional transmittances through every optical path segment. The spectroscopic details of the IR flux transmittance and optical depth computations are presented in Miskolczi (2011) [30], and in [17].

Befor using an RT software designed for directional radiance computations several other test requirements shoud be met. Such requirements are routinly checked through international validation campaigns. The ultimate test is the empirical proof, that under controlled experiments the simulated directional spectral radiances agree with satellite and ground based observations.

The Helmholtz reciprocity principle is demonstrated for vertical and horizontal viewing geometries in Figure 5. It is essential to observe this principle when computing hemispheric transmittances from directional path transmittances. Any RT code is supposed to be able to compute the same directional path transmittance for the reverse trajectory (independently of the viewing geometry).

3.2. Flux density components

To gain knowledge of the radiative structure of the atmosphere first, we need to compute the vertical distribution of all the upward and downward flux density components of a cloud-free air column for altitudes of sufficient vertical resolution.

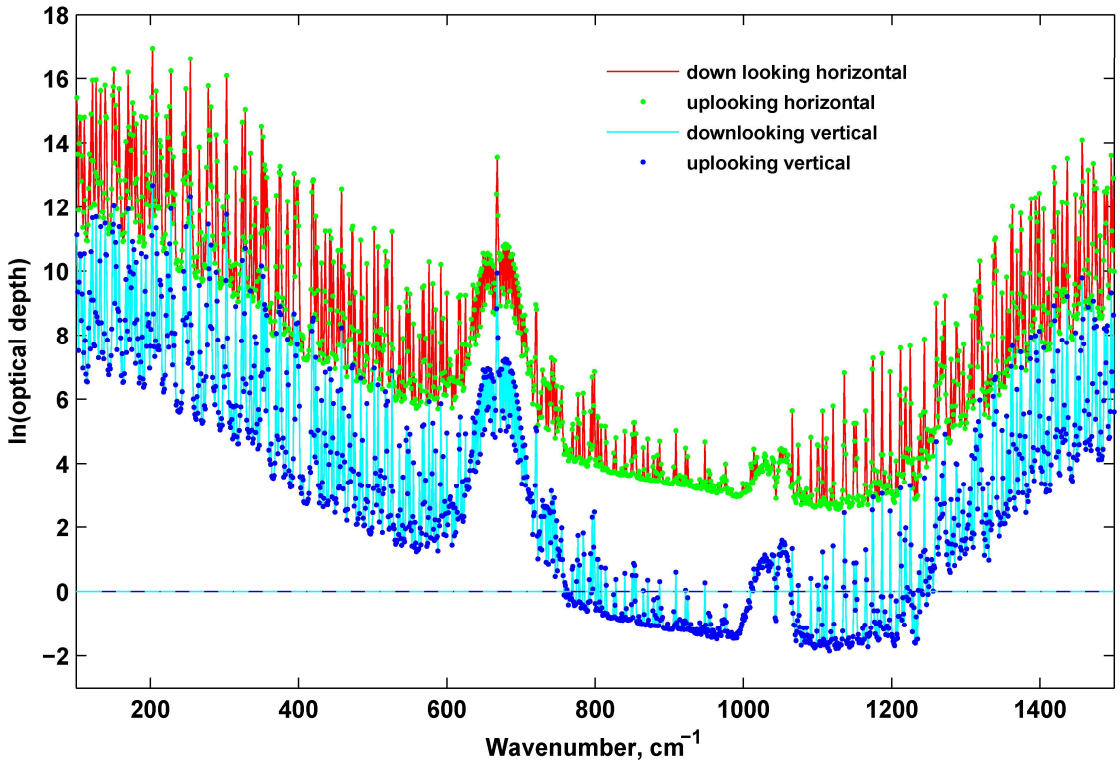

Figure 5: Helmholtz reciprocity principle requires the equal line of sight optical thickness (and path transmittance) for every slanted atmospheric optical paths. In this test vertical and horizontal viewing were considered. High resolution HARTCODE spectral optical thickness computations perfectly reproduce the principle. Note that the Helmholtz principle is not valid for spherically integrated (hemispheric) flux optical thickness.

In vertically inhomogeneous atmosphere showing cylindrical symmetry flux density computations at any altitude (depending on the vertical discretization shown in Figure 3) require angular integration of the path radiances over both the upper and lower hemispheres, and also the altitude integration (both upward and downward direction) of the parts of the atmosphere above and below the given altitudes.

Such computations are presented for the GAT atmospheric structure in Figure 6. Here it is assumed, that at any z altitude a solid or liquid surface discontinuity (cloud layer) is present, emitting isotropic radiation according to the local source function (pink line). The continuous lines are the upward and downward boundary fluxes from the regions bounded by z km and $z_{TOP}=70$ km, (these fluxes are marked in black letters in the legend). The dashed lines are the upward and downward boundary fluxes from the regions bounded by $z=0$ km and z km (these fluxes are marked in red letters at the top of the figure). The upper thin (light blue) horizontal line indicates the altitude where the source function $S_U(z)$ (pink curve) is equal to the $OLR(z)$ (black curve). The lower horizontal line indicates the altitude where $E_U(\mathrm{z})$ and $E_D(z)$ are equal. The small black circle at about $h^C=1.92$ km altitude marks the interception of the $OLR(z)$ and $E_D(z)$ functions where $OLR(h^C)=E_D(h^C)$. At this h^C the global average cloud cover could be in radiative equilibrium with the OLR^C, and in thermal equilibrium with the local source function S_U^C. Of course, the accurate h^C cannot be determined graphically from this figure. In section *4.4* the quantitative procedure of the computation of the accurate h^C, α_B, and S_U^C is discussed.

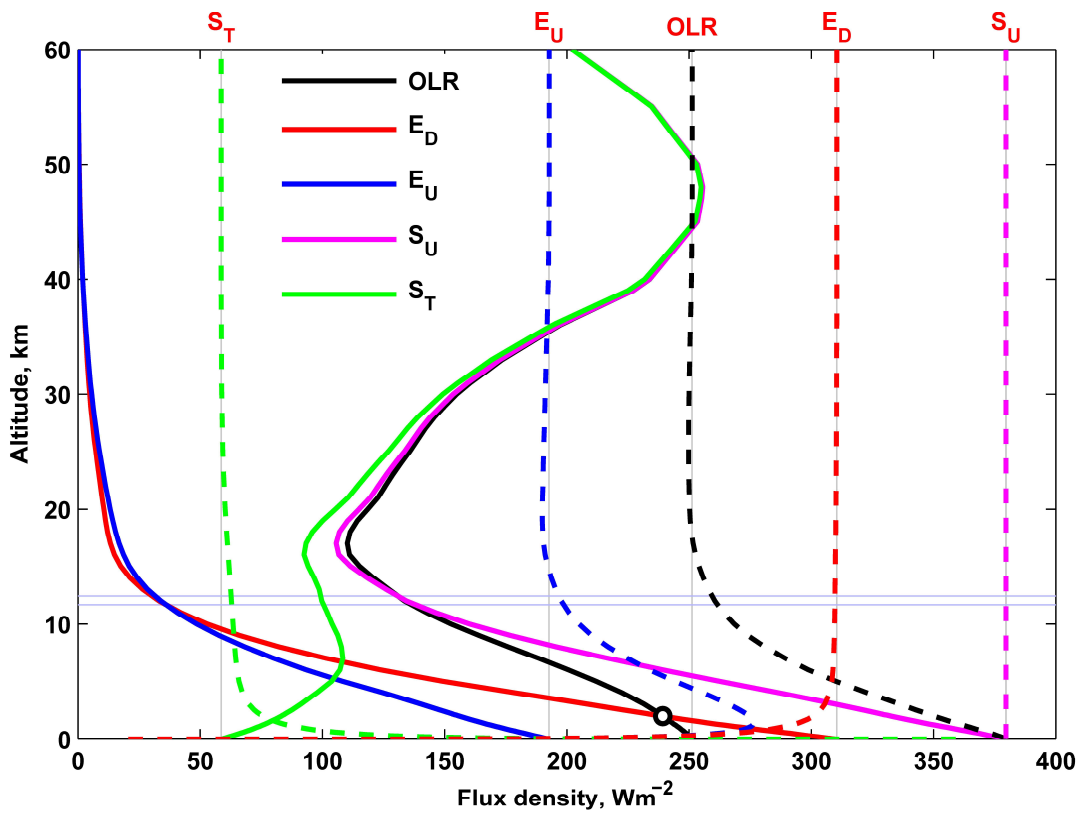

Figure 6: Layer boundary fluxes for the GAT atmosphere. Solid lines are the cumulative upward and downward layer contributions from the regions bounded by the TOA and a given altitude z. Dashed lines are the cumulative layer contributions from the regions bounded by the surface and a given altitude z .

There are many other interceptions of the flux curves which may increase the degree of freedom of the system's response to establish its overall radiative equilibrium. The numerical details of the (surface referenced) flux components of the whole clear air column and the two segments of the same air column divided by the h^C altitude is shown in Figure 7. This figure shows the very first result which revealed some numerical relationships relevant to the global average radiative flux and cloud structure. At h^C altitude the source function is $S_U^C = S_U(h^C) = 333.82\ \mathrm{Wm^{-2}}$ and a global average cloud layer at this altitude should be in radiative equilibrium with $E_D^C = OLR^C = 240.142\ \mathrm{Wm^{-2}}$. It is also shown, that the A_A^C absorbed part of S_U^C (in the blue region) can only leave the system as the clear-sky OLR.

Radiosonde observations show that $t_S = 286.06\ \mathrm{K}$ and the physically meaningful (surface referenced) Δt clear-sky greenhouse effect and the G greenhouse factor are: $\Delta t = 27.9\ \mathrm{K}$, and $G = S_U - OLR = 127.9\ \mathrm{Wm^{-2}}$. The greenhouse effect over the cloud cover is somewhat smaller: $\Delta t^C = 21.89\ \mathrm{K}$, and $G^C = S_U^C - OLR^C = 93.68\ \mathrm{Wm^{-2}}$.

We have seen that the average planetary radiation climate − as a set of scalar climate radiation parameters − assumes an extensive *global average cloud cover* β, at a characteristic *global average cloud altitude* h^C, which breaks up the planetary radiation field into three (not necessarily continuous) major regions.

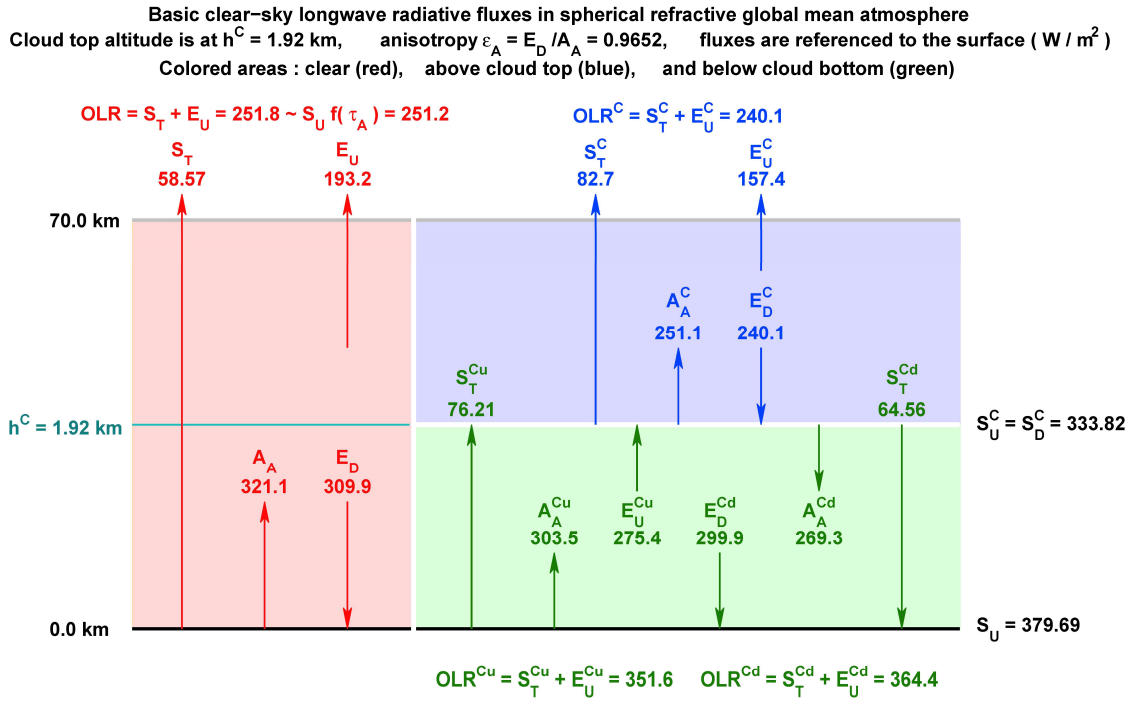

Figure 7: Boundary upward and downward fluxes in the whole average clear air column (red), in the above $h^C = 1.92$ km altitude (blue) and in the below h^C (green) vertical regions. Without the accurate knowledge of the cloud cover the full global mean radiative structure cannot be established.

In Figure 8 the SW and IR as well as the clear and cloudy flux density components are summarized. Here the definitions and the flux density components of interest are displayed together with their numerical value in $\mathrm{Wm^{-2}}$. This figure is based on Figure 7, but here the flux density components are weighted with the cloud cover, and the LW TOA fluxes are referenced to 70 km. altitude. (For example to obtain correct clear-sky transmitted LW flux at the TOA the S_T in Figure 7 must be multiplied by the $(1-\beta)$ clear-sky fraction and the sc spherical correction: $58.57(1-0.6618)0.9789 = 19.39\ \mathrm{Wm^{-2}}$.)

The SW components (F_0 and F_E) are in the top line. In the second line F_E is partitioned by the Bond albedo into F_A absorbed, and F_R reflected parts. In the third line they are further partitioned to clear (F and R) and cloudy (F^C and R^C) components. Remember, that the Bond albedo is not the true reflection properties of the sunlit side of the planet, but – as the ratio of the reflected and absorbed parts of the incoming SW radiation – it is the characteristic of the planetary radiation budget. For further partition of the reflected components into surface and atmospheric origin one must deal with the diurnal cycle and multiple scattering problems, which is not an easy task, and for our purpose it is not needed. After depositing the momentum in the system anywhere, eventually, all scattered SW radiation will leave the system. GE by definition is a LW radiative phenomenon, and more important for us the knowledge of the accurate IR flux density components, which can be directly related to the surface temperature and the TOA net LW flux. It should be emphasized, that this view is not a kind of simplified model, the LW flux density arrows are real global mean fluxes of the GAT atmosphere, they were derived by LBL simulations using first principles, *without any assumptions on the thermal structure and the radiation field*. Even the choices of β and h^C were based on empirical facts shown in Figure 6.

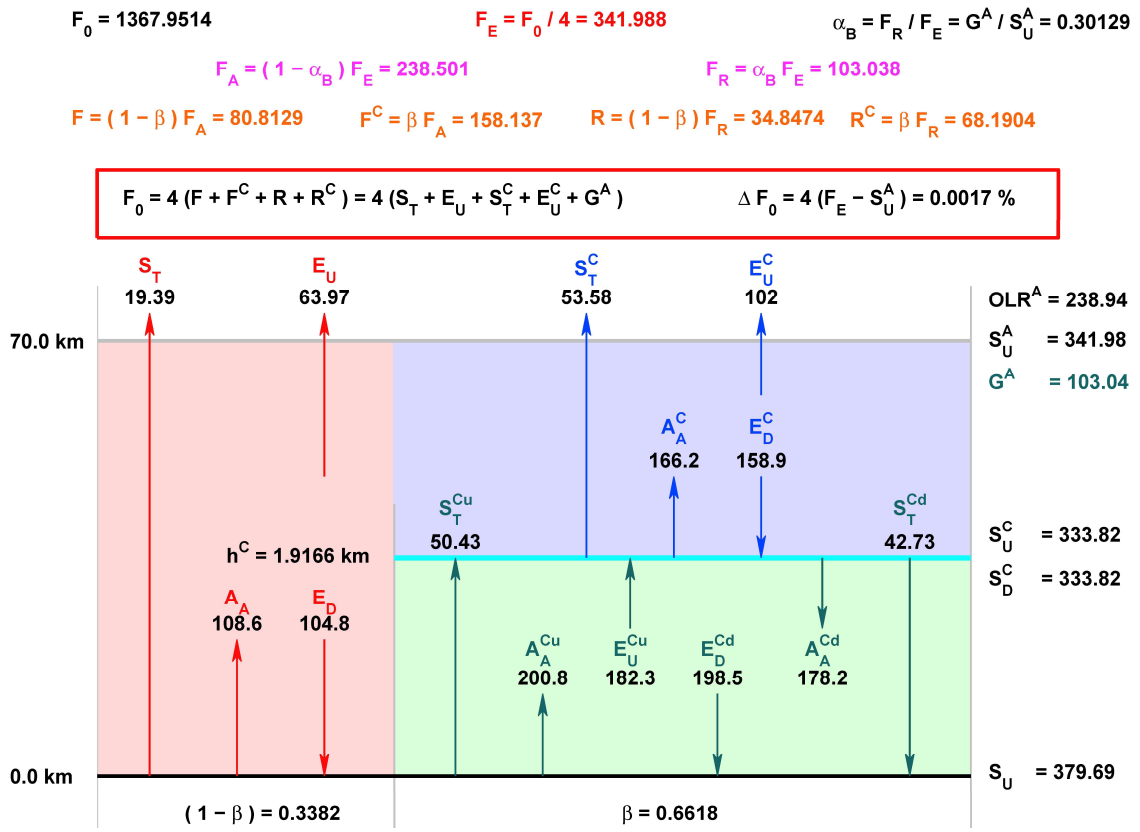

Figure 8: All-sky SW and LW radiative flux components (Wm^{-2}). The red, blue and green regions represent the sum of the clear, above cloud and below cloud portions (spherical shell sectors) of the atmosphere. The equations in the middle show that the F_0 solar constant obtained from the SW and LW flux components agree, therefore the Chandrasekhar-type radiative equilibrium state of the planet is empirically proven.

The IR flux density components are in and around the colored areas at the lower part of the figure. TOA fluxes are referenced to $z_{TOP} = 70$ km altitude; all other fluxes are referenced to the ground surface. The flux absorption of an air column between 70 and 120 km altitudes is less than 0.0005, therefore the flux density contribution from above 70 km is negligible. The numerical accuracy of the flux density components are five significant digits.

The downward upper boundary fluxes at the clear, and above cloud regions are zero. As it was already mentioned, surface fluxes may be referenced to the TOA by applying a spherical correction: $sc = R_E^2 / (R_E + z_{TOP})^2$, where $R_E = 6371 \times 10^3$ m is the volumetric radius of the Earth. Due to refraction, the accurate computation of sc is far more complex and results in an $sc = 0.978918$ (0.0547 % larger) value, which corresponds to an effective altitude of ~ 68.236 km.

In cloud-free areas the ground surface (having a global average radiative temperature t_S) and the semi-transparent atmosphere (with an average GHG and thermal structure) above can directly and freely cool to space. The same is true above an average planetary cloud cover, but with different lower boundary conditions.

The cloud top and cloud bottom altitudes are stochastic variables, the global means of them were set to the same 1.9166 km altitude. Of course, this does not mean that the average cloud cover has zero geometrical thickness.

Remember, the combined lower boundaries of the red and blue areas constitute the APS. From the green area (below the cloud cover) the IR radiation cannot escape (to the atmosphere above the cloud cover, or to the space), and cannot contribute directly to the planetary RE.

Among the flux density components the following trivial relationships must hold (by definitions): $OLR = S_T + E_U$, $OLR^C = S_T^C + E_U^C$, $OLR^{Cu} = S_T^{Cu} + E_U^{Cu}$, and $OLR^{Cd} = S_T^{Cd} + E_U^{Cd}$. Here OLR is the clear sky, OLR^C is the cloudy sky, OLR^{Cu} and OLR^{Cd} are the upward and downward LW boundary fluxes below the cloud layer, respectively.

The *equilibrium equation* (in a red box in the middle of Figure 8) shows that the CRE state of the planet holds, the relative difference of F_0 from the SW and LW components is $\Delta F_0 = 0.0017\,\%$. The TOA flux difference between the SW F_E and the LW $OLR^A + G_E = S_U^A$ (planetary net flux) is 0.00584 Wm^{-2}, indicating that the combined effect of all the computationally ignored planetary thermal flux contributions from non-radiative origin has to be very small indeed. It appears, that the net non-radiative power dissipation in the system is compensated within the system and has no long term observable effect on the planetary radiative equilibrium state of the Earth.

According to the long-term steady state requirement there cannot be any accumulating direct radiant energy in any of the three regions, however, unlimited transfers of thermal energy to-and-from the global latent heat reservoirs are permitted (as it happens in the real environment through the phase boundaries).

The most important conclusion of our computations is the solid empirical proof of the existence of the assumed steady state planetary RE. In Figure 8 the key planetary IR fluxes from the APS are:

$$OLR^A = sc((1-\beta)(S_T + E_U) + \beta)(S_T^C + E_U^C)) = 238.94\ \mathrm{Wm^{-2}}, \tag{18}$$

and

$$S_U^A = sc(S_U(1-\beta) + S_U^C\beta) = 341.98\ \mathrm{Wm^{-2}}. \tag{19}$$

The APS-referenced greenhouse factor is just equal to the all-sky reflected SW flux density $G^A = S_U^A - OLR^A = F_R = 103.04\ \mathrm{Wm^{-2}}$. The astrophysical textbook value for the radiative temperature of the APS (see [11]) $t_{APS} = (16\pi\sigma d_E^2 / L_0)^{-1/4} = 278.68\ \mathrm{K}$ is in perfect agreement with simulated mean all-sky surface temperature of $t_{APS}^S = (S_U^A / \sigma)^{1/4} = 278.68\ \mathrm{K}$ from (19). Here $L_0 = 3.847\times10^{26}$ J/s is the solar luminosity, $d_E = 1.4959789\times10^{11}$ m is the semi-major axis of the Earth's orbit, NASA (2012) [47], and $r_0 = 6.96\times10^8$ m is the solar radius, NASA (2012) [46].

For further consistency check, from the fluxes from (18) and (19) the simulated β^S cloud cover, α_B^S Bond albedo, and F_0^S solar constant were computed and compared, showing reasonably good agreement:

$$\beta^S = \frac{S_U^A / sc - S_U}{S_U^C - S_U} = 0.6615, \tag{20a}$$

$$\alpha_B^S = 1 - \frac{OLR^A}{S_U^A} = 0.3013, \tag{20b}$$

$$F_0^S = 4S_U^A = 1367.93. \tag{20c}$$

3.3. Radiative transfer functions and flux optical thickness

Radiative transfer functions (RTFs)are simple algebraic functions of the flux optical thickness of a semi-transparent planetary atmosphere. In section *2.2* we have already defined the flux optical thickness as $\tau = -\ln(S_T / S_U)$. One can see that the transmission, absorption, transfer and greenhouse functions are explicit functions of this τ. In Figure 9 the fundamental radiative transfer functions and the normalized upward atmospheric emissions $E = E_U / S_U$ for about a thousand weather balloon observations are displayed. The black dots in the yellow-shaded area are clear indication of theoretical constraints exposed by the RT functions. The light grey vertical line is the *annual global average* τ of all the data points.

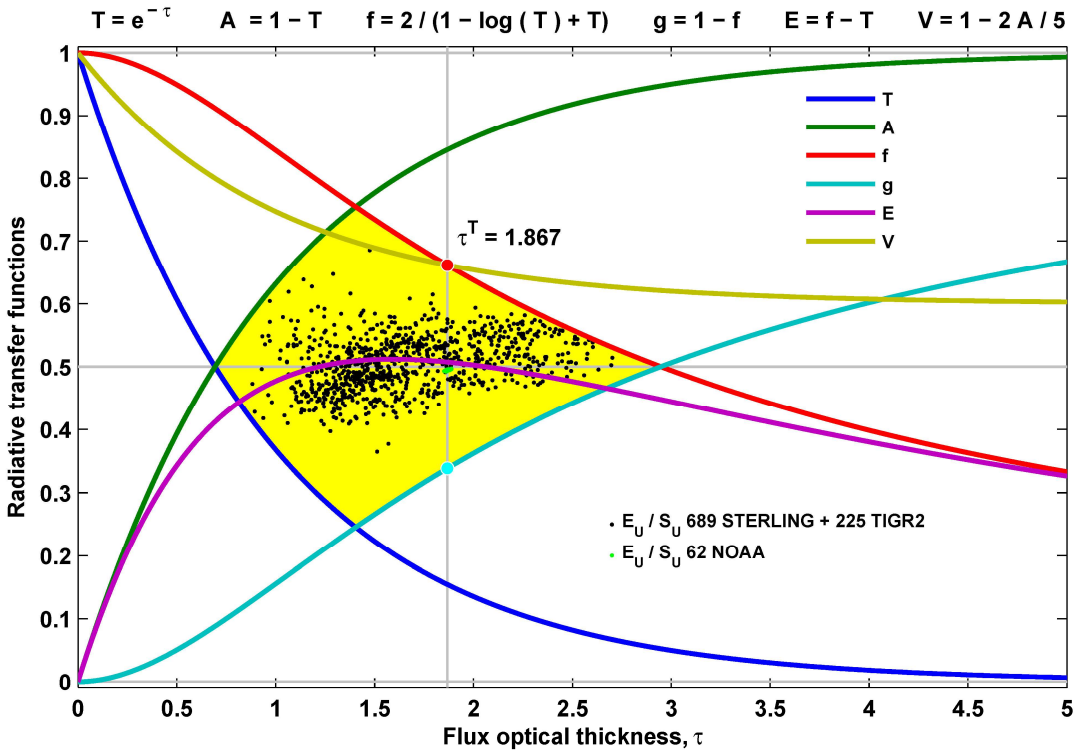

Figure 9: Basic radiative transfer functions. T, A, f, g, E, *and* V *are the transmission, absorption, transfer, greenhouse, emission and virial functions respectively. By definition, the clear-sky* T *and* τ *of an air column are:* $T = S_T / S_U = \exp(-\tau)$ *and* $\tau = -\ln(T)$.

From extended flux density simulations (using diverse radiosonde data) we gained enough confidence to conclude that the Earth's long time global mean flux optical thickness is equal to a theoretically predictable mathematical constant $\tau^T : \tau = \tau^T = 1.86756$. The theoretical τ^T may be computed either from the $f(\tau^T) = V(\tau^T)$ (red dot) or from the $g(\tau^T) = 2A(\tau^T)/5$ (light blue dot) transcendental equations.

The definition of the $V(\tau)$ virial function: $V(\tau) = 1 - 2A(\tau)/5$. This theoretical function takes care of two theoretical requirements (they are empirical facts as well). One is the $S_U = 2E_U$ equality (stems from the Clausius virial theorem), and the other is the constraint known as the transparent limit (without atmosphere *OLR* must be equal to S_U).

In the Earth's atmosphere the theoretical equilibrium optical thickness is the natural constraint on the equilibrium mass of the WV in the atmosphere (the WV column amount in precipitable cm). The average τ of the NOAA-R1 annual global means (green dots) and τ of the GAT atmosphere are equal to τ^T.

The stability of the planetary radiation climate is controlled by the derivatives of T, f, g, E, and V functions: $dT/d\tau = -T$, $df/d\tau = -f^2 A/2$, $dE/d\tau = -f^2 A/2 + T$, $dV/d\tau = -2T/5$. Notice that all the signs of the derivatives are negative, implying a strong tendency of the system to return to its equilibrium state (Braun-LeChatelier principle). Considering the permanent changes of the state of the H_2O in the system it is anticipated that the RE state of the atmosphere will also be affected by dynamical processes related to the condensation and evaporation, permanently present in a global average air column. Our explicit definition of the $_D\tau$ dynamical optical thick-ness is: $E\ OLR\ \tau\ \tau = +\ 1\ 2\ (\ )/\ _D\ _U\ _D$. Remember, condensation will reduce, evaporation will increase $_D\tau$, and what actually happens will depend on the sign of the $_D\tau\ \tau$– difference. Unfortunately, in this article we cannot discuss further interesting and important theoretical questions related to the changes in $_D\tau$.

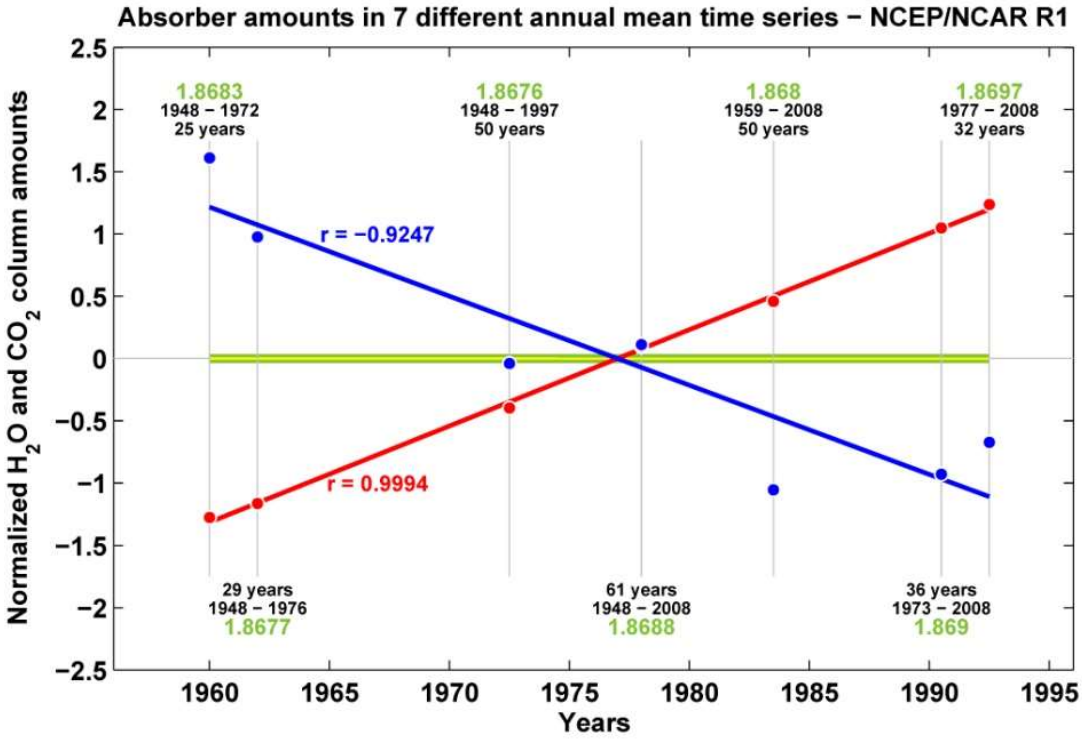

Figure 10: Changes of H_2O (blue) and CO_2 (red) column amounts in 7 different time series. Atmospheric structures are from the NOAA-R1 radiosonde archive. The green and yellow trend lines (deviations from the sample mean and deviations from the τ^T theoretical value show no tendency.

In Figure 10 the constancy of the IR flux optical thickness (light green numbers) is maintained in each randomly selected subset of different length from a 61-year long NOAA-R1 time series. Here the CO_2 (red line) and H_2O (blue line) normalized column amounts are plotted for the 1948-2008-time interval. The sign of the H_2Ocorrelation coefficient (blue number) is a clear indication of the climate stabilizing role of the water vapor. The increase of the atmospheric carbon dioxide is apparently coupled with the decrease of the atmospheric water vapor column amount. The time-averaged CO_2 column amounts − unlike concentrations − increase linearly.

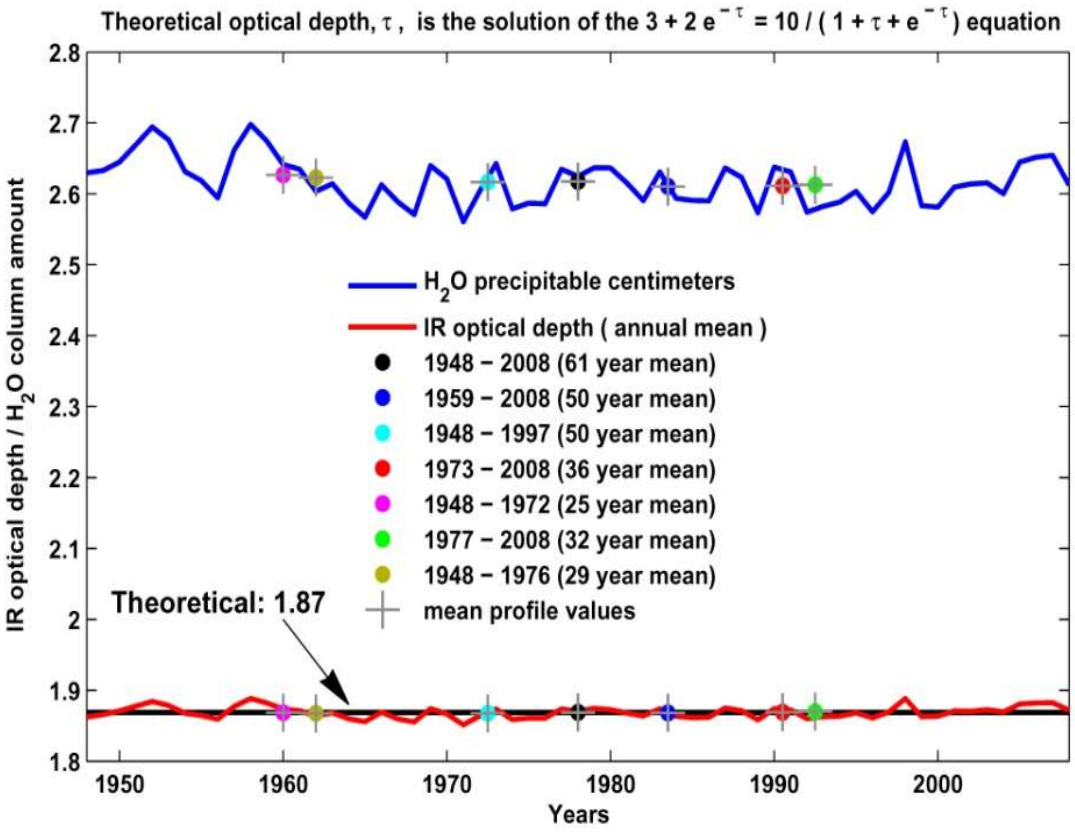

Figure 11: The constancy of the annual mean flux optical thickness in 7-time series of different length (NOAA-R1 radiosonde archive). H_2O column amounts are in prcm.

Time period	Centre	Years	Altitude	Temperature	H_2O	CO_2	Tau
1948–2008	1978	61	0.7931	0.8183	−0.2841	0.9839	0.06488
1959–2008	1983.5	50	0.8059	0.8349	0.04499	0.9937	0.2976
1948–1997	1972.5	50	0.6621	0.6625	−0.4843	0.9827	−0.2284
1973–2008	1990.5	36	0.6947	0.7987	0.1148	0.9974	0.3491
1948–1972	1960	25	−0.005748	0.1731	−0.5907	0.983	−0.4184
1977–2008	1992.5	32	0.58	0.7424	0.03992	0.9973	0.267
1948–1976	1962	29	0.001769	0.0584	−0.6048	0.9804	−0.4396

Figure 12: Trend line correlation summary of seven NOAA-R1 time series. The last five columns on the right are linear regression coefficients for the top altitude of the air column, surface temperature, water vapor and carbon dioxide column amounts, and the flux optical thickness. The IR flux optical thickness has no correlation with time and the strong signal of increasing atmospheric CO_2 content in any time series is not present in the IR flux optical thickness data. Consequently, the atmospheric CO_2 increase cannot be the reason of global warming.

In Figure 11 the changes in the flux optical thicknesses and the H_2O column amounts are also demonstrated. Notice that the random fluctuation in the IR optical thickness (red line) correlate well with the H_2O column amounts (blue line). Again, the constancy of the flux optical thickness is coupled with the constancy of the water vapor content of the air column. The sample means (colored dots) are practically equal to the mean profile values (+ gray symbols) which is an indication that a single column average atmospheric structure can safely be used instead of the global average fluxes from a large data set.

Detailed numerical data of the regression analysis of the key variables − altitude, temperature, H_2O, CO_2, and flux optical thickness − are given in Figure 12. According to Figures 10, 11, and 12 the long-term global mean OLR and S_U cannot change independently, they are linked analytically to the changes in the flux optical thickness by (12) .

The IR flux optical depth has no correlation with time and the strong signal of increasing atmospheric CO_2 content in any time series is not present in the IR flux optical thickness data. Consequently, the atmospheric CO_2 increase cannot be the reason for global warming. It is interesting to note, that in the individual time series the H_2O does not correlate with the time, while in the mean values the negative correlation is quite obvious (in Figure 10).

Based on the NOAA-R1 soundings and simulations Figure 13 shows the no-feedback response and the true observed changes of the OLR in the 200-1500 cm^{-1} spectral range. The real atmosphere does not follow the GHG GE hypothesis of the IPCC. The observed true change in the OLR is positive and the atmosphere and the whole system do not resume the initial state. The fictitious no-feedback response is unrelated to climate change.

Based on the NOAA-R1 soundings and simulations Figure 13 shows the no-feedback response and the true observed changes of the OLR in the 200-1500 cm^{-1} spectral range. The real atmosphere does not follow the GHG GE hypothesis of the IPCC. The observed true change in the OLR is positive and the atmosphere and the whole system do not resume the initial state. The fictitious no-feedback response is unrelated to climate change.

More details are presented in Figure 14 where the no-feedback responses of some other GHGs are also displayed. The observed 23.6 % increase in CO_2 causes -0.75 Wm^{-2} radiative imbalance (red dot). In the same time period, based on the NOAA-R1 archive the real change is 3.02 Wm^{-2} (blue dot). There is no such thing that the OLR remains constant and the surface warms up due to some incorrect GHG GE hypothesis, or because of the outcomes of CO_2 doubling experiments conducted with never validated GCMs.

The changes of OLR due to the pressure induced continuum absorption of N_2 and O_2 are negligible. The contribution to the changes of OLR from the changes of IR absorption of CH_4 (red line) does not seems to be significant either.

IPCC scientists ignore the fact that the clear sky OLR is governed by the unpredictable stochastic nature of the upper tropospheric humidity field (and also the global cloudiness and wind field) which cannot be modelled by any deterministic global climate model. The theoretical constraints governing the global mean radiation flux components are also not part of the GCMs.

In Figure 15 the chaotic nature (in space and time) of the upper tropospheric humidity field is presented, McIDAS (2008) [33]. Evidently, it is impossible to give a reasonable long-term estimate of the OLR^A and t_S, therefore the long-term prediction of climate change is not an appropriate task for GCMs.

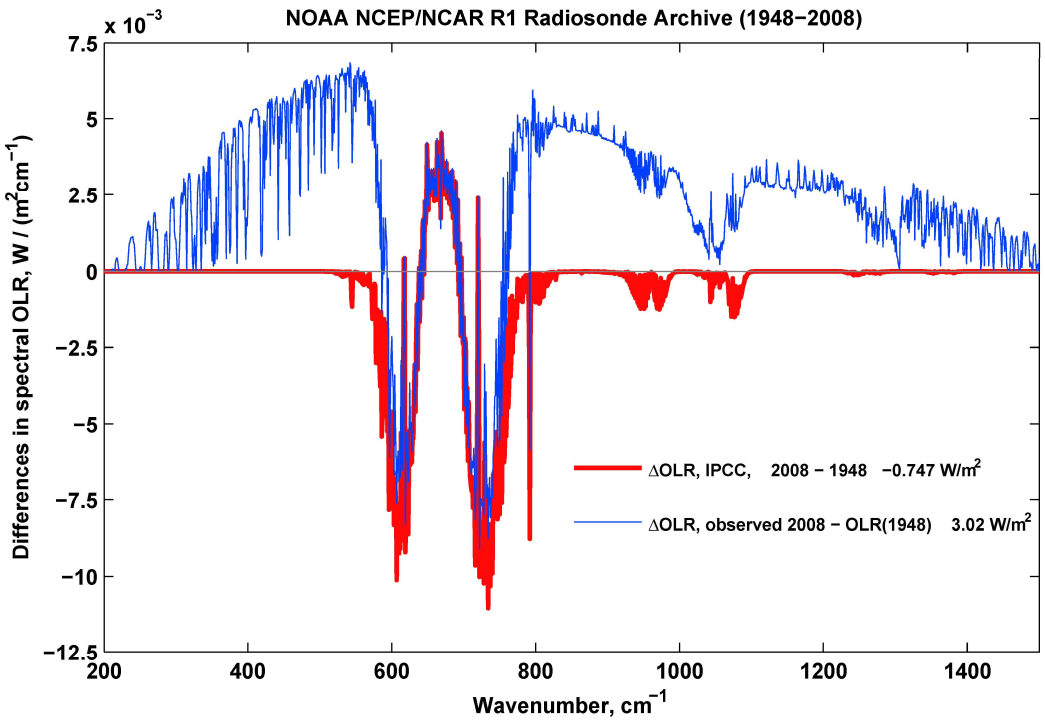

Figure 13: Comparison of the observed and expected changes in the clear-sky spectral OLR . The IPCC type no-feedback response to 23.56 % increase in carbon dioxide is negative, while the true observed changes are definitely positive.

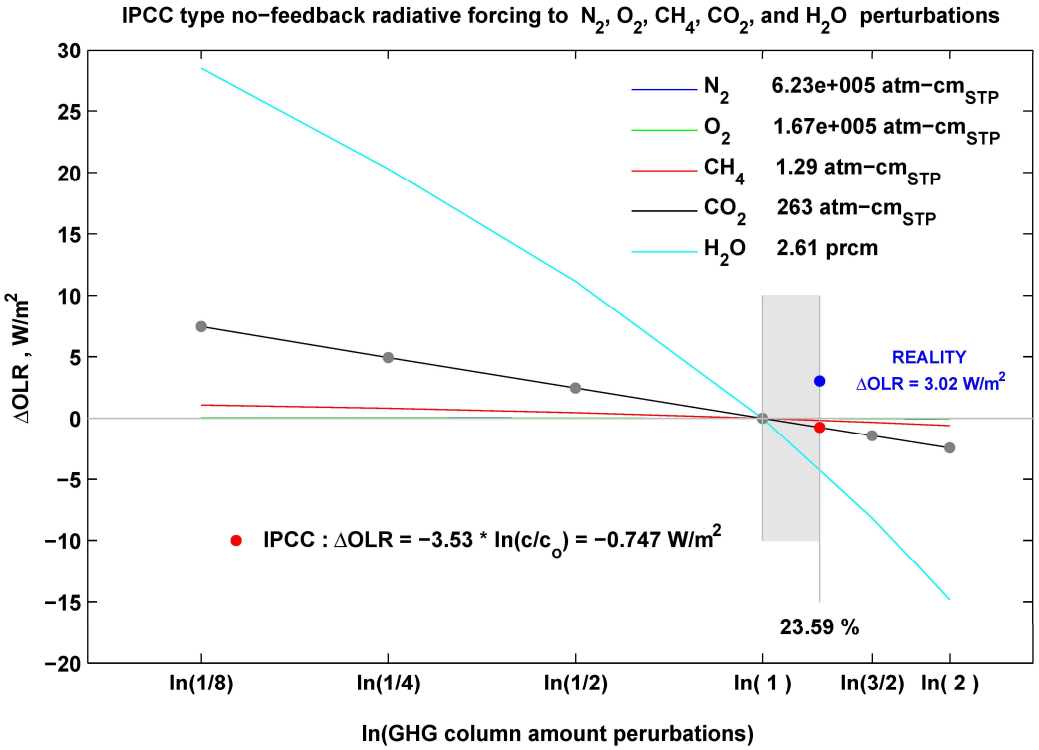

Figure 14: HARTCODE GHG perturbation study shows that at the TOA the no-feedback response of increased atmospheric CO_2 is negative (red dot). CO_2 doubling studies are not consistent with observations.

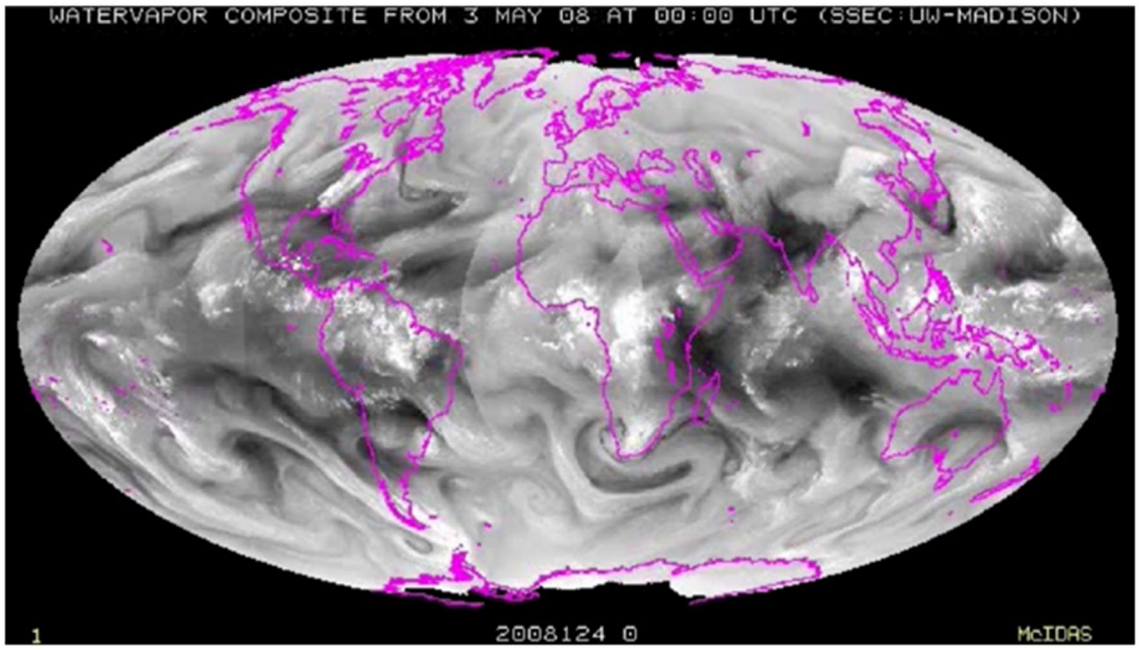

Figure 15: Satellite view of the changes in the upper tropospheric humidity field.

4. The scientific background

In this section some GE related fine details are discussed. Let us list some fundamental IR flux density relationships and the simplest RT functions characteristics of the global mean clear atmosphere:

- Atmospheric Kirchhoff law: $E_D = \varepsilon_A A_A$ (ε_A is the anisotropy factor – discussed later)
- Law of radiative equilibrium: $OLR / S_U = f = 2/(1+\tau+T)$
- Virial function: $OLR / S_U = V = (3+2T)/5$
- Greenhouse identity: $G = S_U - OLR = A_A - E_U$
- Schwarzschild-Milne equation: $OLR = (E_D + E_U)/2$

Based on the equations above, formally, infinite number of valid RT functions may be created by simple (linear) combinations. The new combined functions will all satisfy the clear-sky global RE constraints, but the interpretation of the new equations might not be that simple. In case of the $f = V$ equality and the $\tau^T \cong \tau$ close match the interpretation came relatively easy, but for example to relate the global mean w water vapor column amount to τ, is not that straightforward: $w = w_0/(1-4\exp(-\tau)) = 2.61$ prcm, where $w_0 = 1.0$ prcm.

4.1. Radiative equilibrium at the surface

To establish the radiative equilibrium between the ground surface and the atmosphere above, the ε_A spherical emissivity (or the anisotropy) of the inhomogeneous IR radiation field of the atmosphere has to be considered. The anisotropy of the downward LW radiation is the $\varepsilon_A = E_D / E_{D,I}$ ratio, where E_D is the downward radiation from the real atmosphere, and $E_{D,I}$ is the downward radiation from the isotropic radiation field of temperature t_S (present in the atmosphere).

Because of the $E_{D,I} = S_U(1-\exp(-\tau)) = S_U A = A_A$ mathematical identity, ε_A may easily be expressed as $\varepsilon_A = E_D / A_A = 0.96515341$, where S_U, τ, and $E_{D,I}$ are from GAT LBL simulations. We shall reference this new fundamental relationship as the *atmospheric Kirchhoff law*. The ε_A dimensionless quantity turned out to be one of the most important astronomical parameters of the Earth's radiation climate. In the literature the $\varepsilon_0 = E_D / S_U$ ratio is often termed as sky emissivity, which is not an independent parameter, but related to the ε_A anisotropy factor by the $\varepsilon_0 = \varepsilon_A A$ relationship. Large scale simulations showed that for local atmospheric structures $\varepsilon_0 < 1.0$ always holds, therefore heating of the surface by E_D is impossible. To interpret the theoretical equilibrium global average surface temperature, the following three issues should be taken care of: anisotropy of IR radiation reaching the surface from above; non-radiative energy transport processes at the surface; surface reflection of the downward IR radiation. In a clear atmosphere, the three processes may be easily considered in terms of three parameters ε_A, ε_B, and E_D:

$$E_D / A = \varepsilon_A S_U = \varepsilon_B S_U + (1-\varepsilon_B) E_D, \tag{21}$$

where $\varepsilon_B = E_D S_T / A_A / (S_U - E_D)$ – expressed from (21) – is the *true emissivity* of the surface, taking into account only the non-radiative processes and ignoring the IR surface reflection of E_D. The EBT computed from the $\varepsilon_B S_U$ product defines the t_T *true emissivity temperature* of the surface: $t_T = (\varepsilon_B S_U / \sigma)^{1/4} = 271.43$ K. Obviously, the identity of $1 \equiv \varepsilon_A A + (\varepsilon_A / \varepsilon_B) T$ must also hold. For the S_U isotropic radiation and the t_S EBT there are plenty of exact relationships similar to equations (21) which all satisfy the law of conservation of radiative energy. For example, we may simply write that

$$S_U = A_A \varepsilon_A (1-\varepsilon_B) / (\varepsilon_A - \varepsilon_B), \tag{22}$$

which may suggest that S_U (or t_S) will increase with increasing A_A (due to increased CO_2). This is not the case. Using the definition of A_A, (22) will be reduced to an identity expressing the constancy of the flux optical thickness: $\tau = \ln(\varepsilon_A(1-\varepsilon_B) / (\varepsilon_B(1-\varepsilon_A)))$. We conclude, that once the surface temperature t_S from (17) is physically defined, the equations (21,22) links this t_S to other conservative climate parameters associated with the three most important clear-sky IR radiative processes discussed above.

4.2 The Sun

It should be recognized that the Sun is a very complex object, and the solar constant has its own natural fluctuations. Depending on the state of the Sun F_0 may vary (on different time scales) between $F_0^{\min} = 1359.7$ and $F_0^{\max} = 1376.2$ Wm^{-2} introducing 1.2% (quasi-periodic) changes in the short term averages, Berk et al. (2008) [43]. From $F_0^{\min}$ and $F_0^{\max}$ the F_0^{av} arithmetic average is $F_0 = F_0^{av} = 1367.95$ Wm^{-2}, which is very close to the established long term average ground based observations of 1368 Wm^{-2}. It is not very wise to declare an official solar constant and continuously upgrade it according to the relatively short-term satellite observations. Even NASA warns that their data in the factsheets, NASA (2016) [44] are approximations and they are not appropriate for scientific use. The data are usually given in three or four significant digits and they cannot be consistent with the known physical laws of nature where the key astronomical information and the most fundamental constants of the theoretical physics are given with 10-50 ppm relative accuracy.

To construct a long-term continuous satellite solar constant data base considerable effort has been devoted to reviewing the calibration algorithms of the radiometers involved in different satellite missions. In Scafetta & Willson (2013) [49] one can see largely different composite series from different authors which are the clear sign that the *satellite solar constant problem* is not yet resolved. Once the actual solar constant cannot be known to better than ~0.3 % relative accuracy, (see [49] Fig.15) climate modelers must acknowledge this fact and refer to the reason of their choice of the solar constant.

Sun is the source of the observable radiative and not directly observable entropy flux densities and their specific intensity, radiance, or brightness counterparts. We have found that a theoretical solar constant may be derived from the next equation:

$$F(d) = (\pi / \sigma)^{1/3} d_E^{8/3} r_0^{-2/3} d^{-2} / 10 , \tag{23}$$

where $F(d)$ is the flux density in $\mathrm{Wm^{-2}}$, and d is the distance from the centre of the Sun in meters. In this universal function d may vary from inside the Sun to anywhere in the solar system. This equation stems from the temperature-flux density duality principle which rests on an intrinsic mathematical property of the Planck distribution, Miskolczi & Héjjas (2021) [45]. This analytical form of $F(d)$ is discussed in more details in the Appendix.

Knowing the solar surface area the theoretical solar luminosity, solar surface emission, solar constant and the available SW flux density may easily be computed from the $F(d)$ function: $L_0^T = 4\pi^{4/3}\sigma^{-1/3} d_E^{8/3} r_0^{-2/3} / 10$, $E_0^T = (\pi/\sigma)^{1/3}(d_E / r_0)^{8/3} / 10$, $F_0^T = (\pi/\sigma)^{1/3}(d_E / r_0)^{2/3} / 10$, and $F_E^T = F_0^T / 4$. The theoretical solar constant and the available SW radiation over a unit area at the TOA are: $F_0^T = 1367.95145\ \mathrm{Wm^{-2}}$, and $F_E^T = 341.98785\ \mathrm{Wm^{-2}}$. The diluted theoretical solar entropy flux density is $J_0 = (4/3)\sigma t_{SUN}^3 (r_0 / d_E)^2 = (4/3)\pi^{1/4} \times 10^{-3/4} = 0.31566483\ \mathrm{Wm^{-2}\,K^{-1}}$, which is a mathematical constant. The $t_{SUN}^T = (E_0^T / \sigma)^{1/4} = 5778.0754$ theoretical solar surface EBT is practically equal to $t_{SUN} = (F_0 / d_F / \sigma)^{1/4} = 5778.0738\ \mathrm{K}$. The very important point here is the fact that the $F(d)$ theoretical function depends only on geometrical factors (the solar radius and the semi-major axis of the orbit of the Earth) and of course, independent of any short term or long-term satellite or ground based radiation measurements. Consequently, debate on the theoretical F_0^T solar constant should be restricted to the debate on the accuracy of r_0, and d_E. Of course, the barycenter of the solar system and the steady state center of the Sun (as a fixed geometrical point) do not exist. Sun is not a fixed perfect sphere but a rotating and pulsating gas globe which is subject to gravitational perturbations from other members of the solar system. This physical reality reflected in the singularity of the $F(d)$ function at $d \equiv 0$ where $F(d) = \infty$.

The reference solar constant F_0^T is mathematically consistent with the radiation laws and the known accuracies of the Planck and Boltzmann constants from NIST. It is also consistent with the recent values of r_0, d_E, and the spectral solar constant in Chance & Kurucz (2010) [34]. The existence of the theoretical solar constant does not support the idea of introducing a kind of new standard solar constant (and the backward correction of previous standards) based on purely the newest satellite observations. The accuracy of flux density or radiance measurements will never conquer the accuracy of the measurements of distance, linear size or time. It looks that the extreme stability of the climate over millions of years is linked to the existence of the F_0^T theoretical solar constant.

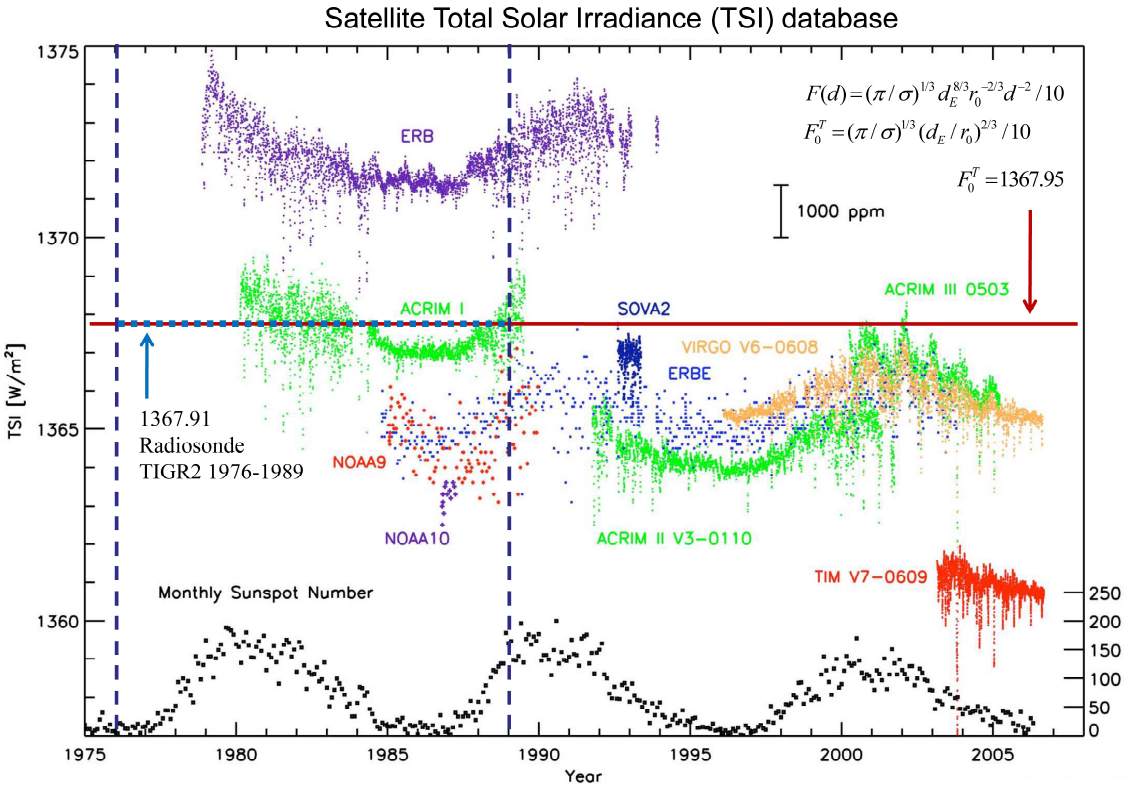

Figure 16: Comparisons of the F_0^T theoretical solar constant with direct satellite observations, and with LW flux density simulations from the TIGR2 archive. The blue dotted line is at $F_0^{obs}=4S_U^A$, and S_U^A is the all-sky global mean surface upward flux density from the APS. The $F_0^{obs}=F_0^T=F_0$ is the indication of planetary radiative equilibrium. All fluxes are in Wm^{-2}.

In Figure 16 F_0^T is compared to the observed F_0^{obs} (quoted under paragraph *2.3*), and the satellite observations from Kopp and Lean (2011) [35]. The $F_0^T=F_0^{obs}=F_0$ equality means that the planet is in strict radiative equilibrium with the theoretical solar constant, where in (23) F_0 mathematically locked to σ, r_0, and d_E.

4.3 Greenhouse gas greenhouse effect

Recently there is a serious problem with the use of the classic definition of the GHG GE. The ambiguity arises from the fact that some scientists recognized that the classic GHG greenhouse effect cannot be discussed without the presence of the global cloud cover and started to use the greenhouse effect terminology in a generalized way, including the cloud effect. For example, in [12] and [13] the authors attribute about ~50 % of the total GE to the H_2O, only 25 % is the contribution of all non-condensing GHGs, and the remaining 25 % is the cloud effect This confusion should be avoided, CO_2 is a greenhouse gas and not a solid or liquid substance. If there is no cloud cover present in an air column one has to talk about the clear-sky GHG greenhouse effect, and in fact, that is what we are interested in.

To answer the question what is the contribution of the individual atmospheric layers to the total greenhouse effect in Figure 17 the vertical distribution of the clear sky greenhouse factor is demonstrated.

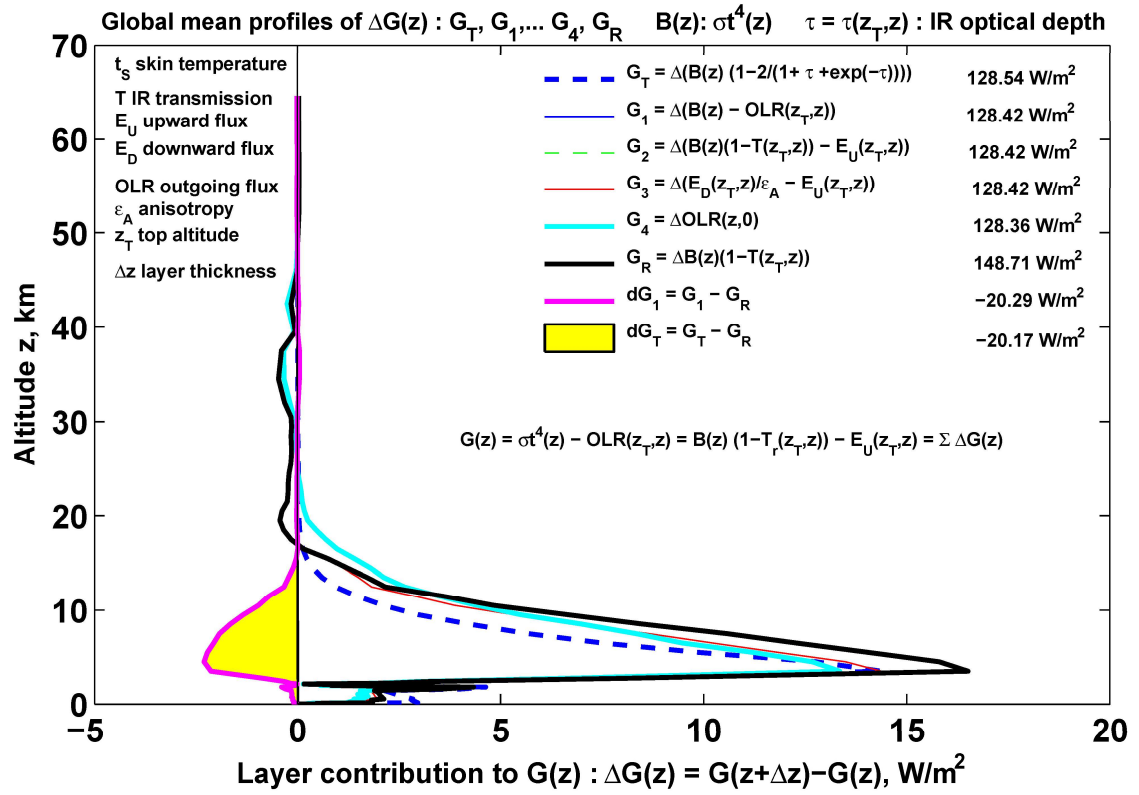

Figure 17: Except G_R the different greenhouse factors (G_T, G_1, G_2, G_3, G_4) are in good agreement. In case of the GAT atmosphere the maximum contribution comes from about 4-5 km altitude.

Apparently, the different numerical computations of the G factors (on the right side) gives consistent results. However, G_R from [10] or from Ramanathan & Inamdar (2006) [36] shows large discrepancy (about 20 Wm^{-2} overestimate). The cause is the incorrect mathematical representation of GF, (see for example equations 1 and 2 in the Nature article [10]). Unfortunately, despite our direct attempt to communicate with the authors, this serious mistake was never acknowledged or corrected, however, this error could effectively invalidate the whole H_2O positive feedback argument in [10].

4..4 Cloud effect

Celestial objects in the Solar system may have no atmosphere at all (Moon), they may have GHG atmosphere which is condensing on the planetary surface (Mars), they may have GHG atmospheres condensing on both the surface and within the atmosphere (Earth), and they may have GHG atmospheres condensing only in the atmosphere (Venus).

Planets may also have diverse set of surface materials which is generally not expected to produce a Bond albedo needed for the planetary radiative equilibrium, see (1,2). It is quite plausible to assume that condensing GHGs in the atmosphere will form an opaque layer of liquid and solid particles (disrupting the propagation of the IR radiation), and will change the Bond albedo in a way that the planetary radiative equilibrium will be established. Theoretically steady state RE of non-condensing semi-transparent GHG atmosphere of a passive planet cannot exist, since the ground surface of such planet would cool down freely to the astronomical limiting temperature depending partly on the local solar constant and Bond albedo, and partly on the outward diffusion of thermal energy from the planetary interior.

In the special case of Earth, the astronomical limiting temperature is practically equal to the temperature of the triple point of H_2O. In other words, at some (sufficiently low) temperature any gas will become a condensing GHG, therefore, without the presence of condensing GHGs in the system there is no atmosphere at all.

The above concept is fully consistent with observations of atmospheres of comets and planets in the solar system. A comet starts to build up atmosphere when getting closer to the Sun and the surface materials start to evaporate. On the reverse trajectory when getting farther from the Sun the atmosphere condenses back to the surface and disappears.

Atmospheres with condensing GHGs might have several internal boundaries (cloud layers) at different altitudes which instantly disrupt the propagation of the electromagnetic radiation, consequently, the global mean cloud cover is the major factor in establishing and maintaining the planetary radiative balance. Note that in gas phase the spectral gas absorption is restricted to certain spectral ranges characteristic of the molecular structure of a particular GHG.

In the interesting case of the thin Martian CO_2 atmosphere − due to the lack of cloud cover − we can only speak of clear-sky GE. The Martian atmosphere contains 33.3 times more CO_2 but the GE is only about ~3 K, indicating that the amount of atmospheric CO_2 is not a major factor in creating the Martian GE. Compared to the ~2.61 prcm of water vapor in the Earth's atmosphere, the Martian atmosphere contains a negligible amount of water vapor (approximately 0.00155 prcm) which is insufficient to form extensive cloud cover and significantly increase GE and GF. In the Martian carbon dioxide atmosphere, the planetary RE is maintained by the diurnal changes of the mass of the GHG atmosphere and the heat (released or received) at the lower boundary by the phase changes of the CO_2. One must conclude that the Earth's clear-sky GE cannot be explained by the CO_2 content of the atmosphere. GE are closely related to the amount of condensing greenhouse gases and their physical state.

In the hot and thick atmosphere of Venus the complex, fully closed multi-layer cloud structure completely decouples the IR radiation field of the ground surface from the *outgoing long wave radiation* (OLR). Below the closed cloud layers, the IR radiation field is a type of cavity radiation in RE. The planetary RE is maintained solely by the radiation from the cloud top (at an effective cloud top altitude) and the atmosphere above. Due to the dramatically different roles of the atmospheric composition, clouds and surface characteristics, the formation and functioning of the greenhouse effect are quite different on the three planets. In Figure 18 the GE of the Martian atmosphere is compared to the GE in the Earth's atmosphere.

In the Earth's atmosphere (14) shows that the planetary radiative equilibrium cannot be established without involving the cloud cover in the greenhouse problem. The concept of the numerical evaluation of the equilibrium cloud cover is presented in Figures 19 and 20.

As a first step we define the $\beta^A(F_A, h^C)$ and $\beta^E(F_E, h^C)$ global mean cloud covers relevant to the TOA and APS radiative balance requirements. From a set of β^A and β^E (computed for large number of different α_B and h^C) and using a multi-parameter optimization algorithm the global average α_B and h^C can be calculated. In the two-dimensional optimization problem, only one global average cloud layer is assumed, and the norm of $\| \beta^A - \beta^E \|$ is to be minimized. As a computational detail, the accuracy of our global average cloud cover largely depends on the vertical resolution of the LBL code used. In our case around 2 km altitude the layer thickness was set to 40 m.

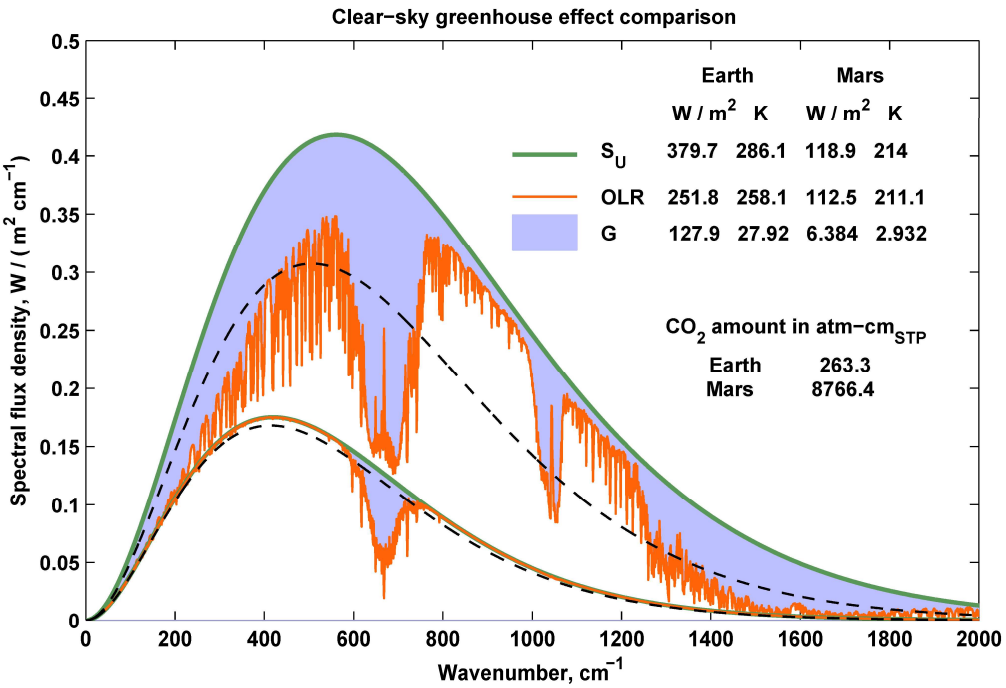

Figure 18: Comparison of the greenhouse effect on Earth and Mars. The clear sky GE, $(S_U/\sigma)^{1/4}-(OLR/\sigma)^{1/4}$ and GF, $S_U - OLR$ are not controlled by the CO_2 content of the atmosphere. The black dashed lines are the EBFs of the two planets.

$$F_A = (1-\beta^A)\,OLR + \beta^A\,OLR^C$$

$$F_E = (1-\beta^E)\,S_U + \beta^E S_U^C$$

$$\beta^A(F_A, h^C) = (F_A - OLR)/(OLR^C(h^C) - OLR)$$

$$\beta^E(F_E, h^C) = (F_E - S_U)/(S_U^C(h^C) - S_U)$$

$$F_A = (1-\alpha_B)F_E$$

$$\min(\,\|\,\beta^A(h^C,\alpha_B) - \beta^E(h^C,\alpha_B)\,\|^2\,)$$

Figure 19: Radiative equilibrium cloud cover constraints. At the TOA LW fluxes from the APS must be equal to F_E the all-sky outgoing LW radiation must be equal to F_A, and the cloud covers from the two constraints must be equal $\beta^A \equiv \beta^E$.

From a 20-year long time series data of ISCCP−D2 in Van Andel 2010 [61] a global mean of 66.38 +/− 1.48 % was reported. In Figure 21 satellite cloud climatology data are in excellent agreement with our theoretical cloud cover of $\beta = 0.6618$. The equilibrium cloud cover must be equal to the theoretical transfer function: $\beta = 2/(1+\tau^T+\exp(-\tau^T))$, where $\tau^T = 1.8676$ is the theoretical equilibrium flux optical thickness. In the case of Earth the CRE situation holds and from the equilibrium equation in Figure 8 follows the $\alpha_B = g^A$ equality. Knowing the accurate β, S_U, and S_U^C the g^A can be checked against the next theoretical equation in [17]:

$$g^A = g/(1+\beta S_U^C/(1-\beta S_U)) + g^C/(1+(1-\beta)S_U/(\beta S_U^C)) = 0.30129061. \qquad (22)$$

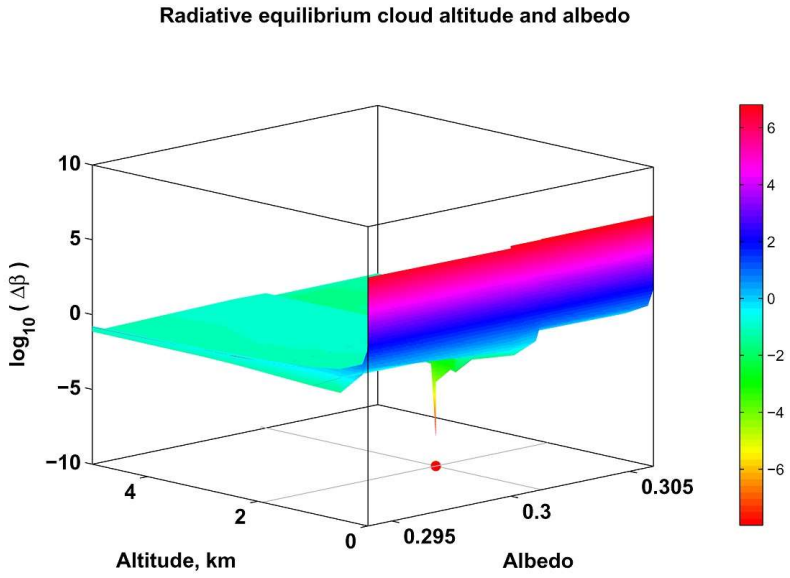

Figure 20: The multi-parameter optimization algorithm. Sharp minimum of the $\| \beta^A - \beta^E \|$ *norm found at* $\alpha_B = 0.30129$ *and* $h^C = 1.1916$ *km.*

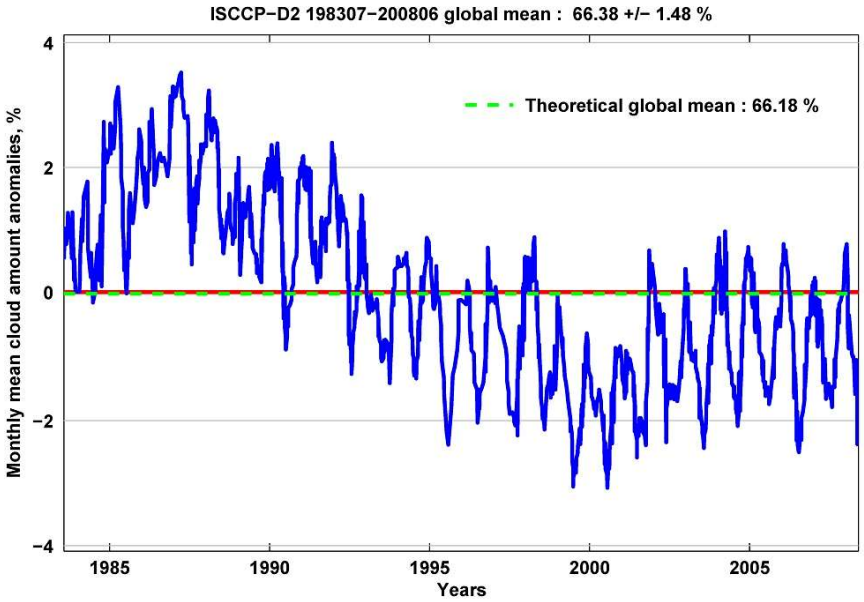

Figure 21: The theoretical cloud cover (green dashed line) is compared with satellite observations in the 1983-2008-time interval (red line). The agreement is well within the uncertainty of the satellite observations.

The $\alpha_B = F_R / F_E = (S_U^A - OLR^A) / S_U^A = g^A = 0.30129061$ equality is evident, therefore, the use of (17) with the S_U^C and β above is quite justified: $t_S = ((F_0 / (4sc) - \beta S_U^C) / (1-\beta) / \sigma)^{1/4} = 286.075$ K. This t_S is practically equal to the global average surface radiative temperature from radiosonde observations.

4.5 Water vapor

Compared to Mars and Venus on Earth the planetary RE situation is far more complex. Since the phase changes of the H_2O may happen at any time and anywhere in the system the Earth has an extremely variable cloud, surface ice and snow cover. The combined surfaces where the water vapor is in direct contact with liquid water, snow, and ice will be termed as the phase boundary. Through this hypothetical complex surface the total amount of water vapor in the atmosphere will change by the release or buildup of the latent heat by evaporation, condensation or sublimation. In steady state the net condensation and evaporation associated with rain droplets (within the atmosphere) must be zero and the mass balance of the atmosphere is maintained by the evaporation or sublimation from the ground surface and precipitation or deposition to the ground surface. These processes will result in a decrease or increase of the flux optical thickness which is coupled with the mass exchange trough the lower boundary.

The total mass (or the potential energy) of the atmosphere and the flux optical thickness are controlled by the virial theorem, (see [17]). The mass conservation in the hydrological cycle expresses indirectly the conservation of the flux optical thickness.

The observed and theoretically predicted constant flux optical thickness (see [27]) is plain proof of the climate control by the water cycle. In other words, increasing or decreasing the energy input to the system will result in the release or storage of the required amount of radiant or thermal energy through the phase boundary to assure the radiative equilibrium while keeping the temperature of the phase boundary unchanged.

To clarify further the water vapor feedback problem, from the NOAA-S archive 689 high quality all-sky radiosonde observations were processed to show the relationship between the local mean layer temperature and water vapor column density. During 1992-1993 from the high resolution (6 second) data 654130 individual layer mean temperature and water vapor column density pairs were collected.

In Figure 22 the primary measured relative humidity and the computed H_2O column density profiles are plotted showing no correlation. The H_2O column density directly enters to the LBL computation of the layer flux transmittance and optical thickness.

In Figure 23 the linear correlation coefficient between the temperature and natural logarithms of the column density is 0.99, which − considering the relevant quantitative theoretical relationships − is not a surprise. The light blue dot around 5 km (in the right plot) is the observed maximum altitude of the H_2O condensation temperature at Sterling. Many climatologists mistakenly call this relationship as positive feedback. It must be clear that locally the temperature and water vapor content of the air parcels are alternative variables, and they are not connected by some ad-hoc positive or negative feedback parameter.

According to thermodynamics phase transitions are controlled by the changes in the molar free energy and entropy. In view of the known analytical dependence of the ambient temperature on the water vapor content (of an individual air parcel) the whole positive H_2O feedback hypothesis seems to be nonsense.

In Figure 24 we show the dependence of the CO_2 and H_2O column amounts in 7 different NOAA-R1 time series. The column amounts were computed in two sections: the lower part (green dots), the upper part (red dots), and also for the total air column (blue dots). While below about 2 km both the H_2O and CO_2 increased, above 2 km the relationship reversed. The net effect for the whole air column is decreasing H_2O with increasing CO_2 (with a sufficiently large linear correlation coefficient).

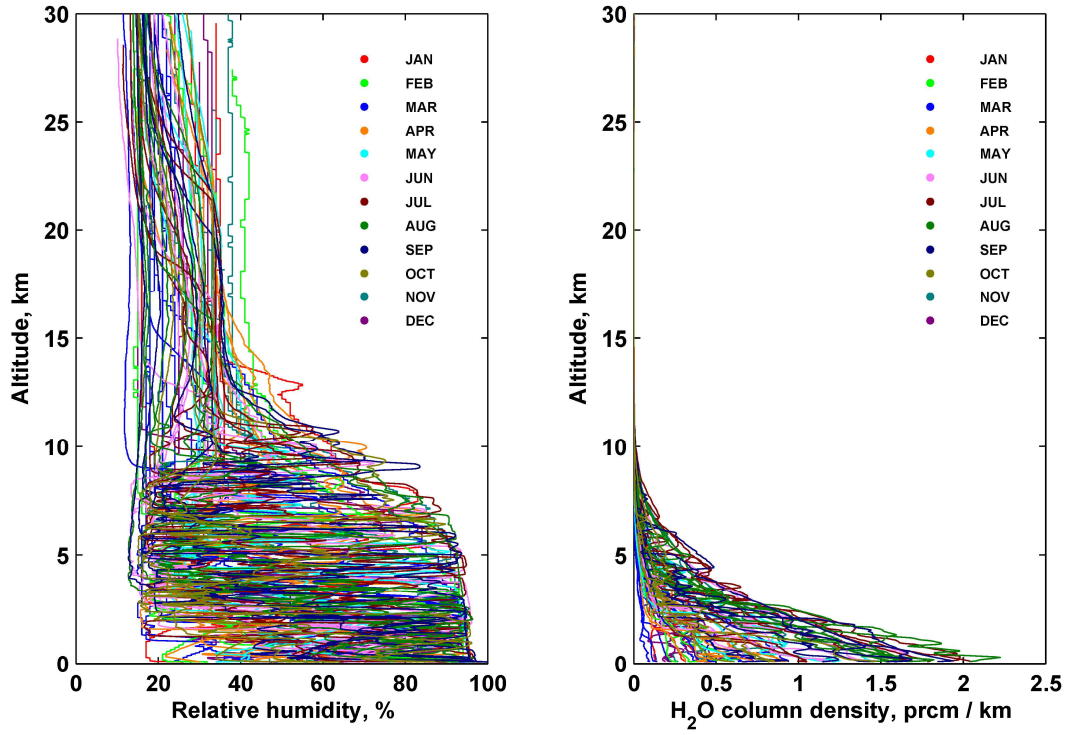

Figure 22: High resolution radiosonde observations from NOAA Sterling, Virginia. The left panel shows, that the tropospheric relative humidity is a true stochastic component of the climate system.

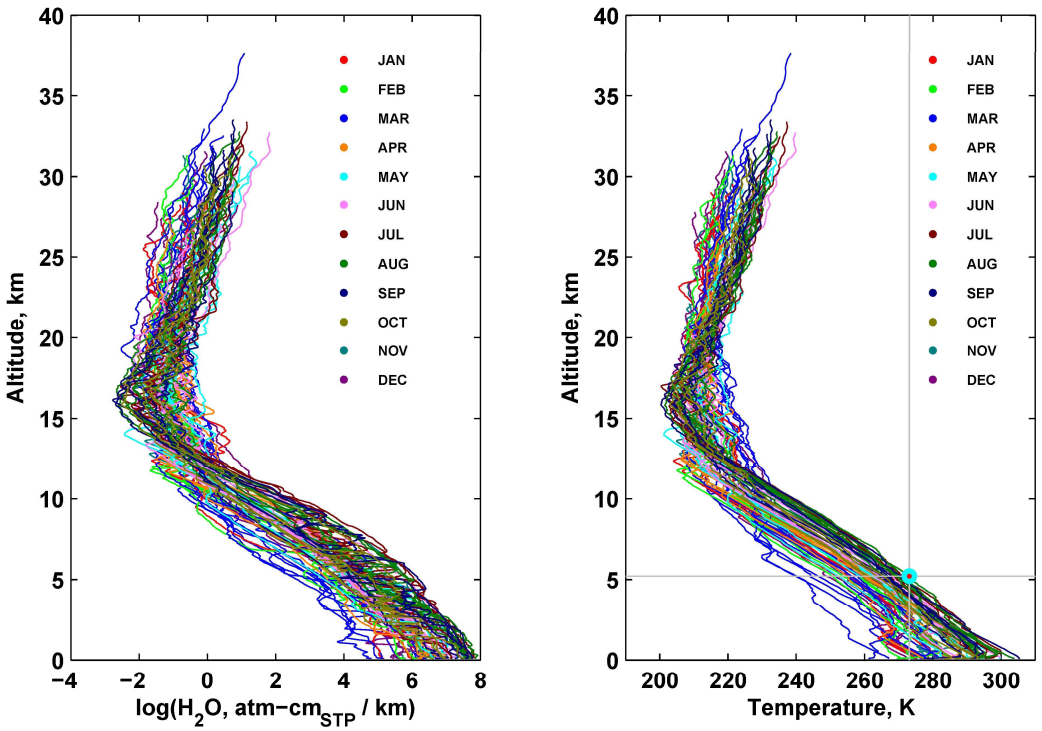

Figure 23: High resolution radiosonde observations from NOAA Sterling, Virginia. The temperatures and H_2O column density are highly correlated, and they follow the relevant theoretical relationships.

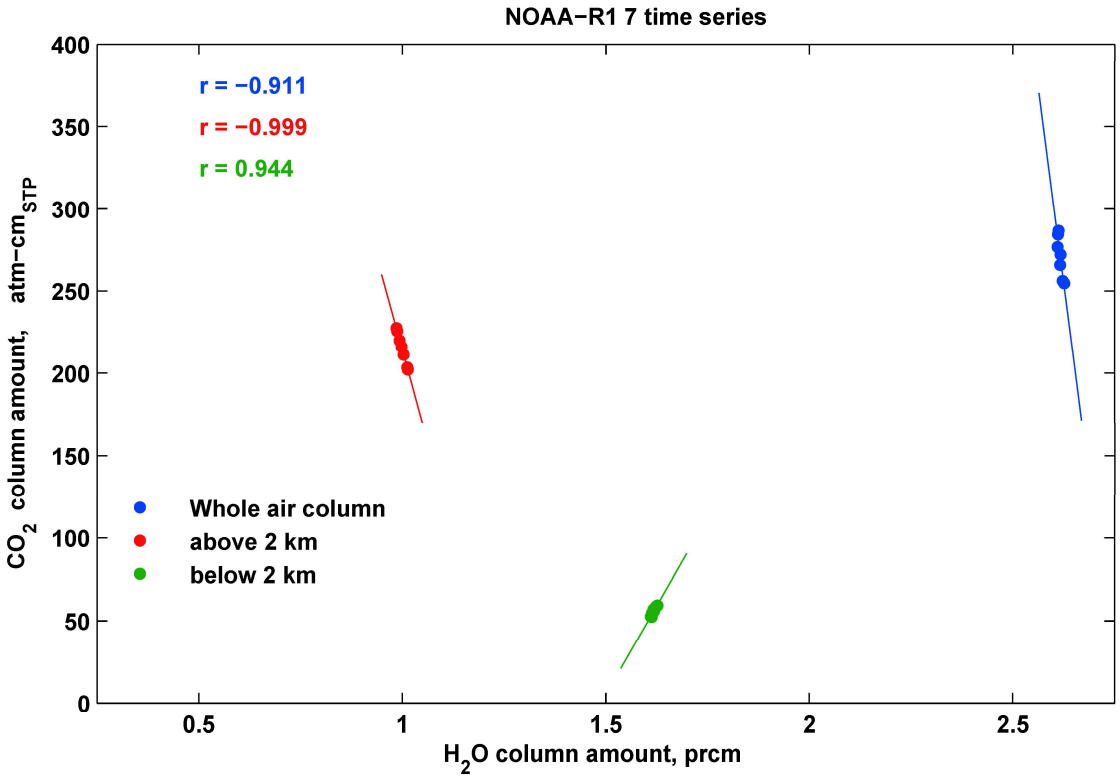

Figure 24: Changes in the CO_2 and H_2O column amounts in the 7 NOAA-R1 time series (presented in Figures 10, 11, and 12).

The blunt statement of the IPCC on the positive water vapor feedback mechanism is probably based on the increasing H_2O in the lower atmosphere with increasing CO_2 (green dots). However, the response of the dynamical system evidently coupled with reduced H_2O in the upper levels, in such a way, that the net change of H_2O in the total air column is negative. One should not forget that this figure is not proof that increasing CO_2 concentration will decrease the water vapor. Rather, it is proof that the system may adjust its IR absorption properties to the actual CRE requirements by restructuring the vertical water vapor distribution.

4.6 Energy budget cartoons

The usual way to support the idea of the classic greenhouse effect is to present planetary energy budget schemes where the global radiative flux density components as well as the sensible and latent heat fluxes in the system are estimated either from direct measurements or from radiative transfer computations.

The most well-known is the Kiehl & Trenberth (1997) [39] energy budget. In Miskolczi (2014) [17], based on 13 years of radiosonde observations, it was first shown with high degree of accuracy that the Earth-atmosphere system is in the state of radiative equilibrium. The *radiative imbalances* at the upper and lower boundaries of the atmosphere that appear in peer-reviewed radiative budget cartoons (Trenberth et al., (2009) [40]; Stephens et al. (2012) [41]; Wild et al. (2012) [42]; NASA (2010) [38]) do not exist. The radiative equilibrium stems from energy conservation and energy minimum principles and it is the natural state of the Earth-atmosphere system. So far none of the published planetary energy budgets give any bearing to the origin and physics of the atmospheric greenhouse effect and unfortunately, almost all of them suffer from serious errors in the methodology and evaluation. Some of them are listed below.

1. Quantitative discussion of the greenhouse effect should be based on the strict, detailed, clear, and physically meaningful definition of the phenomenon. For example, in Schmidt et al. (2010) [12] and Lacis et al. (2010) [13], we see published totally misleading quantitative results about how the share of the present-day global GE is distributed between GHGs. They state that the contributions of H_2O and CO_2 are 50 % and 20 % subsequently. In common understanding these data means that the CO_2 absorption in the 15μm band is about half of the absorption of the H_2O in the whole IR, which is sheer nonsense.

2. Due to the heavily overlapping nature of the terrestrial spectral radiation field it is mathematically impossible to decompose the flux optical thickness into the contributions of the individual molecular species, (see [16], Appendix A). The LBL computational technique was developed to remove the uncertainties due to the spectral overlaps of the absorption coefficients of different GHGs.

3. Clouds (or any kind of solid or liquid particles in the atmosphere) radiate continuous IR spectra and have nothing to do with the IR spectral absorption of the greenhouse gases. The cloud forcing approach to the greenhouse problem does not help to clarify and quantify the planetary radiative budget. The $F_E = S_U^A$ and $F_A = OLR^A$ equalities show clearly that the global average atmosphere is in radiative equilibrium with a well-defined t_S surface temperature, β cloud cover and the equilibrium cloud top temperature.

4. From the confirmed $G^A = S_U^A - OLR^A = F_R$ and $F_E = S_U^A$ equalities follow the conservation of radiant energy, radiative equilibrium, and they give solid empirical support to the theoretically introduced equivalent blackbody temperature. Because of the two-layer structure of the global average atmosphere the ground surface referenced GE cannot contain any dependences on the albedo, cloud cover, radiative temperature, LW absorption, or flux optical thickness, rendering the GE to observations of t_S, and OLR^A, and leaving the greenhouse problem entirely to the mercy of the GCMs and their unphysical assumptions and countless ad-hoc tuning parameters.

5. No quantitative constraints on the shortwave system albedo, cloud cover and cloud altitude are established. These are key climate parameters, and some kind of theoretical expectation must be referenced or developed. The steady state planetary radiative balance is abandoned in favor of a hypothetical man-made greenhouse warming. In science the quantitative estimate of 0.6 ± 17 Wm^{-2} missing heat in Stephens, 2012 [41] means that climatologists have no idea why and how the hidden (thermal and radiant) energy is distributed among the different latent heat reservoirs.

6. In the budgets the global mean thermal and GHG structure of the atmosphere is not specified. Generally, the LW fluxes relevant only to the USST76 are used as the global average. The most recent [38] budget (presented in Figure 25) adopted the flux density components from the [39] radiative budget which is obviously wrong. Transmitted flux densities from the surface (40 Wm^{-2}) in [39] were computed for the USST76 atmosphere and its 390 Wm^{-2} surface upward flux. 15 years later, in the NASA picture the corresponding fluxes are 40.1 and 398.2 Wm^{-2} which is nonsense. About ~10 Wm^{-2} increase in surface upward flux and practically unchanged surface transmitted flux density deserves some explanations. Another problem is the net non-radiative flux density into the atmosphere which supposed to be zero for an isolated planet.

7. Due to the fatal mistake of using the USST76 atmospheric model, not even one flux density component is close to the ones from the GAT structure. The 0.6 Wm^{-2} fictitious missing heat (white number) is meaningless and violates energy conservation principles (atmospheric Kirchhoff law). For reference, our simulated flux density terms are inserted (black numbers). In the blue and red squares are the top of the atmosphere and the surface referenced flux components.

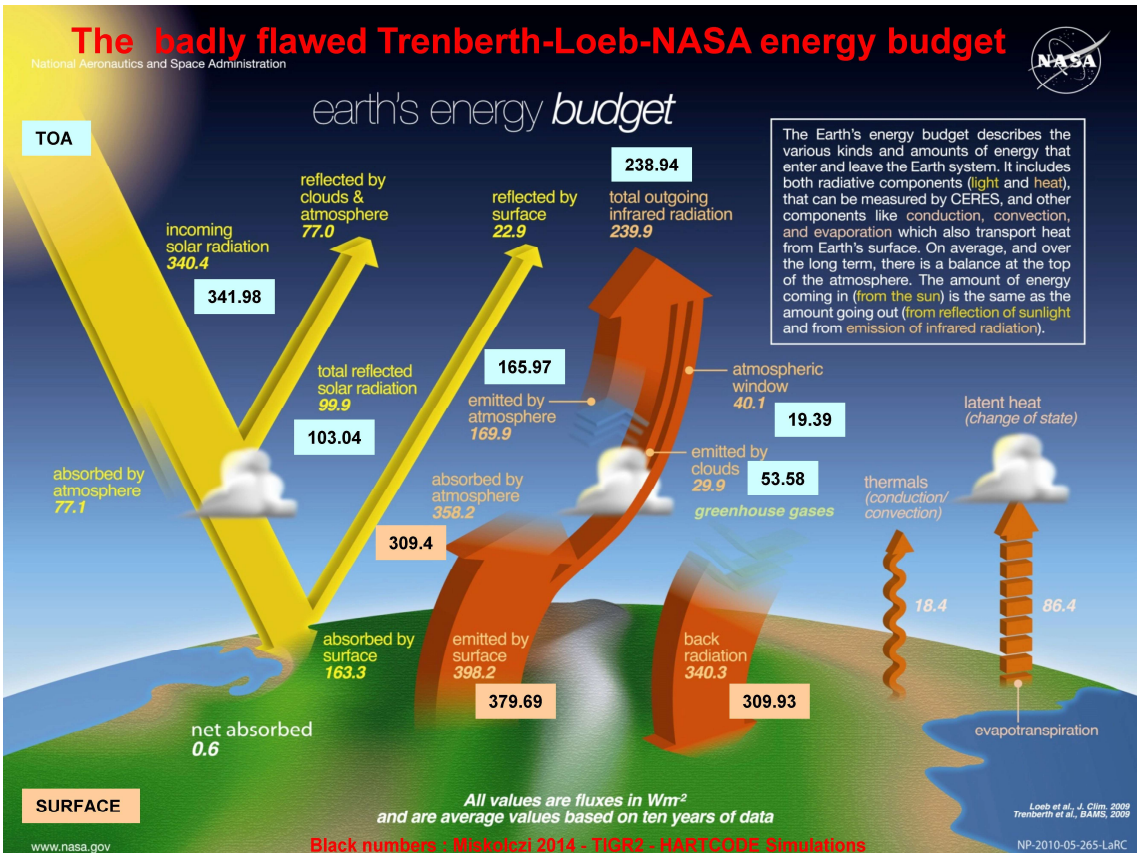

Figure 25: All-sky energy budget of the Earth-atmosphere system, adopted from NASA.

8. The most serious problem with the cartoons is the ignorance of a long line of well-known fundamental concepts and principles of theoretical physics. Some of them are: energy and momentum conservation principles of the radiation field, Wien's law, virial theorem, energy minimum principle, Maxwell rule, Kirchhoff law, Helmholtz reciprocity principle, Vogt-Russel theo- rem, Br a un-LeChatelier principle. Apart from the ignorance of the newest laws of atmospheric radiative transfer, one has to observe that the complexity of the climate system is not a free ticket for violating the first principles of physics.

Further on, it is not apparent that climatologists have access to an accurate RT software for the calculation of correct atmospheric flux densities. Note, that remote sensing applications use high accuracy inter-calibrated LBL radiance codes developed for special applications. However, there is a long way to go to arrive at a correct LBL flux density software from simple directional LBL radiance-transmittance codes.

4.7 Deliberate data manipulation of climatological data

We have discovered that vital climatological data sets were deliberately manipulated. The verification of the planetary energy budget and radiative balance require high quality primary information from global scale radiosonde observations. If the radiosonde observations are wrong then no one will trust in the satellite retrievals of the temperature, humidity or ozone structures. Satellite products depend on the calibration and tuning (of the instruments and retrieval algorithms) based on the ground truth information.

The common mistake of the climatologists is to assume that satellite information is always correct, no matter what. This is not true; satellite information cannot ever be more accurate than the ground truth.

It should be kept in mind that most of the vital flux density components cannot theoretically be measured by any instrument. For example, the so called windows radiation (usually defined in the 721-1260 cm^{-1} spectral range) is not a good representation of the true S_T surface transmitted flux density. That is, the S_T (or S_T^C) flux density component can never be accurately measured even by broad-band or ideal Fourier spectrometers.

Scientists must also be aware that government research institutions may deliberately manipulate their databases to reflect their wild imagination on how the GE works. A good example is the NOAA-R1 archive which was used in our trend analysis study in Miskolczi, 2010 [27]. This global archive shows consistently that between 1948 and 2008 the flux optical thicknesses from the profiles are equal to the theoretical τ^T of 1.867 (see Figure 9).

However, the true equilibrium optical thickness of the NOAA-R1 time series is $\tau_E = 1.937$ and it is far off from τ^T, which is a sign that none of the annual mean profiles are close to the radiative equilibrium. The $\tau_E - \tau^T = 0.06$ optical thickness difference corresponds to about 250 % increase in CO_2 concentration. This is of course impossible; the Earth cannot be out of radiative balance by about 4 Wm^{-2} at the TOA for 61 years.

Such a situation can only happen by altering the thermal structure (especially the close to surface temperature field). Much more serious is the problem with the USST76 atmosphere and the [39] budget, where due to the unrealistic temperature and humidity structure the imbalance in the OLR at the TOA is about 29.38 Wm^{-2}. The NOAA-R1 archive may be used for trend analysis, but − because it violates the energy conservation principle − it is useless for global energy budget research.

Other examples are the TIGR2 and the updated TIGR2000 archives. A closer look at the TIGR2000 revealed that more than half (915 out of 1761) profiles are coincidental, and they are included in both archives. The humidity and ozone structures in those coincidental profiles were poorly modified in an obvious way that the original thermal structures were preserved.

The authors of the database should have known that the H_2O, O_3, and the thermal structures in real atmospheres are highly correlated, which property is widely used in water vapor and ozone statistical retrievals from satellite spectral measurements.

In Figure 26 we present one sample (out of the 915 manipulated profiles) where the increased H_2O and ozone content resulted in increased flux optical thickness (to a value corresponding to CO_2 doubling). The left plot shows the unchanged temperature profile, the right two plots show the manipulated H_2O and O_3 profiles respectively.

As a result of the data manipulation the TIGR2000 archive now contains 915 unrealistic atmospheric structures (mostly with increased upper tropospheric humidity and ozone amounts) which makes the database useless for both remote sensing and radiative budget applications. Creating fake radiosonde observations to support the belief in CO_2 GE based global warming is not a scientific approach.

The upper tropospheric humidity problem (if there is any) will not be resolved by artificial increase of the humidity data in the raw radiosonde observations. Unfortunately, there is evidence of extended data manipulations in other climate data sets that renders the whole climate science to a hiding game, and largely reduces the chances to obtain scientifically sound answers to the role of the GHGs in the global warming.

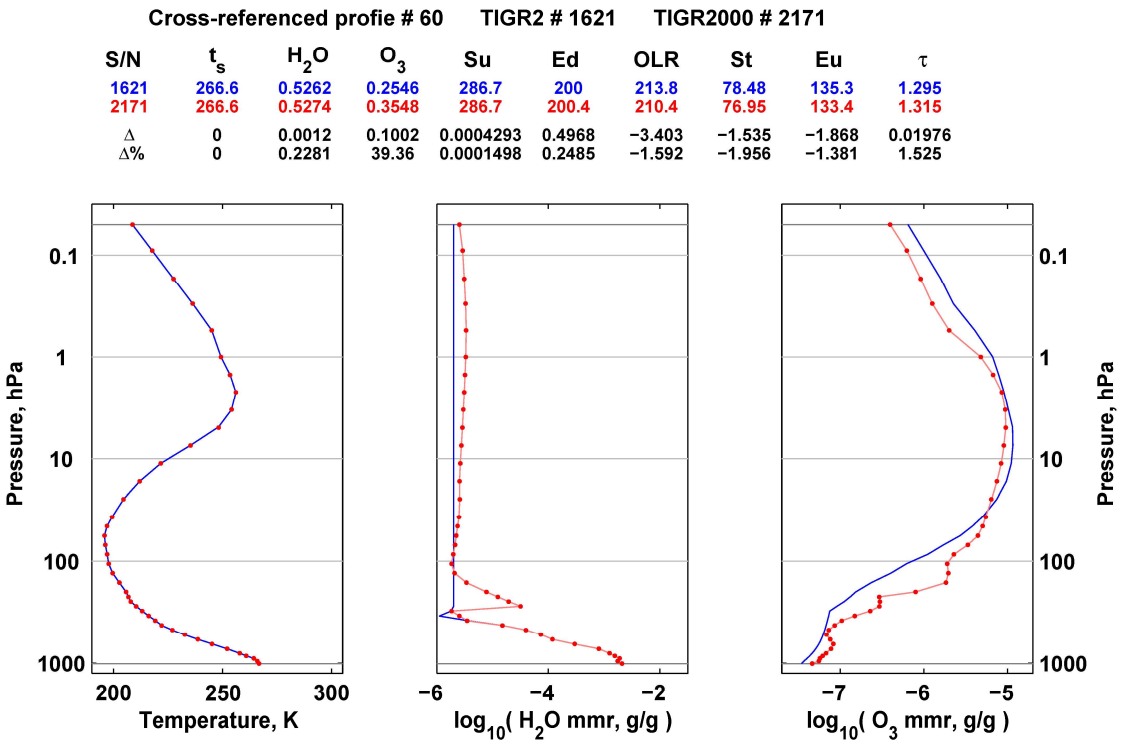

Figure 26: Evidences of large scale data manipulation in radiosonde observations. Comparing the two versions of the TIGR database shows that in more than 50 % of the profiles the upper tropospheric H_2O and O_3 mass mixing ratio were increased (red dots). In this example the changes resulted in 3.4 Wm^{-2} decrease in OLR and significant increase in the flux optical thickness.

4.8 Overview of spectral flux density components

Summarizing our quantitative results in Figures 27, 28, and 29 the spectral distributions of the most important flux density components are presented. The spectrally integrated fluxes are accurate up to 4-5 significant digits. In these figures the meaning of the subscript 'A' (in t_A and t_A^{NASA}) refers to the global mean emission temperature of the Earth for the GAT atmosphere, and for the NASA (computed from the EBTs of the all-sky OLRs).

In Figure 27 the $B(t_A)=B(t_A^{NASA})$ and $B(t_S)=B(t_S^{NASA})$ equalities are indications that the GAT atmosphere is very close to the real global average atmospheric structure. The black dotted line(over the yellow line) is the Planck blackbody curve of the GAT t_e^{bt} mean color temperature showing the maximum entropy of the OLR^A.

While the surface referenced equilibrium clear sky GF ($\sigma t_S^4/\varepsilon_A - OLR = 154.5\ \mathrm{Wm^{-2}}$) has no clear physical meaning, in Figure 28 the APS referenced GF can easily be associated with the deposited momentum by the reflected radiation: $G_{APS}=S_U^A-OLR^A=F_0\alpha_B/4=103.04\ \mathrm{Wm^{-2}}$. In the figure G_{APS}^e (black curve) is the Planck blackbody function of the EBT of the G_{APS} (206.47 K). This temperature is apparently equal to the SW effective equivalent reflection temperature: $t_R=(F_R/\sigma)^{1/4}=206.469\ \mathrm{K}$.

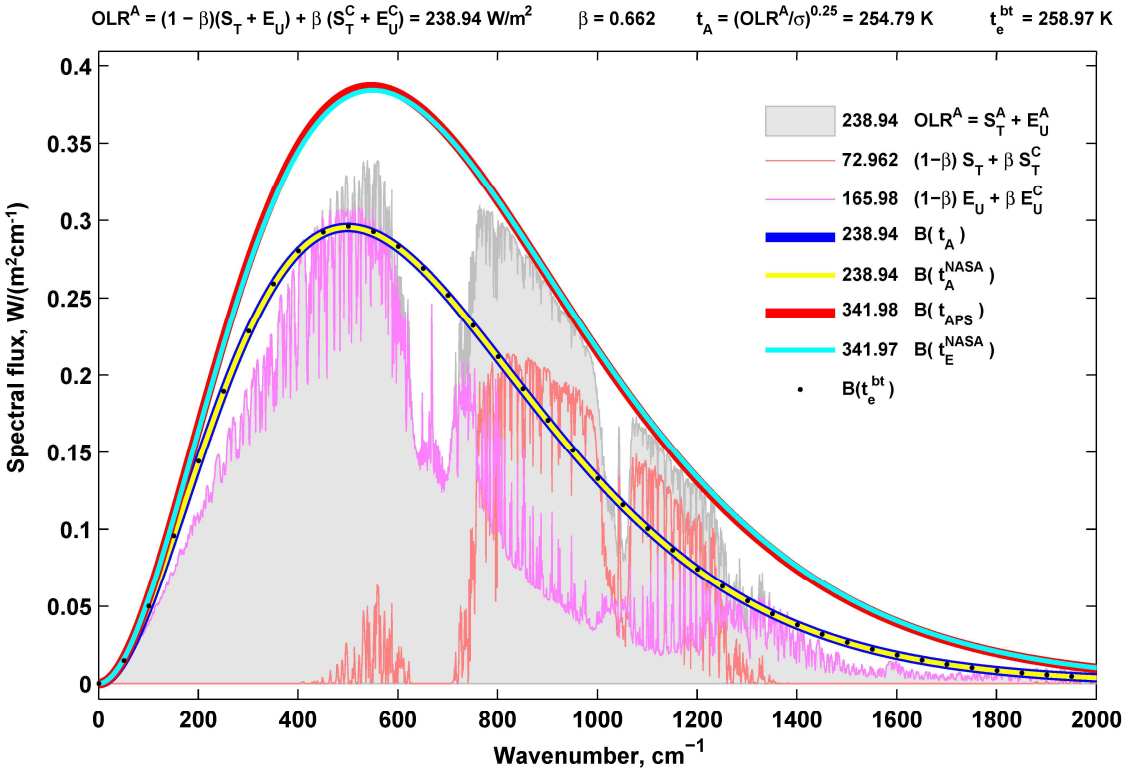

Figure 27: Flux density spectra of the all-sky GAT atmosphere. The equivalent blackbody spectra $B(t_A)$, and $B(t_e)$ from GAT are equal to the equivalent spectra from $B(t_A^{NASA})$, and $B(t_e^{NASA})$.

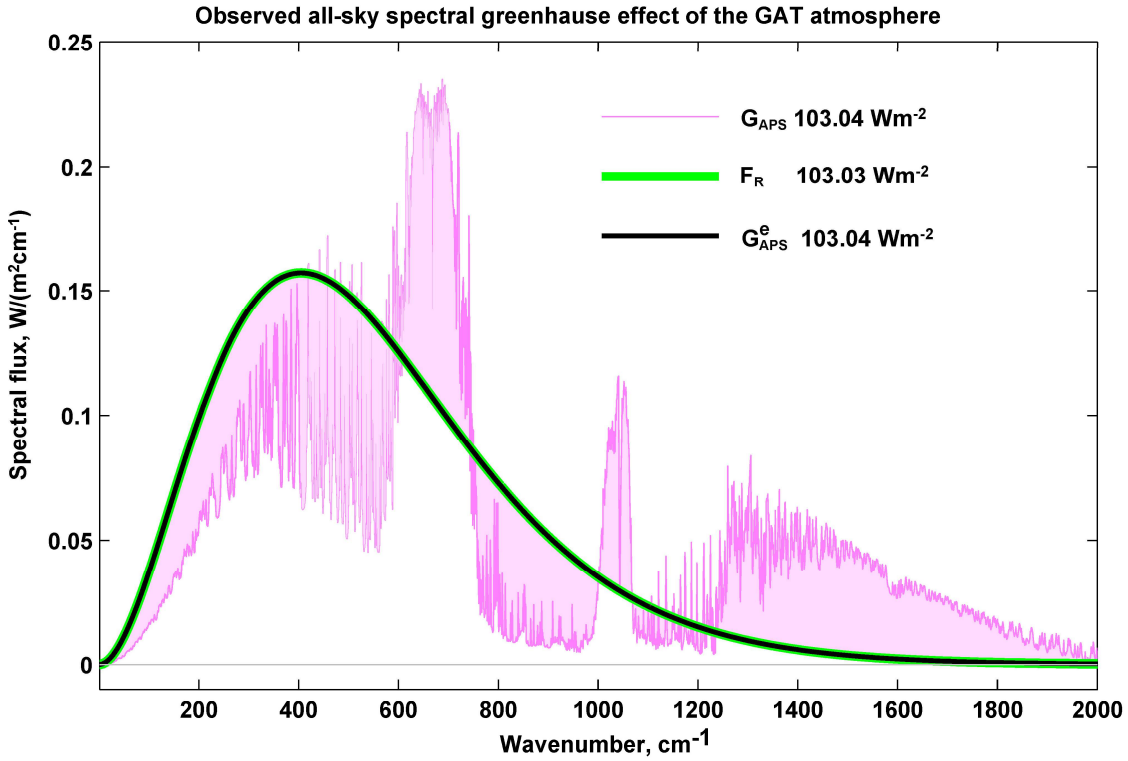

Figure 28: Spectral all-sky greenhouse effect referenced to the APS. The integrated flux densities from the G_{APS}^{e} and F_R curves agree quite well.

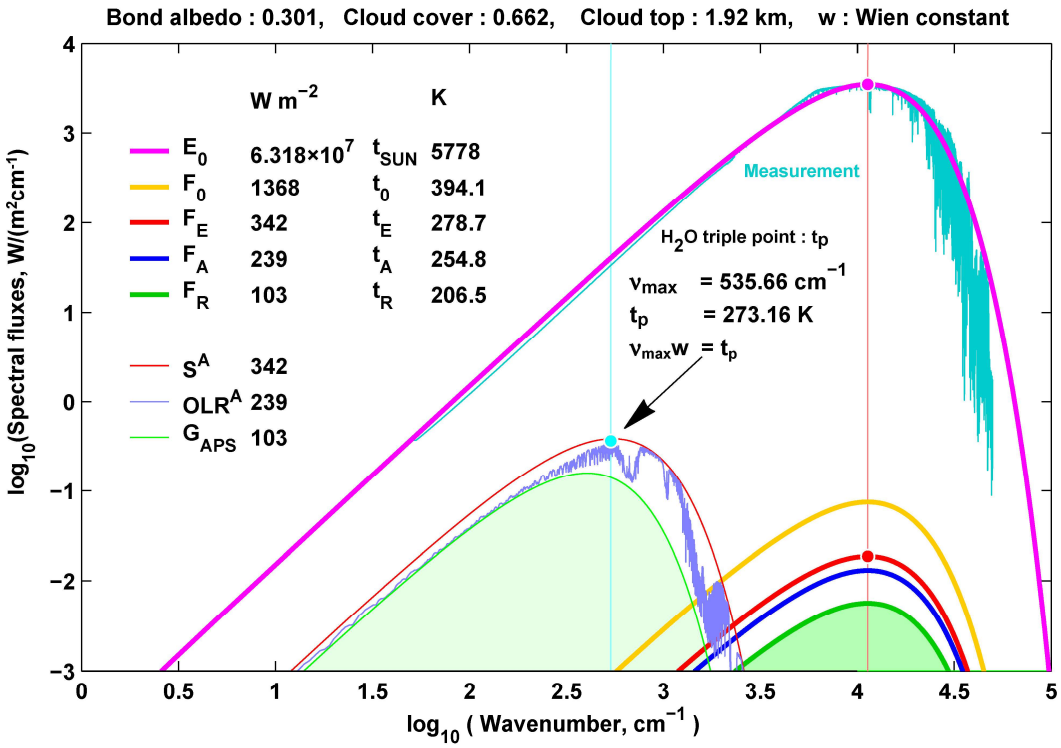

Figure29: Solar and terrestrial equilibrium blackbody spectra. The observed solar reference spectrum (dark cyan line) is from the Chance and Kurucz, 2010. The light blue line is the observed TOA OLR_{ν}^{A} *from the TIGR2 radiosonde archive.*

In Figure 29 all the SW and LW equivalent effective blackbody fluxes of the Sun-Earth system are presented. One must recognize, that at large, the Earth-atmosphere system is nothing but a converter of the low entropy SW solar radiation to maximum entropy terrestrial radiation. Theoretically the J^A entropy flux density of OLR^A may be expressed by the maximum of the spectral flux density of OLR^A: $J^A = c_e OLR^A_{\max,\nu}$, where $c_e = 4.2337344\,\mathrm{cm^{-1}K^{-1}}$, and $OLR^A_{\max,\nu} \approx 0.338\,\mathrm{Wm^{-2}/cm^{-1}}$ (at $\nu_{\max} \approx 535\,\mathrm{cm^{-1}}$). The light blue dot shows that the Earth has a special orbit where the Wien temperature is equal to the t_P phase temperature of the H_2O. Obviously the empirical spectral OLR^A has the maximum entropy flux density. The Wien constant in wavenumber representation is $w = 0.50994751\ \mathrm{K/cm^{-1}}$.

4.9 Comments on the new view of greenhouse effect

Almost all attempts to publish the results presented in this paper failed. Articles were routinely rejected by the mainstream scientific journals − Science, Astrophysical Journal, Tellus, Journal of Quantitative Spectroscopy and Radiative Transfer, Journal of Geophysical Researches etc. − mostly without sending for review. For example, the review of the Hungarian Science magazine (Magyar Tudomány) rejected the publication of the above results saying that it should be published first in some elite journals. Probably this is the reason why it is hard to find any useful critical comments on the presented quantitative results in the peer reviewed literature.

However, the blogosphere is flooded with academically illiterate comments from self-declared experts. As an example, it is worth reading the comments of A. Lacis (moderated by J. Curry at her Climate Etc. blog) on the Miskolczi's article [17].

The whole comment is just an ad hominem attack, probably motivated by the lack of his knowledge of basic radiative transfer concepts. There is a number of posts and comments on various websites like J. Curry, Science of Dooms and Real Climate etc. They don't deserve to be repeated in this journal.

They do not sound very scientific. Let us have a closer look into the *best* rebuttal. In Spencer 2010 [59] he wrote an *executive summary* on my [27] E&E article. Spencer simply ignored the important fact that in the whole article I dealt with clear sky conditions only. Since the clear and all sky fluxes are not directly (and quantitatively) comparable, his numerical comparisons with the [39] radiative budget is totally meaningless.

He is also, in my opinion, confused in a series of radiative transfer details: does not comprehend what anisotropy means and how to compute it (he called the spherical emissivity a *fudge factor*), what is the flux density form of the Kirchhoff-Planck relationship, what is the Virial theorem and how to apply it, what is directional and flux optical thickness.

If the blog comment above − without correct quantitative references to my well documented computational results − represent the matured opinion of the global warming community on the greenhouse science, then certainly the open scientific discussion must be improved on this topic.

One should remember that real science cannot ever be settled. Planetary climate science is not an exception; it will eventually make its progress with or without the 'consensus' of the politically oriented IPCC. The various hypotheses and approximations must be scientifically evaluated and eventually rejected, accepted or improved.

It is worth to look at what the consensus science means regarding the global mean surface radiative temperature. In Figure 30 we compare theoretical and empirical temperatures (in ºC) of the GAT atmosphere and some published temperatures in the mainstream literature in the last 30 years.

The title of the figure shows the theoretical equations (17) and (21), and there are other 20 numbered equations (inside the figure) giving the surface upward flux density S_U as the function of different flux density components and other RT parameters. The black dots are temperatures computed from the 20 equations via the SB law, the average is 12.93 ºC, and the standard deviation is 0.87 % (of the mean).

The red line is the GAT radiosonde observations which perfectly agrees with the (17,21) theoretical expectations. The magenta line with the black '+' symbols are the temperatures of the APS computed form F_E and S_U^A (5.53 ºC) apparently agreeing very well.

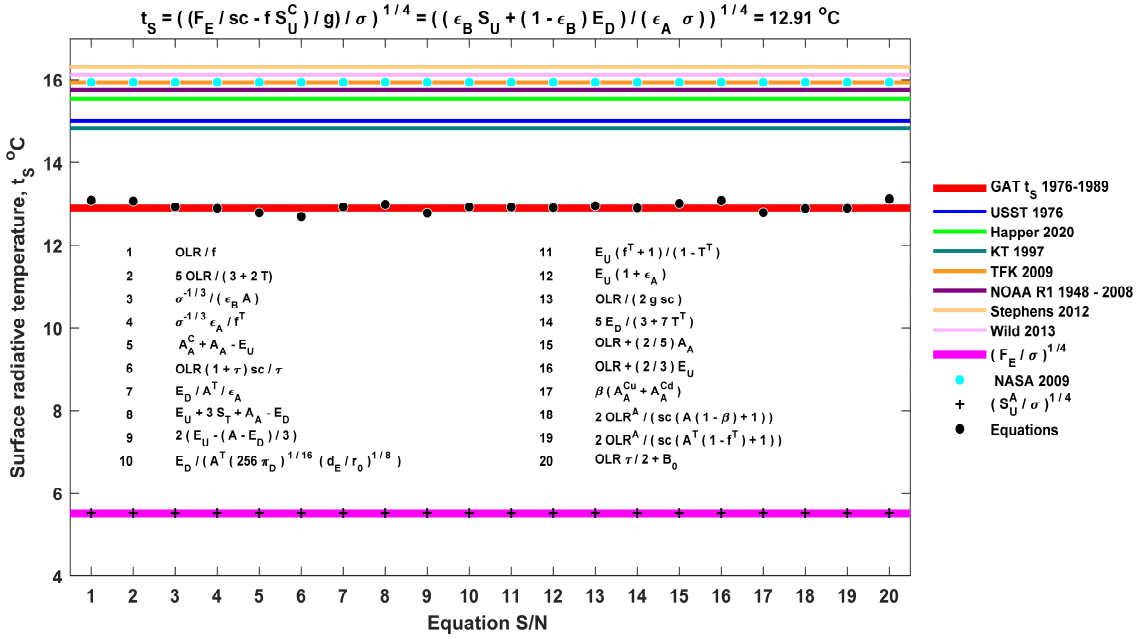

Figure 30: The global mean surface temperature from real science and from IPCC consensus. The published surface temperatures above 15 °C (in the upper part of the plot) are all erratic, they are more than 2 °C warmer than the real observed and theoretically expected ~ 13 °C. The public may deserve to know this information.

The upper part of the figure shows the diverse surface temperatures published in the peer-reviewed elite journals by the IPCC followers. None of them are anywhere close to the observed reality therefore they are useless for any climate study. No one may seriously expect to quantify a hypothetical small GHG surface warming effect if the initial surface temperature has an error of a magnitude larger.

5. Summary

The classic GH effect hypothesis is not a theory and it is unable to establish the required quantitative relationship between the GHG content of the atmosphere and the planetary surface temperature. In climate science the arbitrary definition of the GE is not suitable to associate the heat absorption properties of the atmosphere with the amount of GHGs present in the atmosphere. The reason it is invalid is the two-level radiative structure of the atmosphere and the unlimited supply of the water vapor in its three phases.

In addition to this the strongly stochastic nature of the humidity field makes the tracking of the phase changes of the H_2O impossible therefore the quantitative knowledge on the changes of the dynamical optical thickness (that is related to the phase transitions of the H_2O) is unknown. The large number of new physical relationships − and new universal constants of radiation physics − converging to form a coherent picture of the planetary IR radiative processes which ultimately establishes the correct radiative budget of the Earth-atmosphere system. Compared to surface and satellite flux density observations the rigorous numerical testing of the new equations has not produced any contradictory results. The new equations and constants were presented in a series of published papers, open conference presentations, and in NASA science team meetings. So far neither the equations nor the numerical results were openly challenged by radiative transfer experts or wider climate science community.

The theoretically constant equilibrium flux absorption coefficient of the Earth's atmosphere negates the existence of the Arrhenius type greenhouse gas greenhouse effect. If there are no changes in the greenhouse effect, then there is no climate sensitivity to man-made increase of the atmospheric CO_2. The excess optical thickness from increased CO_2 will condense into water droplets and will rain out from the atmosphere without the IPCC or government permission. Alternatively, structural variations in the global wind and humidity field, or the cloud cover may easily restore the equilibrium flux optical thickness. Evaluating the global average flux density components from ground truth observations it is evident, that the Earth-atmosphere system is in CRE with a theoretical solar constant. Some simple empirical manifestations of this equilibrium include:

1. equality of the Bond albedo and the empirical normalized all-sky greenhouse factor referenced to the APS:
   $g^A = G^A / S_U^A = \alpha_B = 0.3013$;
2. equivalence of the APS referenced greenhouse factor and reflected solar flux:
   $G^A = (S_U^A - OLR^A) = F_R = \alpha_B F_0 = 103.04\,\mathrm{Wm^{-2}}$;
3. equality of the sum of the radiative fluxes from the cloud top and cloud base and the total infrared radiation absorbed in the three regions of the atmosphere:
   $S_U^C + S_D^C = A_A + A_A^C + A_A^{Cu} + A_A^{Cd} = 653.8\,\mathrm{Wm^{-2}}$;
4. constancy of the global average atmospheric equilibrium infrared flux optical thickness:
   $\tau^T = \tau = \ln(S_U / S_T) = 1.86756$;
5. constancy of the radiative equilibrium water vapor column amount:
   $w = w^0 / (1 - 4T) = w^0 / (1 - 4T^T) = 2.612\,\mathrm{prcm}$;
6. theoretical and empirical equivalence of the cloud cover, transfer, and virial functions:
   $\beta = f = V = f^T = 0.661$;
7. equivalence of the theoretical intercepted absorbed available solar flux density from astronomical parameters and the empirical all-sky planetary TOA IR fluxes from the APS:
   $F_A = F_0(1 - \alpha_B) = OLR^A = S_T^A + E_U^A = 238.95\,\mathrm{Wm^{-2}}$;
8. equality of EBT of the intercepted available solar radiation over a unit area and the empirical EBT temperature of the APS:
   $(F_E / \sigma)^{1/4} = (S_U^A / \sigma)^{1/4} = 278.68\ \mathrm{K}$;
9. equality of the theoretical solar constant, empirical solar constant, and the long term observed average solar constant:
   $F_0^T = F_0^{OBS} = F_0 = 1367.95\,\mathrm{Wm^{-2}}$;
10. equality of the above cloud downward flux and the above cloud OLR:
    $E_D^C = OLR^C = 155.58\,\mathrm{Wm^{-2}}$;
11. equality of the simulated phase temperature and the H_2O triple point temperature:
    $t_P = (\sigma^{-1/3} + \varepsilon_A^{1/4} t_S) / 2 = 273.18\,\mathrm{K.}$;
12. equality of the SW and IR anisotropy factors:
    $\varepsilon_A = E_D / A_A = \varepsilon_A^T = 2^{-1/2} t_0 / (t_0 / \sigma)^{1/4} = 0.965153$;
13 equality of the surface radiative temperature from the Kirchhoff law, the solar constant, and from radiosonde:
    $t_S = (E_D / (A\varepsilon_A\sigma))^{1/4} = ((F_E / sc - \beta S_U^C / (1 - \beta)) / \sigma)^{1/4} = 286.06\,\mathrm{K}$;
14 equality of the SW virtual temperature and the empirical virtual temperature:
    $\hat{t}_0 = (t_0 / \sigma)^{1/4} = ((2(S_U^A + OLR^A / (1 - g^A)) / \sigma)^{1/4} / \sigma)^{1/4} = 288.744\,\mathrm{K}$;
15 equality of the SB constant from fundamental physical constants and from astronomical parameters:
    $\sigma = 10^{-4}(2/3)\pi^5\, \mathrm{c}_2 / \mathrm{c}_1^4 = (d_E / (r_0 F_0^{3/2}))^2 / \pi_D = 5.669833697 \times 10^{-8}\,\mathrm{Wm^{-2}K^{-4}}$

Science is not a talk-show, all arguments and critiques against the new view of the greenhouse effect must be quantitative. If this situation remains for long, then the system of new equations will be upgraded to the *only greenhouse theory* which explains the observed facts and obeys the fundamental principles of physics. The easily verifiable numerical facts mentioned above are only a fraction of the infinite number of possible quantitative relationships that all ensure the stability of the Earth's climate.

Scientific facts are stubborn things, they cannot be changed by fraud, misinformation, manipulation of climate data, censorship or democratic voting. Unfortunately, understanding the greenhouse effect phenomenon requires detailed knowledge of radiation physics, which can only be expressed in complex mathematical relationships, equations and formulae. Basic principles of radiation physics are not expected to be known by the general public, nor by climatologists, environmentalists and politicians who are boldly making statements on the subject but are not familiar even with the simplest physical concepts.

A good example is the most recent public announcement of a Hungarian politician Orsolya Ferencz who recently declared in a TV show that the Miskolczi Greenhouse Theory (MGT) is *officially invalid*, Ferencz (2022) [58]. It is clear, that the only purpose of her politically motivated statement is the misinformation of the people and, as such, it has no scientific value. Obviously, her scientific background information on the atmospheric radiative transfer is missing, and unfortunately, she has no idea about the falsification protocol of a scientific theory. One should remember that in the Middle Ages there was an official, government-approved view of the structure of solar system and how the inquisition worked to suppress new ideas. I hope climate science will proceed in a better way.

6. Conclusions

In this article all the arguments are focused on the theoretical and observational issues of the greenhouse effect and not on the question whether the global surface temperature is changing or not. The most valuable result of this research is the theoretical foundation of the observed radiative structure of the Earth's atmosphere. A long line of new radiation laws and their empirical validation together constitute the backbone of the physics of the greenhouse effect. Our planet enjoys the stable climate because the hydrological cycle forces the climate system to maintain the chaotic upper tropospheric humidity and wind field, the equilibrium cloud cover and precipitation, and moves the latent heat among the different geological reservoirs – as required by the planetary energetics. The role of the non-condensing GHGs stems from the fact that they do not participate in the hydrological cycle, they cannot contribute to the entropy production, but they can regulate the transmitted flux density to the level required by the Milne-Eddington equations. The greenhouse effect terminology of the climatologists refers to the steady state temperature difference between t_S and t_A. However, the $\Delta t_A \approx 28\,\mathrm{K}$, and the related $G_A \approx 128\,\mathrm{Wm^{-2}}$ clear-sky temperature and flux density differences are constants, they cannot violate the planetary radiative equilibrium and energy conservation principles. One should admit that Δt_A and G_A are practically meaningless parameters and they cannot be related to the IR atmospheric absorption of the CO_2. Any perturbations to the flux optical thickness by non-condensing GHGs will force the hydrological cycle to restore the theoretical equilibrium state. The greenhouse effect predicted by the Arrhenius greenhouse theory is inconsistent with the existence of the CRE. Hence, the CO_2 greenhouse effect as used in the current global warming hypothesis is impossible. Let us emphasize the overall conclusion:

The Arrhenius type greenhouse effect of the CO_2 and other non-condensing GHGs is an incorrect hypothesis and the CO_2 greenhouse effect based global warming hypothesis is also an artifact without any theoretical or empirical footing.

Without scientific proof the debate on the CO_2 GE based catastrophic AGW should be abandoned and policymakers should focus on the more urgent environmental and social issues of humanity. The recent worldwide energy crisis is a warning sign that the promotion of the so-called green energy is neither solving energy shortages nor helping to protect the environment from pollution. The climate does not need protection, but the clean environment does.

Funding: This work did not receive any funding.

Guest-Editor: Ole Henrik Ellestad; Reviewers: anonymous.

List of acronyms with the page numbers of first occurrences

SW	shortwave (1)
IR	infrared (1)
LW	long-wave (1)
APS	active planetary surface (1)
GHG	greenhouse gas (2)
RE	radiative equilibrium (2)
TOA	top of the atmosphere (2)
CRE	Chandrasekhar-type radiative equilibrium (2)
WV	water vapor (3)
GE	greenhouse effect (4)
LTE	local thermodynamic equilibrium (4)
AGW	anthropogenic global warming (4)
SB	Stefan-Boltzmann (5)
NIST	National Institute of Standards and Technology (5)
EBT	equivalent blackbody temperature (5)
RT	radiative transfer (6)
EBF	Planck equivalent blackbody spectral flux density (7)
GAT	global average TIGR2 atmospheric structure (9)
IPCC	Intergovernmental Panel on Climate Change (9)
GCM	global climate models (10)
NOAA	National Oceanic and Atmospheric Administration (11)
NOAA-S	testing facility in Sterling Virginia (11)
LBL	line-by-line (12)
HARTCODE	High-resolution Atmospheric Radiative Transfer Code (12)
RTF	Radiative transfer function (15)
OLR	outgoing longwave radiation (28)
MGT	Miskolczi Greenhouse Theory (44)
MCT	mean color temperature (48)
ECS	equilibrium climate sensitivity (51)

Acknowledgements

I am indebted to A. Rörsch, C. Wiese, E. Berry, A. Harvey, D. Hagen, S. Welcenbach, C. Game, K. Gregory, and N. Van Andel, for their substantive professional discussions. Also, thanks are due to K. Sifrin, K. Vinnikov, I. Wilson, J. Pompe, R. Tscheuschner, D. Brooks, W. Guang, Y. Shao-min, R. Tattersall, L. Szarka, E. Petz, I. Héjjas, I. Kalmár, Z. Korényi, L. Livo, F. Tompa, S. Nagy, Z. Kolláth, S. Kenyeres, E. Fuggerth, A. Bazso-Dombi, S. Balogh, and all those who have followed my many years of research and contributed with their useful advices to clarify numerous theoretical problems that have arisen in the course of my work. I am very grateful to D. Lawson, and the editors and reviewers for their comments and the help with the technical preparation of the manuscript.

References

[1] Kandel, R., and Viollier, M., 2004: *Planetary radiation budgets*, Space Science Reviews (2005) 120: 1–26DOI: 10.1007/s11214-005-6482-6, pp. 4

[2] Chandrasekhar, S., 1960: *Radiative Transfer*. © 1960 by Dover Publications, Inc.

[3] Scafetta, N., 2010: *Empirical evidence for a celestial origin of the climate oscillations and its implications.* Journal of Atmospheric and Solar-Terrestrial Physics 72 (2010) 951

[4] Miskolczi, F., 2016: *Expert opinion on the greenhouse gas theories and the observed infrared absorption properties of the Earth's atmosphere.* https://climatecite.com/ferenc-miskolczi-testimony-in-mann-vs-ball-libel-case/

[5] Manabe, S. and Wetherald, R. T., 1967: *Thermal Equilibrium of the Atmosphere with a Given Distribution of Relative Humidity.* Vol. 24, No. 3 JAS, (1967) 242

[6] Andrews, D. E., 2023: *Clear Thinking about Atmospheric CO2.*Science of Climate Change, Vol. 3.1 (2003), pp. 1-13, https://doi.org/10.53234/scc202301/13

[7] le Pair C. and de Lange C.A., 2022: *On the Theory of the Earth's Physical Parameters, Distributed in Space and Time. Science of Climate Change*. Vol. 2.3 (2022) pp. 302-309

[8] Kramm, G., and Dlugi, R., 2011: *Scrutinizing the atmospheric greenhouse effect and its climatic impact*. Natural Science, Vol.3, No.12, 971-998 (2011), http://dx.doi.org/10.4236/ns.2011.312124

[9] Mohr P. J., Taylor B. N. and Newell D. B., 2007: *CODATA Recommended Values of the Fundamental Physical Constants: 2006*. National Institute of Standards and Technology, Gaithersburg, Maryland 20899-8420, USA

[10] Raval, A., and Ramanathan, V., 1989: *Observational determination of the greenhouse effect*. NATURE 342 (1989) 758-761

[11] Ahren, J. L., 2004: *Planets*. http://zebu.uoregon.edu/~js/glossary/albedo.html, © 2004, Judson L. Ahern

[12] Schmidt, G., A., Ruedy, R., A., Ron L. Miller, R., L., Lacis, A. A., 2010: *Attribution of the present-day total greenhouse effect*. JGR, Vol. 115, D20106, doi:10.1029/2010JD014287, 2010, pp. 3

[13] Lacis, A., Schmidt, G.A., Rind, D., Ruedy, R., A., 2010: *Atmospheric CO_2: Principal Control Knob Governing Earth's Temperature*. Science 330 (2010) 356-359

[14] NOAA, 1976:*US Standard Atmosphere 1976*. NOAA, NASA, USAF, Washington, D.C. October1976, NOAA-S/T 76-1562

[15] Miskolczi, F. and Mlynczak M., 2004: *The greenhouse effect and the spectral decomposition of the clear-sky terrestrial radiation*. Időjárás, 108, 4, 209–251, Corpus ID: 44927545, https://www.met.hu/en/ismeret-tar/kiadvanyok/idojaras/index.php?id=261

[16] Miskolczi, F. M., 2007: *Greenhouse effect in semi-transparent planetary atmospheres*. IDŐJÁRÁS, Quarterly Journal of the Hungarian Meteorological Service, Vol. 111, No. 1, January–March 2007, pp. 1– 40

[17] Miskolczi, F. M., 2014: *The Greenhouse Effect and the Infrared Radiative Structure of the Earth's Atmosphere*. Development in Earth Science Vol. 2, 2014, http://www.seipub.org/des, https://www.researchgate.net/publication/268507883

[18] Arrhenius, S.,1896: *On the Influence of Carbonic Acid in the Air upon the Temperature of the Ground*. Philosophical Magazine and Journal of Science Series 5, Vol. 41, April 1896, 237-276.

[19] Pierrehumbert, R. T., 2011: *Infrared radiation and planetary temperature*. © 2011 American Institute of Physics, 8·0031·9228·1101·010-6, Jan. 2011, Physics Today, 33-38

[20] Lindzen, R. S., 2007: *Taking Greenhouse Warming Seriously*. E&E, Vol. 18, No. 7+8, 2007, 937–950

[21] Nurse, P. and Cicerone, R. J., 2014: Climate Change, Evidence & Causes. An overview from the Royal Society and the US National Academy of Sciences, RS & NAS Feb. 27th 2014

[22] Smith, A. P., 2008: *Proof of the Atmospheric Greenhouse Effect*. American Physical Society, 1 Research Road, Ridge NY, 11961, PACS numbers: 92.60. Vb,05, 90. +m, (2008) http://arxiv.org/abs/0802.4324v1

[23] Schwarzschild, K., 1906: *On the equilibrium of the Sun's atmosphere*. Nachr. v. d. Königlichen Ges. d. Wissenscaften zu Göttingen. Math-Phys. Klasse, Vol. **195,** 41-53.

[24] Poyet, P., 2022: *The Rational Climate e-Book*. The Extended 2nd Edition https://patricepoyet.org/

[25] Miskolczi, F., 1989: *High resolution atmospheric radiative transfer code (HARTCODE)*.https://www.researchgate.net/publication/287994595DOI: 10.13140/RG.2.1.2319.6240

[26] Rizzi, R., Matricardi, M., and Miskolczi, F., 2002: *Simulation of up-looking and down-looking high-resolution radiance spectra with two different radiative transfer models*. Applied Optics, Vol. 41, No. 6, 20 Feb. 2002, 940-956

[27] Miskolczi F. M., 2010: *The stable steady-state value of the earth's global average atmospheric Planck-weighted greenhouse gas optical thickness*. Energy & Environment 21, 4 (2010) 243-262

[28] Kratz, D. P., Mlynczak, M. G., Mertens, C. J., Brindley, H., Gordley, L. L., Martin-Torres, J., Miskolczi, F. M., and Turner, D. D., 2005: *An inter-comparison of far-infrared line-by-line radiative transfer models*. Journal of Quantitative Spectroscopy & Radiative Transfer 90 (2005) 323–341

[29] Saunders, R., Rayer, P., Brunel, P., von Engeln, A., Bormann, N., Strow, L., Hannon, S., Heilliette, S., Liu, X., Miskolczi, F., Han, Y., Masiello, G., Moncet, J.-L., Uymin, G., Sherlock, V., and Turner, D. S., 2007: *A comparison of radiative transfer models for simulating Atmospheric Infrared Sounder (AIRS) radiance*s. JGR-Atmosphere, Vol. 112, D01S90, 2007, 1-17, http://onlinelibrary.wiley.com/doi/10.1029/2006JD007088/epdf

[30] Miskolczi, F. M., 2011: *The stable stationary value of the Earth's global average atmospheric infrared optical thickness*. European Geophysical Union, EGU 2011, Vienna, 13662, 1-20, http://presentations.copernicus.org/ EGU2011-13622_presentation.pdf

[31] Scott, N., 2009: *TIGR, Thermodynamic Initial Guess Retrieval 2000*. http://ara.lmd. polytechnique.fr/htdocs-public/products/TIGR/TIGR.html

[32] NOAA NCEP, NOAA Earth System Research Laboratory, 2012: *Time series*. http://www.cdc.noaa.gov/cgi-bin/Timeseries/timeseries1.pl

[33] McIDAS Water Vapor Composit_2008: http://www.ssec.wisc.edu/data/composites.html

[34] Chance, K., and Kurucz, R., L., 2010: *An improved high-resolution solar reference spectrum for earth's atmosphere measurements in the ultraviolet, visible, and near infrared*. Journal of Quantitative Spectroscopy & Radiative Transfer 111 (2010) 1289–1295

[35] Kopp, G., and Lean, J., L., 2011: *A new, lower value of total solar irradiance: Evidence and climate significance*. Geophysical Research Letters, Vol. 38, L01706, doi:10.1029/2010GL045777

[36] Ramanathan, V., and Inamdar A. K., 2006: *The radiative forcing due to clouds and water vapor*. In Frontiers of Climate Modeling, Cambridge University Press, 2006, 119-151

[37] Shaviv, N., J., Shaviv, G., and Wehrse, R. 2012: *The Maximal Runaway Temperature of Earth-like Planets*. 2011, Icarus, 216, 2, 403-414

[38] NASA, 2010: *Earth's energy budget.* http://www.nasa.gov, Document: NP-2010-05-265-LARC, http://scienceedu.larc.nasa.gov/energy_budget

[39] Kiehl, J., T., and Trenberth, K., E., 1997: *Earth's Annual Global Mean Energy Budget.* AMS, BAMS, Vol. 78, No. 2, 1997, pp.199

[40] Trenberth, K., E., Fasullo, J., T., and Kiehl J., 2009: *Earth's Global Energy Budget.* AMS, BAMS, March 2009 pp. 311-323

[41] Stephens, G., L., et al., 2012: *An update on Earth's energy balance in light of the latest global observations.* Nature. Geo-science. 5 (2012) 691–696, doi:10.1038/ngeo1580

[42] Wild, M., Folini, D., Schar, C., Loeb, N., Dutton, E. G., Konig-Langlo, G., 2012: *The global energy balance from a surface perspective.* Climate Dynamics (2013) 40:3107–3134, DOI 10.1007/s00382-012-1569-8

[43] Berk, A., Anderson, G., P., Acharya, P., K., Shettle, E., P., 2008: *MODTRAN5.2.0.0 User's Manual*. ftp://ftp.pmodwrc.ch/pub/Claus/Vorlesung2009/ModtranDaten_etc/ MODTRAN(R) 5.2.0.0.pdf

[44] NASA, 2016: *Notes on the Fact Sheets.* NASA Official: Ed Grayzeck, edwin.j.grayzeck@nasa.gov, Last Updated: 29 February 2016, DRW

[45] Miskolczi, F. & Héjjas, I., 2021: *The self-regulation of climate*. *Ferenc Miskolczi's climate theory with comments by István Héjjas.* In Hungarian: *Az Éghajlat Önszabályozása. Miskolczi Ferenc klímaelmélete Héjjas István magyarázataival.* Püski 2021, [ISBN 978-963-302-328-0]

[46] NASA, 2012: *Sun Fact Sheet*.nssdc.gsfc.nasa.gov/planetary/factsheet/sunfact.html

[47] NASA, 2012: *Earth Fact Sheet*. nssdc.gsfc.nasa.gov/planetary/factsheet/earthfact.html

[48] Mihalas, D. & Mihalas, B. W., 1984: *Foundations of radiation hydrodynamics*. Oxford University Press, 1984, pp. 328

[49] Scafetta, N. & Willson, R. C., 2014: *ACRIM total solar irradiance satellite composite validation versus TSI proxy models*. Astrophysics and Space Science. DOI 10.1007/s10509-013-1775-9

[50] Wu, W. and Liu Y., 2010: *Radiation entropy flux and entropy production of the Earth system*. Rev. Geophysics. 48, RG2003, doi:10.1029/2008RG000275.

[51] Scafetta, N., Milani, F., Bianchini, A., Ortolani, S., 2016: *On the astronomical origin of the Hallstatt oscillation found in radiocarbon and climate records throughout the Holocene.* Earth-Science Reviews162, 24–43, 2016. http://dx.doi.org/10.1016/j.earscirev.2016.09.004

[52] Scafetta, N., 2022: *CMIP6 GCM ensemble members versus global surface temperatures.* Climate Dynamics, https://doi.org/10.1007/s00382-022-06493-w

[53] NIST, 2018: *Fundamental Physical Constants—Extensive Listing* http://physics.nist.gov/constants

[54] NASA, 2016: *Jupiter Fact Sheet*. nssdc.gsfc.nasa.gov/planetary/factsheet/earthfact.html NASA Official: Ed Grayzeck, edwin.j.grayzeck@nasa.gov, Last Updated: 19 April 2016,dave.williams@nasa.govNIST

[55] Willman, A., J., 2012: *Planetary System Data.* Copyright © 1996 A. J. Willman, Jr. All rights reserved. http://www.princeton.edu/~willman/planetary_systems/,This page was last updated: 2012 September 20

[57] VanWijngaarden, W. A. and Happer, W., 2020: *Dependence of Earth's Thermal Radiation on Five Most Abundant Greenhouse Gases*. arXiv:2006.03098v1 [physics.ao-ph] 4 Jun 2020

[58] Ferencz, O., 2022: https://hirtv.hu/video/261689

[59] Spencer, R., W., 2010: *Comments on Miskolczi's (2010) Controversial Greenhouse Theory.* https://www.drroyspencer.com/2010/08/comments-on-miskolczi%E2%80%99s-2010-controversial-greenhouse-theory/

[60] Shaviv, N., 2006: *On Climate Sensitivity and why it is probably small.* http://www.sciencebits.com/OnClimateSensitivity

[61] VanAndel, N., 2010: *Note on the Miskolczi Theory*. E&E, Vol. 21, No. 4, 2010, pp.277-292

[62] Harde, H., 2019: *What Humans Contribute to Atmospheric CO2: Comparison of Carbon Cycle Models with Observations*. International Journal of Earth Sciences. Vol. 8, No. 3, pp. 139-159.

[63] Berry, E., X., 2021: *The Impact of Human CO2 on Atmospheric CO2*. Science of Climate Change, Vol. 1.2 (2021) pp. 213-249

[64] Peixoto, J., P., Oort, A., H., 1992: *Physics of Climate*. American Institute of Physics, New York, Printed in the United States of America. Third printing, 1993

Appendix

Duality of flux density and radiation temperature

1. Planck radiation laws

Let us recall the most fundamental equations of the Planck radiation laws. The wavenumber, wavelength, and frequency representations are all suitable for spectral characterization of radiative processes. Further on we use the wavenumber representation, usually found in IR spectroscopy, where the $b_\nu(t_\nu)$ spectral radiances are expressed in units of mW/(m^{2}cm^{-1}sr):

$$b_\nu(t_\nu) = c_2\nu^3(\exp(c_1\nu / t_\nu) - 1)^{-1}, \tag{a1}$$

where c_1 and c_2 are the radiation constants appropriate for the wavenumber domain, and the t_ν color temperatures are expressed in K. In case of isotropic radiation field $t_\nu \equiv t$ is a constant, the Kirchhoff-Planck relationship holds and $b_\nu(t)$ is called the Planck (spectral) distribution of blackbody radiance. From (a1) follows the definition of the color (or brightness) temperature, commonly used in remote sensing applications:

$$t_\nu(b_\nu) = c_1\nu / \ln(c_2\nu^3 / b_\nu + 1). \tag{a2}$$

In case of gaseous materials, the spectral structure of t_ν may be very complex, and the $\overline{t}_\nu$ average may not be equal to EBT. We have seen that, the *mean color temperature* (MCT) of the Sun is about 292.71 K smaller: $t_{SUN} = 5778.075$, $\overline{t}_{\nu,SUN} = 5485.362$ K. In isotropic case $t = t_\nu = \overline{t}_\nu$. In Table 1 some characteristic parameters of the SW solar radiation are presented. Detailed explanations of the symbols are given in section *2*.

Table 1: Radiative parameters of the Sun.

EBT and *MCT* are the equivalent blackbody, and mean color temperatures

Parameters	*EBT*	*MCT*	Units	Symbols
1 *temperatures*	5778.0758	5485.36	K	$\tilde{t} = \overline{t}_\nu$
2 *Wien's law*	5778.0623	5485.3524	K	$W_\nu\nu_{\max}$
3 *SB law*	63197970	51332316	Wm^{-2}	$\sigma\tilde{t}^4$
4 *flux density*	63197967	51332316	Wm^{-2}	$B(\tilde{t})$
5 *MCT*	5778.0754	5485.36	K	$\tilde{t}$
6 *virtual temperatures*	565.00621	557.71036	K	$\hat{t}$
7 *dual flux density*	5778.0754	5485.36	Wm^{-2}	$\tilde{B}(\hat{t})$
8 *maximum of* $B_\nu(\tilde{t})$	3444.5702	2947.1405	Wm^{-2}/cm^{-1}	$B_{\max,\nu}$
9 *maximum wave number*	11330.7	10756.7	cm^{-1}	$\nu_{\max}$
10 *entropy flux density*	14583.396	12477.415	Wm^{-2}/K	J

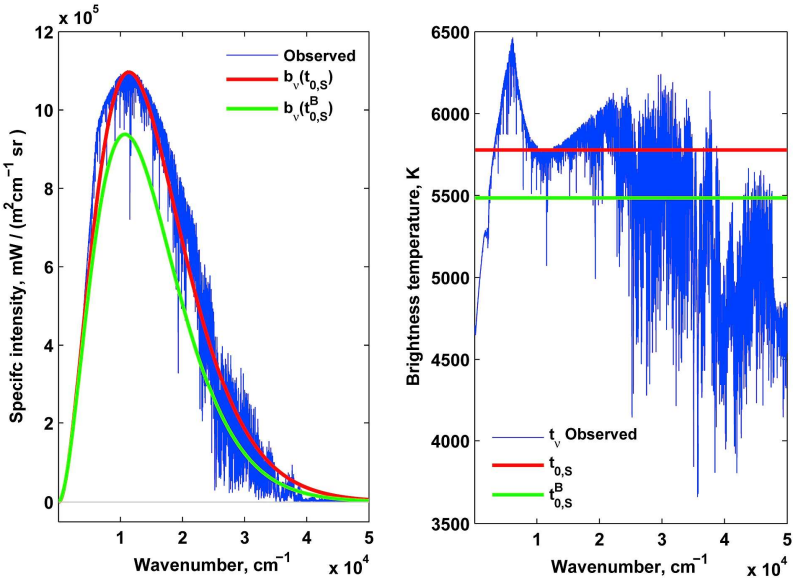

Figure 31: Spectral characteristic of the observed solar specific intensity (left plot) and brightness temperature spectra (right plot). The Sun is definitely not a blackbody radiator.

In Figure 31 the solar spectral radiance and color temperature spectra are shown. From the $b_\nu(t_{0,S})$ and $b_\nu(t^B_{0,S})$ specific intensity spectra – in the left plot – the solar constant could be ~18 % (257 Wm^{-2}) less if computed from $b_\nu(t^B_{0,S})$ instead. See also row 4 and 5 in Table 1. This figure actually is a proof, that the solar radiation is not blackbody radiation, therefore, any *equilibrium climate sensitivity* (ECS) study of GCMs – related to the variations in the solar constant – cannot be based on the SB law or the Planck response, Shaviv (2015) [60].

The form of the Kirchhoff-Planck relation for radiative flux densities is obtained by integrating (a1) by solid angle and wavenumber. The conversion of spectral radiances from units of $mW/(m^2cm^{-1}sr)$ into $B_\nu(t)$ spectral flux densities in $W/(m^2cm^{-1})$ means a multiplication by the $\pi_D = \pi \times 10^{-3}$ factor. Spectrally integrated $B_\nu(t)$ will result in the $B(t)$ flux density function in Wm^{-2}, which depends only on the temperature. The wavenumber and solid angle integral of (a1) yields the Stefan-Boltzmann (SB) law:

$$B(t) = \sigma t^4 . \qquad \text{(a3)}$$

In the wavenumber domain the SB constant may be expressed with the c_1 and c_2 radiation constants: $\sigma = 10^{-4}(2/3)\pi^5 c_2 / c_1^4 = 5.669833697 \times 10^{-8}\ Wm^{-2}K^{-4}$, where $c_1 = 1.438786\ K/cm^{-1}$, and $c_2 = 1.1909596 \times 10^{-5}\ mWm^{-2}cm^{-4}sr^{-1}$. By definition, the t temperature obtained from (a3) is the $t = (B/\sigma)^{1/4}$ EBT, (for the Earth $t_0 = (F_0/\sigma)^{1/4} = 394.101649\ K$).Specifically for the Earth, the $\sigma \equiv \pi_D E_0 / F_0^4 \equiv \pi_D (d_E / r_0)^2 / F_0^3$ relationships numerically also holds exactly. (In double-precision arithmetic '*exact*' means a numerical accuracy up to 15 significant decimal digits.)

The form of the SB law for the $U(t)$ energy density of the radiation field: $U(t) = at^4\ Jm^{-3}$, where $a = 4\sigma / c\ Jm^{-3}K^{-4}$, and c is the speed of the light in vacuum. Differentiation of (a1) by wavenumber

yields Wien's displacement law:

$$t / \nu_{\max} = W_{\nu}, \tag{a4}$$

where $W_{\nu} = 0.50994751$ K/cm^{-1} is the Wien constant in the wavenumber representation, and $\nu_{\max}$ is the wavenumber of the maximum of the $B_{\nu}(t)$ function. The radiation entropy flux density may be expressed in different forms, Wu & Liu (2010) [50]:

$$J = cat^3 / 3 = (4/3)\sigma t^3 = (4/3)\sigma^{1/4} B^{3/4} = (4/3)B/t\,. \tag{a5}$$

At a unique temperature of $t_M = \sigma^{-1/3}$ K, and unique flux density of $B_M = \sigma^{-1/3}$ Wm^{-2} (a3) reduces to a mathematical identity of $t_M \equiv B_M = \sigma^{-1/3} = 260.301$, and the temperature and flux density cannot be numerically distinguished. At t_M and B_M the entropy flux density – from (a5) – is exactly 4/3 Wm^{-2}/K.

At this point we did not pay much attention to the numerical value of $\sigma^{-1/3}$, and we just introduced the $\sigma_M = \sigma^{-1/3}$ and $c_M = \pi_D^{1/3}\sigma_M = 38.123536778$ notions, where σ_M and c_M quantities can equally have dimensions of K or Wm^{-2}, and called this strange situation to temperature-flux density duality. We may call t_M and B_M *mixing temperature* and *mixing flux density*, and refer to the c_M parameter as *dual entropy constant*.

However, empirical evidence shows that σ_M cannot be discarded as a physically meaningless quantity. Radiosonde observations showed that $2t_P - t_S \cong \sigma_M$, indicating that σ_M, (or c_M) is quantitatively associated with the phase temperature of the H_2O and the global mean surface temperature, (see [17]). Flux density simulations show that the $t_T + E_D - A_A \cong \sigma_M$ empirical relationship also holds, indicating that mixed (temperature and flux density) mathematical expressions of physical quantities are also associated with σ_M.

Using astronomical parameters of the Earth and Sun ($E_0, t_{SUN}, F_0, r_0, d_E, d_F$) and the SB law, later we were running into several mathematical identities where the dimensions of the involved quantities did not match:

$$F_0 = \pi_D t_{SUN}, \quad \sigma F_0^4 = \pi_D E_0, \quad (4/3)\sigma F_0^3 = (4/3)\pi_D d_F\,. \tag{a6}$$

In the 1st equation of (a6) the left side is flux density in Wm^{-2},the right side is temperature in K. In the equivalent form of this equation $F_0 \equiv (\pi_D E_0 / \sigma)^{1/4}$, where the E_0 flux density virtually has the dimension of radiance. Taking the 4th power of this equation and multiplying with σ we get the 2nd equation, where both sides are flux densities but on the left side F_0 must be temperature in K, as required by the SB law. In the 3rd equation the right side is a dimensionless quantity, while the left side (assuming that F_0 is temperature in K) may be taken as entropy flux density in Wm^{-2}/K, see the second equation of (a5) . Perhaps the $\pi_D^{1/4} t_{SUN} = 1367.9514$ K quantity may be called as the t_{π}K *entropy temperature* of the Sun.

Rearranging the 3rd equation of (a6) and using the $d_F = (r_0 / d_F)^2 = F_0 / E_0$ definitions of the dilution factor, the solar constant equation (23) in *4.2* may easily be derived: $F(d) = c_M d_E^{8/3} r_0^{-2/3} d^{-2}$. Obviously, for the Earth $d = d_F$, $F(d_E) = c_M d_F^{-1/3}$ and here c_M is Wm^{-2}. Notice, that because of the

$d_E^{8/3}$ term in (23), the $\sigma = \pi_D E_0 / F(d)^4$ relationship – from the 2nd equationof (a6) – cannot be valid for any other planets.

Further interesting fact is, that the radiation entropy flux density from (a5) for the t_π entropy temperature is 193.51 Wm^{-2}/K, which is numerically very close to the GAT clear-sky emission of $E_U = 193.24\,Wm^{-2}$, (see Figure 7). Similar coincidences, without straightforward physical explanations, used to be termed as tele-connections. Such surprising numerical relationships are the $F_0 = (15/(\pi^4 c_2 d_F))^{1/3} c_1^{4/3}$, or $\sigma = \pi_D E_0 / F_0^4$ expressions, where c_2, c_1, and σ are known functions of the fundamental physical constants.

All of the strange relationships just mentioned point to a hidden mathematical property of the Planck radiation laws, and also to the very special astronomical parameters of the Sun and the Earth's orbit. Because of the mixed dimensions (a3) may not be a unique relationship between flux densities and temperatures. Looks like (a3) structurally represents physically meaningful relationships among long lines of different RT quantities.

2. Law of radiation-temperature duality

Let $\tilde{t} = \overline{t}_\nu$ be the MCT of the spectral t_ν over the whole wavenumber domain. Let us also define the $\hat{t} = (\tilde{t} / \sigma)^{1/4}$ *virtual temperature* as the EBT from the flux density being numerically exactly equal to $\tilde{t}$. The virtual notation indicates that $\hat{t}$ is a mixed physical quantity, meaning that $\tilde{t}$ in K may formally enter into the SB law as flux density in Wm^{-2}.

A very important mathematical property of equations (a1-a5) is the exact mathematical equivalence of the $\tilde{B}(\hat{t})$ Wm^{-2} integrated $\tilde{B}_\nu(\hat{t})$ spectral flux density, and the average color(or brightness) temperature $\tilde{t}$ K:

$$\tilde{t} \equiv \tilde{B}(\hat{t}) = \pi_D \int_0^\infty c_2 \nu^3 / (\exp(c_1 \nu / (\overline{t}_\nu / \sigma)^{1/4}) - 1) d\nu \,. \qquad \text{(a7)}$$

Equation (a7) is a new insight not found in the literature and will be referred to hereafter as the *law of radiation-temperature duality*. Further on, $\tilde{B}(\hat{t})$ and $\tilde{t}$ will be termed as *dual flux density* and *dual temperature*. Remember, that for ideal blackbody radiation $\tilde{t}$ is the t temperature itself. To prove that the law of duality holds for temperature t_M is relatively simple. Using (a1) one has to show quantitatively that (a7) is true:

$$t_M = \pi_D \int_0^\infty b_\nu(t) d\nu = \pi_D c_2 \int_0^\infty \nu^3 (\exp(c_1 \nu / t_M) - 1)^{-1} d\nu \,, \qquad \text{(a8)}$$

where $t_M = \sigma^{-1/3} = (\pi_C c_2)^{-1/3} c_1^{4/3}$, and $\pi_C = \pi^5 / 15000$. Substituting ν with the $x = \nu c_2 \pi_C / c_1$ new variable we arrive at the next equation:

$$(\pi_C\, c_{2,\nu})^{-1/3} c_{1,\nu}^{4/3} = \pi_D c_{2,\nu} (c_{2,\nu} \pi_C / c_{1,\nu})^{-4/3} \int_0^\infty x^3 (\exp(x) - 1)^{-1} dx \,, \qquad \text{(a9)}$$

where the Riemann sum of the right integral is $\pi^4 / 15$, which reduces (a9) to an identity, independent of t_M. Since any t temperature can be expressed (scaled) by t_M with a constant of proportionality, our statement holds for any t temperature.

In Figure 32 HARTCODE GAT simulations of the all-sky OLR_ν^A and the relevant t_ν brightness temperature spectra are presented. On the contrary to the solar spectra in Figure 31, the terrestrial radiation is a fair approximation of the maximum entropy blackbody radiation.

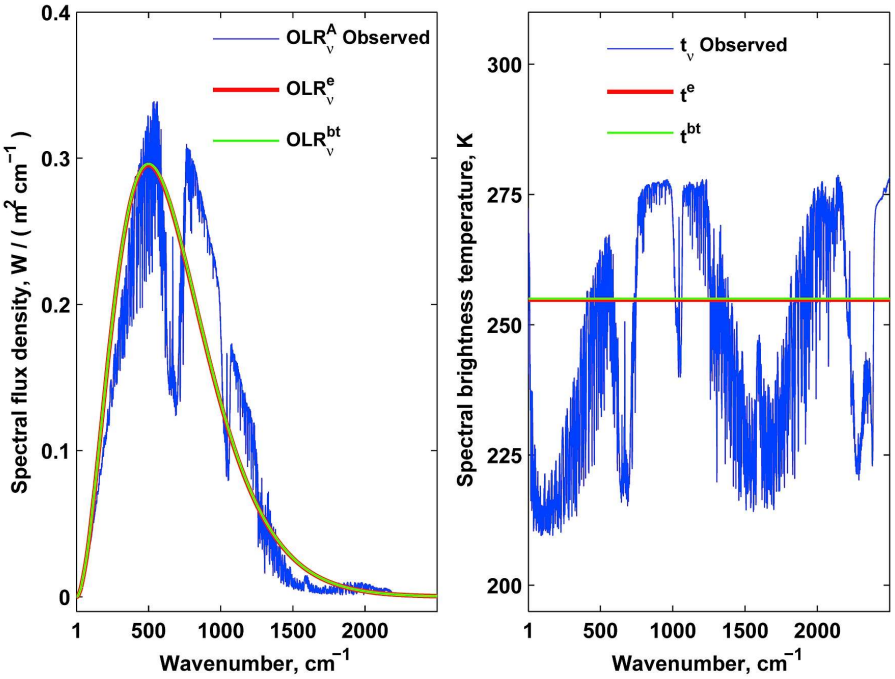

Figure 32: Spectral OLR_ν^A and t_ν (thin blue lines) of the GAT atmosphere. In the right plot the t^{bt} mean brightness temperature and the t^e EBT are practically equal. In the left plot OLR_ν^e EBF, and OLR_ν^{bt} flux density from t^{bt} are also equal. The IR radiation leaving the Earth is close to ideal blackbody radiation.

The integral flux densities of OLR_ν^e and OLR_ν^{bt} are about equal, and the SB law for ECS estimations in CO_2 doubling studies theoretically may safely be applied. Based on the SB law and GCM simulations without feedback processes, the ECS in Scafetta (2022) [52] would result in ~1 K surface temperature rise.

Of course, this is a plain nonsense, the stochastic climate system is not controlled by the SB law, but by the random combination of the most diverse physical processes, laws, and principles of nature, which is ultimately able to produce the OLR_ν^A maximum entropy IR radiation of the Earth-atmosphere system. On the other hand, popular CO_2 doubling studies in GCM simulations are based on artificial atmospheric structures, therefore producing quite unrealistic results which are violating the Schwarzschild-Milne equations.

The means of conversion of the incoming SW solar to outgoing LW terrestrial radiation are based on the stochastic processes in the global hydrological cycle, which is – using the infinite supply of water from the oceans – creating the global average equilibrium cloud cover.

The duality of flux density and temperature is independent of the spectral structure of the radiation field, should therefore be regarded as an intrinsic mathematical property of the Planck distribution.

In the context of the Planck distribution, this fact is probably not of great novelty to mathematicians working on theory of the distribution functions, but it may be of some interest to physicists, astrophysicists or astronomers. The duality of flux density and temperature provides the theoretical background for number of unexplained tele-connections.

The SW solar radiation field must obey the law of duality. At d_E distance from the Sun a virtual $\hat{t}_0 = (t_0 / \sigma)^{1/4} = 288.74448$ K temperature can be computed, which will be consistent with the t_0 EBT, and the numerical identity of $B_0 = \sigma \hat{t}_0^4 \equiv (F_0 / \sigma)^{1/4} = t_0 = 394.11692$ Wm^{-2} or K. Just like t_0, $\hat{t}_0$ is an astronomical parameter and has nothing to do directly with the t_S global mean surface radiative temperature (from (17) in paragraph *2.2*). By definition, the $\varepsilon_A^T = t_E / \hat{t}_0$ dimensionless ratio is the *theoretical anisotropy factor of the incoming directional SW radiation field* at the d_E distance from the Sun. The numerical value of $\varepsilon_A^T = 0.9651535$ may be expressed by several mathematical identity:

$$\varepsilon_A^T = t_E / \hat{t}_0 = 2^{-1/2} t_0 / \hat{t}_0 = 2^{-1/2} (F_0 / \sigma_M)^{3/16} = \pi_N / d_F^{1/16} = \pi_N (d_E / r_0)^{1/8}, \qquad \text{(a10)}$$

where $\pi_N = (\pi_D / 256)^{1/16}$. To establish the relationship between t_S and t_0 the anisotropy of the solar and terrestrial radiation fields has to be evaluated. It was shown in paragraph *4.1* that the ε_A IR clear-sky anisotropy factor of the GAT atmosphere practically equal to ε_A^T: $\varepsilon_A^T \cong \varepsilon_A = E_D / E_{D,I} = 0.96515341$. The close agreement of ε_A and ε_A^T is a proof that the structure of the global mean atmosphere is such, that the SW and IR anisotropy factors are exactly the same.

As a prominent example, the $\hat{t}_0^{obs}$ empirical virtual temperature from GAT simulation is in very good agreement with the true $\hat{t}_0$: $\hat{t}_0^{obs} = ((2(S_U^A + OLR^A / (1 - g^A)) / \sigma)^{1/4} / \sigma)^{1/4} = 288.74395$ K. The relative deviation of $\hat{t}_0$ and $\hat{t}_0^{obs}$ is ~1.83×10^{-4}%. As expected, the atmospheric Kirchhoff law also gives a perfect match with t_S: $t_S = (E_D / (\varepsilon_A A \sigma))^{1/4} = 286.06469$ K.

Assuming constant E_0 and F_0, we can easily determine the local $F(d)$ theoretical solar constant as a function of d distance from the Sun to any point in the solar system. Let $(r_0 / d)^2$ be the local dilution factor associated with the distance d, and let us use the next duality of the solar surface emission $E_0 = c_M d_F^{-4/3} = c_M (r_0 / d_E)^{-8/3}$.

By multiplying both sides with $(r_0 / d)^2$, the left hand side will define the $F(d) = (r_0 / d)^2 E_0$ function, and the right hand side will be transformed to the next mathematical identity: $c_M (r_0 / d_E)^{-8/3} (r_0 / d)^2 = c_M r_0^{-2/3} d_E^{8/3} d^{-2}$. The final form of $F(d)$:

$$F(d) = c_M r_0^{-2/3} d_E^{8/3} d^{-2}, \qquad \text{(a11)}$$

where r_0 and d_E are the proper *time averages* of the Sun's radius and the semi major axis of the Earth's orbit. Using the $F_0 = c_M d_F^{-1/3}$ duality, and the $r_0^{-2/3} d_E^{8/3} = d_F^{-1/3} d_E^2$ identity, $F(d)$ may be expressed in $d_a = d / d_E$ astronomical units:

$$F(d_a) = F_0 d_a^{-2}. \qquad \text{(a12)}$$

The precise determination of the relevant r_0 and d_E is the subject of solar physics, and perturbation calculations in celestial mechanics. The EBT temperature expressed from (a11) may be written as: $t(d) = c_M 10^{3/4} \pi^{-1/4} d_E^{2/3} r_0^{-1/6} d^{-1/2}$. The effective surface temperature of the planets in astrophysical sense is $t_0(d) = 2^{-1/2} t(d)$ K.

Outside the Sun, using Kepler's third law, $F(d)$ can also be expressed in terms of the orbital periods of the planets:

$$F(\mathrm{P}) = c_M \kappa_E^{-2/9} \mathrm{P}_E^{16/9} r_0^{2/3} \mathrm{P}^{4/3}, \qquad \text{(a13)}$$

where P is the orbital period in seconds of any planet, $\mathrm{P}_E = 3.155941209 \times 10^7$ s is the orbital period of the Earth, and $\kappa_E = 2.97496184 \times 10^{-19}$ s^{-3}m^2 is the Kepler constant for the Earth.

Equation (a11) has a singularity at $d = 0$ – at the center of the Sun or the barycenter of the solar system – which would physically imply an infinitely high temperature and an infinitely large flux density, which of course cannot exist. In principle, the solar system is in constant motion and a static geometrical center representing its center of gravity cannot be assigned. Using (a11) at $d = d_E$ we may formally define the $F_0^T = c_M r_0^{-2/3} d_E^{8/3} d_E^{-2} = 1367.954$ Wm^{-2} theoretical solar constant, which is agreeing well with F_0 and F_0^{obs}.

Apart from the singularity at $d = 0$, the distance d can vary from the Sun's interior to any point in the solar system. As already mentioned, the accuracy of (a11-a13) depends solely on the accuracy of measured geometric distances and times, and therefore it is free from the calibration problems often encountered in radiation measurements which makes F_0^T a real good candidate for a reference solar constant.

Based on model calculations the temperature at the center of the Sun is 1.571×10^7 K, NASA (2012) [46]. If we wonder what equation (a11) considers to be the Sun's center, we gradually decrease the distance d to the hypothetical center of the Sun in our equation and find when the resulting flux density of the radiation temperature calculated from the SB law equals the temperature of NASA's above. Our result shows that at 94.15 m from a hypothetical solar center the temperature is 1.5710053×10^7 K. This distance (in terms of astronomical distances) is a good approximation to the solar center, so our equation practically confirms the NASA complex model calculations. Further reducing the distance from a hypothetical solar center (d in (a11)), the radiative temperature increases rapidly, reaching 1.52436097×10^8 K degrees at a distance of 1 meter. At extremely small distances, such as the unit Planck length ($l_P = 1.61622938 \times 10^{-35}$ m, CODATA (2018) [53]), the temperature is 379.17×10^{23} K, which is of course still far from infinity.

It is also worth examining the accuracy of (a11) for much larger values of d. Again, referring to NASA data, Jupiter has a solar constant of 50.26 Wm^{-2}, a Bond albedo of 0.343, a distance d of 778.57×10^9 m, and an equilibrium absorption temperature of 109.9 K, NASA (2016) [54]. Similar data can be found in the planetary database of Willman (2012) [55]. From (a11), the theoretical solar constant of Jupiter is $F(d) = 50.504$ Wm^{-2}, which is about equal to the NASA data. The equilibrium absorption temperature of Jupiter is $(F(d)(1-0.343)/(4\sigma))^{1/4} = 109.9804$ K, which is also equal to the NASA data. The above examples show that (a11) does indeed accurately reproduce the wide range of solar constants in the solar system.

The point of our equation is not to show the trivial dependence of the flux density on distance d, but rather to show that the solar constant of any planet depends specifically on the semi-major axis of the Earth's orbit. Consequently, the Earth plays a very special role in the energetics of our solar system. It may even be that we should reconsider our ideas about the origin and formation of the solar system and our heliocentric worldview.

The law of duality interconnected the F_0 solar constant, the σ Stefan-Boltzmann constant and the r_0 solar radius into an accurate mathematical expression for the d_E semi-major axis of the Earth's orbit, where the working hydrological cycle assures the maximum radiation entropy of the OLR while maintaining a stable planetary climate: $d_E = (\sigma\pi_D)^{1/2} F_0^{3/2} r_0 = 1459789$ m. To answer the question why it is so needs further studies of planetary evolution.

To show the distinguished characteristics of the Earth's orbital position in the solar system in Figure 33 and 34 we compare planetary solar constants and anisotropy factors of the five inner planets. In these figures the black dots mark the unique orbital position of the Earth where the duality based F_0, $F_P(d)$ and $\varepsilon_P(d)$ parameters exactly reproduce the empirical data.

In Figure 33 the F_0^T and F_0^{obs} are equal and they numerically agree with the t_π entropy temperature. The maximum and minimum relative differences of F_0^T and the satellite records between 1978 and 2018 (in Scafetta [49], figure 1) are 0.44 % and -0.58 %, corresponding to about 1.0 K change in t_0.

In Figure 34 the SW ε_P were computed from the $\varepsilon_P = t_E / \hat{t}_0$ using the $\hat{t}_0$ (red dots), and from the $\varepsilon_P = \pi_N d_F^{-1/16}$ using d_F (green dots). The black dot marks the unique orbital position of the Earth where the empirical IR $\varepsilon_A = E_D / E_{D,I}$ and both SW ε_P are equal.

Finally, returning to our prominent example, using the $t_S = (E_D / (\varepsilon_A A\sigma))^{1/4}$ atmospheric Kirchhoff law, the $\varepsilon_A^T = \pi_N (d_E / r_0)^{1/8}$ anisotropy, and the $\varepsilon_A \cong \varepsilon_A^T$ close agreement, the E_D^T theoretical equilibrium downward atmospheric emission of the global average atmosphere will depend only on the ε_A^T astronomical parameter, and the τ^T theoretical IR equilibrium global mean flux optical thickness: $E_D^T = \varepsilon_0^T S_U$, where $\varepsilon_0^T = \varepsilon_A^T (1 - \exp(-\tau^T))$, and ε_0^T is the theoretical equilibrium clear-sky emissivity. The relative differences of $E_D - E_D^T$ and $\varepsilon_0 - \varepsilon_0^T$ are 0.0286 %.

Our planetary mean climate is particularly fond of the constants ε_A^T and τ^T, and leaves no room for any greenhouse gas perturbations. The message of our equations is quite clear and does not require the official approval of the Hungarian Academy of Sciences, or the academically illiterate politicians and their IPCC.

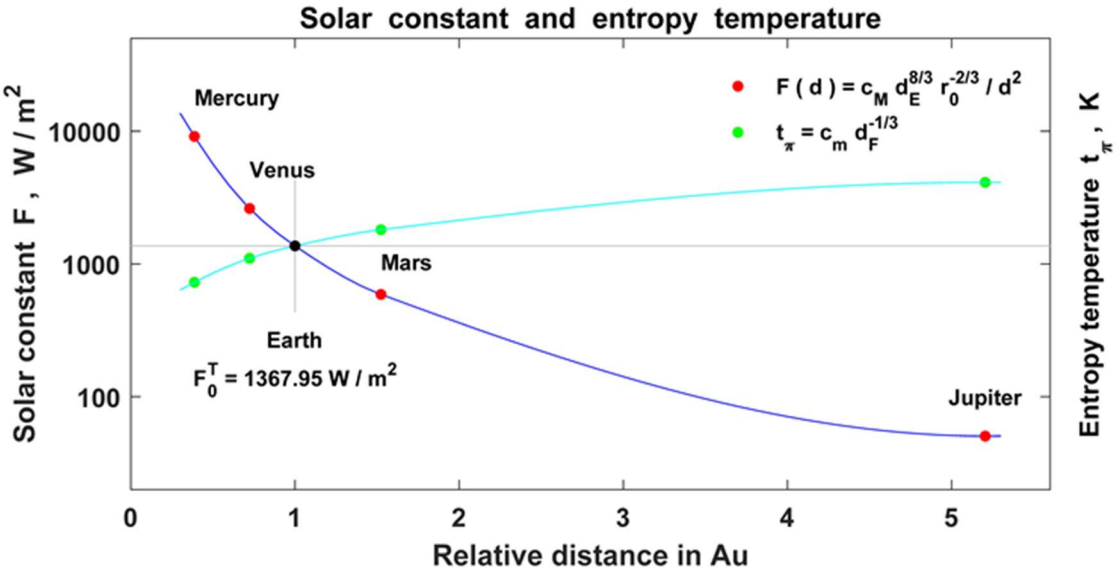

Figure 33: Numerical comparisons of the planetary solar constants from the $F(d)$ function (red dots) with the entropy temperatures from $t_\pi = \pi_D^{1/4} t_{SUN} = c_M d_F^{-1/3}$ dualities (green dots). The empirical F_0^{obs} (black dot) from GAT simulations perfectly agrees with F_0^T.

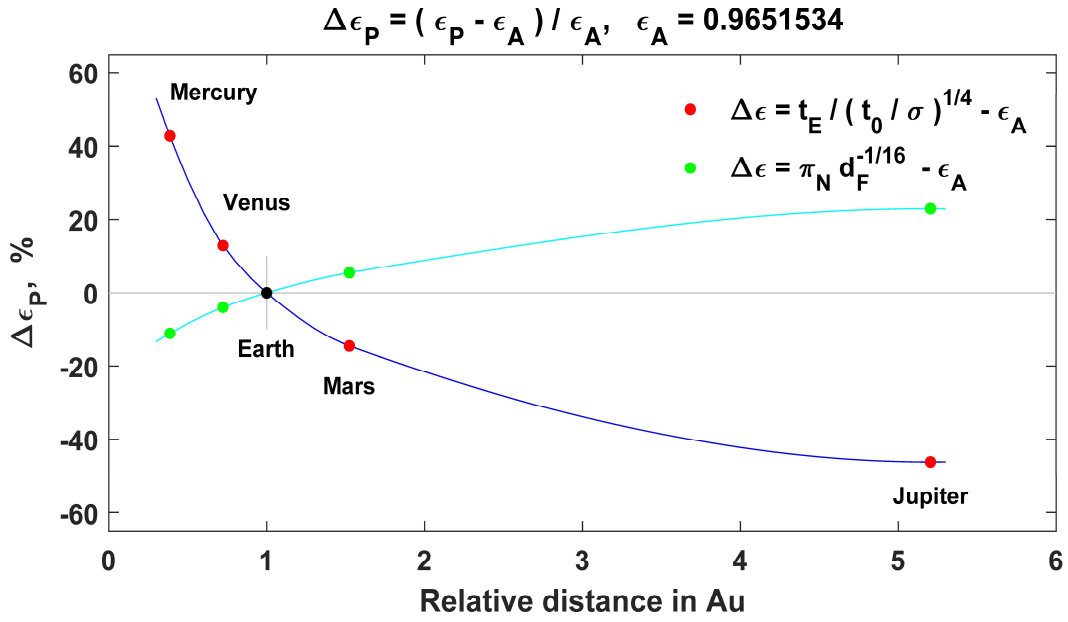

Figure 34: Comparisons of the ε_P SW anisotropy factors of the planets from the law of duality with the ε_A IR anisotropy factor of the GAT atmosphere from the atmospheric Kirchhoff law.